

**T.R.N.C.**  
**NEAR EAST UNIVERSITY**  
**INSTITUTE OF HEALTH SCIENCES**

**HUMAN PLACENTAL GLUTATHIONE S-TRANSFERASE P1-1**  
**(*hp*GSTP1-1): INHIBITORY ACTIVITY AND MOLECULAR DOCKING**  
**STUDIES OF DELTAMETHRIN**

**Victor MARKUS**

**MEDICAL BIOCHEMISTRY PROGRAM**  
**MASTER OF SCIENCE THESIS**

**NICOSIA**

**2017**

**T.R.N.C.**  
**NEAR EAST UNIVERSITY**  
**INSTITUTE OF HEALTH SCIENCES**

**HUMAN PLACENTAL GLUTATHIONE S-TRANSFERASE P1-1**  
**(*hp*GSTP1-1): INHIBITORY ACTIVITY AND MOLECULAR DOCKING**  
**STUDIES OF DELTAMETHRIN**

**Victor MARKUS**

**MEDICAL BIOCHEMISTRY PROGRAM**  
**MASTER OF SCIENCE THESIS**

**SUPERVISOR**  
**Professor Nazmi ÖZER, PhD**

**NICOSIA**

**2017**

## 1. INTRODUCTION

Glutathione transferases (E.C.2.5.1.18, referred also as Glutathione S-transferases, GSTs) are a significant large family of enzymes, primarily responsible for the phase II detoxification of endogenous and exogenous noxious chemical compounds by catalyzing their conjugation to the nucleophile reduced glutathione (GSH) for easy excretion out of the body through bile or urine (Whalen and Boyer, 1998; Sheehan *et al.*, 2001). Four types of GSTs have been identified: the soluble Canonical GSTs, Kappa-class or Mitochondrial GSTs, MAPEG (Membrane-associated Proteins in Eicosanoid and Glutathione metabolism) otherwise known as Microsomal GSTs, and the fosfomycin resistance protein from bacteria (Morgenstern *et al.*, 1982; Armstrong, 1991; Sheehan *et al.*, 2001; Bernat *et al.*, 2004; Ladner *et al.*, 2004; Josephy, 2010). Soluble canonical GSTs (sometimes called cytosolic GSTs) have been well characterized than other types of GSTs, and were originally grouped into A, M, P and T (Alpha, Mu, Pi and Theta respectively) classes on the basis of their structure similarities (primary and tertiary), specificity (substrate and inhibitor) and immunological identity (Sheehan *et al.*, 2001). GSTP1-1, one of the cytosolic or soluble GSTs, regulates cell survival and apoptosis by interacting with C-Jun-N terminal kinase-1 (JNK-1), maintaining it in an inactive form, thereby protecting the cells against hydrogen peroxide-induced cell death (Sheehan *et al.*, 2001; Zimriak, 2007; Dalmizrak *et al.*, 2016). The crystal structures of soluble GSTs revealed bound substrates or products in which the “canonical fold” has N-terminal  $\alpha/\beta$  domain that serves as GSH-binding site (“G-site”) and the second, a  $\alpha$ -helical domain that serves as the “H-site” which binds the electrophilic substrate (Josephy, 2010). GST gene expression is induced by many of its substrates and other nonsubstrate molecules such as  $H_2O_2$  including other reactive oxygen species (Whalen and Boyer, 1998). While it is commonly known that enzymes catalyze only one kind of reaction, GSTs belong to a enzymes family that metabolize xenobiotic such as cytochrome P450 enzymes which catalyze the biotransformation of a wide variety of substrates with diverse kind of functional groups (Josephy, 2010). GSTs have other several functions than the detoxification of xenobiotics. They include isomerase and peroxidase activities, regulating signaling cascades through protein-protein interaction, synthesis of steroids, synthesis and degradation of eicosanoids, degradation of aromatic amino acids, and also possess the ability to bind a wide range of non-catalytically exogenous and endogenous ligand molecules such as heme, bilirubin and steroid hormones (Sheehan *et al.*, 2001; Dalmizrak

*et al.*, 2016). In a case where there is a problem with GSTs in a cell, aside from other effects, detoxification of reactive electrophiles would not be possible. This, therefore, would result in accumulation and persistence of these electrophilic substrates in the cell, thereby bringing deleterious interactions with essential cellular components such as nucleic acids, lipids, and proteins.

Toxic electrophiles are a major source of assaults and insults to the human body. One of the sources of these electrophiles is pesticides-chemical substances widely used to control disease vectors (Hernández *et al.*, 2013). The increase in food production due to population growth has caused a significant rise in the use of pesticides over the years. The production of pesticides in the world has been shown to have increased to about twentyfold from 1960 to 2000 and risen from 1.0 billion tons to 1.7 billion tons from 2002 to 2007 (Hu *et al.*, 2015). Human exposure to these pesticides are from a variety of sources, including residues in food and water as a result of their extensive usage in modern agricultural practices to enhance food production, applications to public spaces in controlling disease vector in public health, domestic use in garden and lawn, and in occupation during production in factories (Alavanja *et al.*, 2004; Hernández *et al.*, 2013). Although pesticides have been very useful, their impact on human health has attracted substantial attention in recent years (Hu *et al.*, 2015). The mechanism of toxicity of various pesticides, including organophosphates (OP), organochlorines (OC), N-methylcarbamate (NMC), pyrethroids (PYR), neonicotinoids, triazines, paraquat, and dithiocarbamates has been chiefly through oxidative stress (Hernández *et al.*, 2013), the process that precipitate many disease condition by the production and accumulation of free radicals in the cells, induction of lipid peroxidation and alteration of the antioxidant enzymes system capability (Abdollahi *et al.*, 2004). Studies have shown that pesticide exposure induces cancer (Alavanja *et al.*, 2004; Bassil *et al.*, 2007), neurodegeneration (Steenland *et al.*, 2000; Alavanja *et al.*, 2004; Parrón *et al.*, 2011; Hu *et al.*, 2015), disorders of protein, lipid, and carbohydrate metabolism (Karami-Mohajeri and Abdollahi, 2011), defects in blood cells, liver, pancreas, muscles and other health disorders (Karami-Mohajeri and Abdollahi, 2011; Hu *et al.*, 2015), including death. About 220,000 people die each year in the world from OP pesticides exposure alone (Ekinici and Beydemir, 2009). There has been more concern that fetuses and babies are greatly endangered by toxic effects of pesticides than adults as there are pieces of evidence of pesticide residues in placenta, fetal

organs, subcutaneous fat tissues, umbilical cord blood and body fluids (Martínez *et al.*, 1993; Waliszewski *et al.* 2000; Perera *et al.*, 2004; Souza *et al.*, 2005). The enterohepatic clearance system of the fetus is immature (Beath, 2003; Dalmizrak *et al.*, 2016), and the body defense system of neonates is not well developed (Grijalva and Vakili, 2013), thus the high possibility of a more severe effect of pesticides in fetuses and babies. Although pre- and perinatal deleterious effects on fetal and neonatal development have been shown in a population exposed to pesticides, information relating to possible effects of low dose environmental residue of pesticides is scarce (Souza *et al.*, 2005). Most reported cases of the effect of pesticide exposure have been self-reported, and the degree of effect and other detailed information is difficult to reconstruct (Souza *et al.*, 2005). This makes it needful for more information on the effect of pesticides and their possible mechanism of action.

Deltamethrin (DEL) is a common name for a synthetic pyrethroid insecticide [ $\alpha$ -cyano-3-phenoxybenzyl-(1R, S)-cis, trans-3-(2, 2-dibromovinyl) -2, 2-dimethylcyclopropanecarboxylate] (Chargui *et al.*, 2012). The effects of organochlorine as a result of their bioaccumulation and organophosphates high toxicity especially to non-target organisms have made pyrethroids potential alternative (Yekeen and Adeboye, 2013). Aside from been used extensively in agriculture, pyrethroids have found application in public health in reducing the morbidity and mortality of malaria (Hougard *et al.*, 2002; Pennetier *et al.*, 2008). They are the only class of insecticides recommended by both the Center for Disease Control and Prevention (CDC) and the World Health Organization (WHO) to treat nets for the control of malaria (Pennetier *et al.*, 2008). As of one of the members of type II pyrethroids, DEL has been shown to have enhanced usage both indoor and outdoor due to its high potency on several of pests having three times power than some other pyrethroids (Chargui *et al.*, 2012; Yekeen and Adeboye, 2013), and owing to the fact that it has low toxicity and rapid metabolism to other non-target organisms including humans (Chargui *et al.*, 2012). Pyrethroids, particularly DEL have been considered to be safe (Rehman *et al.*, 2014). However, studies have revealed that low dose of DEL has harmful effects in pubescent female rats by causing DNA damage and disrupting renal and hepatic function (Chargui *et al.*, 2012). Studies on toxic effects of DEL on humans are very scarce (Rehman *et al.*, 2014). There is need therefore to evaluate the toxicity of DEL and assess its impact in the event of human exposure.

This study was aimed to elucidate the interaction of human placental glutathione transferase P1-1 (*hpGSTP1-1*) with DEL. First, the enzyme was characterized by determining the subunit molecular mass, temperature optimum and pH optimum. Then its concentration dependent inhibition was investigated using different DEL concentrations. From the data obtained, kinetic parameters were determined using different kinetic models (Segel, 1975) and STATISTICA '99 (StatSoft, Tulsa, OK). Lastly, a molecular docking approach was carried out to evaluate the best geometrical arrangement and strength of association between the pesticide and the enzyme.

## 2. GENERAL INFORMATION

### 2.1. Oxidative Stress and the Antioxidant System

Oxidative stress is a homeostatic imbalance that occurs when the level of free radicals (reactive oxygen species (ROS) and reactive nitrogen species (RNS)) overwhelm the body's ability to regulate (Cao *et al.*, 2005; Lobo *et al.*, 2010). These free radicals are molecular species with unpaired electron in their atomic orbital (**Table 2.1**) and capable of existing independent, making them unstable and highly reactive to donate an electron to or accept an electron (as oxidants or reductants) from other molecules (Yan *et al.*, 2008; Lobo *et al.*, 2010). They are generated by our body's various endogenous systems as a normal part of cellular metabolism, pathological states, and exposure to different physiochemical conditions (Lobo *et al.*, 2010).

Although ROS play a crucial role in normal cellular function where they serves an important mediators in cellular immunity and signal transduction pathways (Cao *et al.*, 2005), however, due to their highly reactive nature, they are detrimental when they are in excess as they can react with a number of cellular molecules such as DNA, proteins, and lipids, damaging cell structure and bringing about aging (Yan *et al.*, 2008; Lobo *et al.*, 2010). Alterations and deregulations in oxidative biology are hallmarks and critical events associated with cancer, inflammatory diseases (vasculitis, arthritis, lupus erythematosus, glomerulonephritis, adult respiratory diseases syndrome), ischemic diseases (stroke, heart diseases, intestinal ischemia), acquired immunodeficiency syndrome, hemochromatosis, organ transplantation, emphysema, preeclampsia and hypertension, gastric ulcers, neurological or psychiatric disorder (Alzheimer's disease, muscular dystrophy, Parkinson's disease), smoking-related diseases, alcoholism, and many others, (Lobo *et al.*, 2010; Dalmizrak *et al.*, 2011; Erkmen *et al.*, 2013). Redox homeostasis, therefore, is necessary to maintain proper physiological function and handle deleterious reactions such as lipid peroxidation, protein carbonylation, and DNA oxidation that damage cell structure and trigger a number of diseases (Cao *et al.*, 2005; Lobo *et al.*, 2010).

**Table 2.1.** Free radicals (from Lobo *et al.*, 2010; modified).

Free Radicals	Description
Superoxide ion ( $O_2^{\cdot-}$ )	Superoxide is produced by the addition of one $e^-$ to $O_2$ in autoxidation reactions or/and electron transport chain. It removes $Fe^{2+}$ from ferritin and iron-sulfur containing proteins.
Hydrogen peroxide ( $H_2O_2$ )	In the cell $O_2^{\cdot-}$ is converted to $H_2O_2$ by superoxide dismutase (SOD) or spontaneous reaction. It also converted to $\cdot OH$ radicals by metals ( $Fe^{2+}$ , $Cu^{1+}$ ). It is lipid soluble, it is able to diffuse across membranes.
Hydroxyl Radical ( $\cdot OH$ )	This is produced by Fenton and Haber-Weiss reaction and by the breaking down of peroxy nitrite. It reacts extremely and attacks most cell constituents.
Organic hydroperoxide (ROOH)	This is produced by radical reactions with cell components like nucleobases and lipids.
Alkoxy ( $RO\cdot$ ) and peroxy radicals ( $ROO\cdot$ )	These are oxygen centered organic radicals produced by hydrogen abstraction and radical addition to double bonds. Lipids are degraded in lipid peroxidation reaction.
Hypochlorous acid (HOCL)	This is formed by myeloperoxidase from hydrogen peroxide. It is highly reactive, lipid soluble, and can oxidize constituents of proteins including amino groups, thiol groups, and methionine readily.
Nitric oxide ( $NO\cdot$ )	It is synthesized by nitric oxide synthetase (NOS) from arginine. It is called as vital poison. It has many important physiological functions but it is also very toxic.
Peroxynitrite ( $ONOO^-$ )	This is produced in a rapid reaction between $NO\cdot$ and $O_2^{\cdot-}$ . It is similar to hypochlorous acid in reactivity and lipid soluble. When Peroxynitrous acid, produced from protonation undergoes homolytic cleavage to forms nitrogen dioxide and hydroxyl radical.

One of the mechanisms employed by the cell in response to oxidative stress is the used of the antioxidant system (Cao *et al.*, 2005). In the cell, nuclear transcription factor erythroid 2 p45-related factor 2 (Nrf2) is a very important transcription factor for the induction of Phase II enzymes and regulating antioxidant enzymes (Erkmen *et al.*, 2013). The enzyme system glutathione transferase (GST), superoxide dismutase (SOD), Catalase (CAT), glutathione peroxidase (GPX) and glutathione reductase (GR) play critical roles in redox homeostasis, acting cooperatively and synergistically to scavenge ROS because none of them can handle all the forms of ROS single-handedly (Yan *et al.*, 2008; Dalmizrak *et al.*, 2012). These enzymes protect the organism against ROS and xenobiotics (**Figure 2.1**).

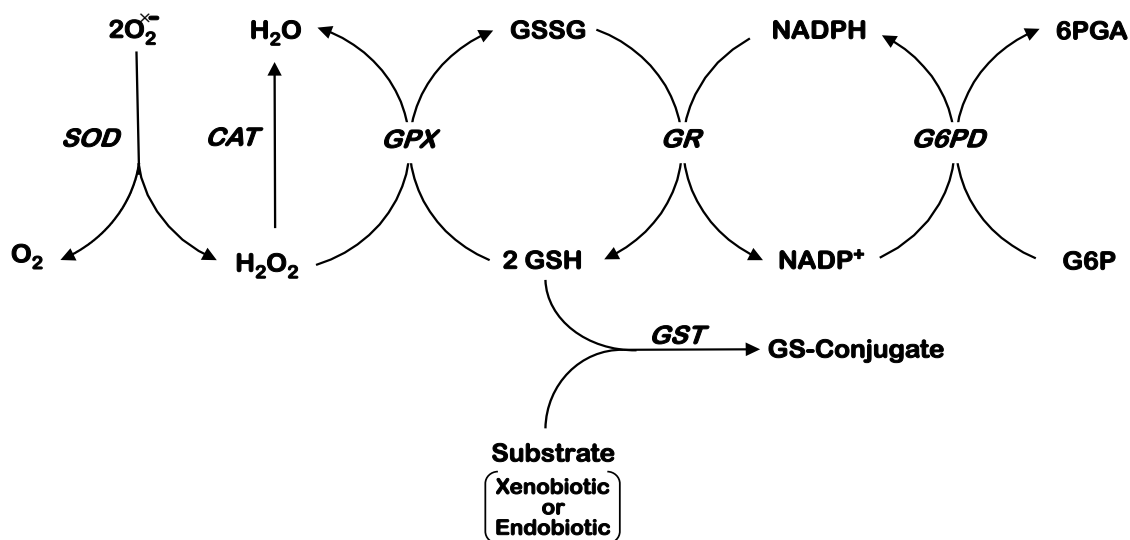


**Figure 2.1.** Schematic summary of detoxification and antioxidant systems: SOD reduced two superoxide anions ( $O_2^{\bullet -}$ ) to form hydrogen peroxide ( $H_2O_2$ ) and molecular oxygen, and then GPX takes the  $H_2O_2$  and reduced it through oxidation of two molecules of glutathione (GSH) to glutathione disulfide (GSSG) which subsequently is reduced by GR with the utilization of NADPH. And GST catalyzes the conjugation of glutathione to electrophilic substrates.

## 2.2. Glutathione Transferases

Glutathione Transferases (GSTs) are promiscuous enzymes that catalyze various kinds of reactions, with wide varieties of substrates (Angelucci *et al.*, 2005). These substrates are toxic and reactive products of environmental chemical carcinogens, therapeutic drugs, and oxidative stress (Morel and Aninat, 2011; Dalmizrak *et al.*, 2012). Their primary function, particularly in higher organisms, is the detoxification of both endobiotics and xenobiotics through their conjugation to reduced glutathione (GSH) (Armstrong, 1991; Dalmizrak *et al.*, 2012) and maintains normal redox homeostasis (Erkmen *et al.*, 2013). Other function of GSTs enzymes include isomerase and peroxidase activities, regulating signaling cascades through protein-protein interaction, synthesis of steroids, synthesis and degradation of eicosanoids, degradation of aromatic amino acids, and able to bind several non-catalytically exogenous and endogenous ligands such as heme, bilirubin and steroid hormones (Sheehan *et al.*, 2001; Tuna *et al.*, 2010; Dalmizrak *et al.*, 2016).

## 2.3. Distribution of GSTs

GSTs are ubiquitous. Analysis of the DNA sequence relationships and evolutionary history (Phylogenetics) among organisms indicate that they are widely distributed in nature (Board and Menon, 2013). They are present in plants, most aerobic microorganisms, and animals, including humans (Armstrong, 1991; Board and Menon, 2013). In animals, they are mostly found in the cytosol (Sheehan *et al.*, 2001) and other compartments of the cell such as the mitochondria and microsomes Dalmizrak *et al.*, 2016). In biomedical research, the mammalian soluble cytosolic GSTs are prominent as a result of the roles played by many members of the family in the metabolism of drug and xenobiotic (Board and Menon, 2013).

## 2.4. Classification of GSTs

The division of GSTs into classes is based on sequence similarity (Mannervik and Danielson, 1988; Mannervik *et al.*, 2005; Josephy, 2010). Basically they are classified into four groups: soluble Canonical GSTs (Armstrong, 1991; Sheehan *et al.*, 2001; Board and Menon, 2013), Mitochondrial (Kappa-class) GSTs (Ladner *et al.*, 2004; Morel and Aninat, 2011), MAPEG

(Membrane-associated Proteins in Eicosanoid and Glutathione metabolism) or otherwise known as Microsomal GSTs (Morgenstern *et al.*, 1982; Josephy, 2010), and the bacterial fosfomycin resistance protein (Bernat *et al.*, 2004). Humans consist of three of the classes: cytosolic GSTs, Kappa-class or mitochondrial GSTs, and MAPEG (Membrane-associated Proteins in Eicosanoid and Glutathione metabolism) or otherwise known as Microsomal GSTs (**Figure 2.2**). The soluble canonical GSTs (also called cytosolic GSTs) have been well studied and characterized than other types of GSTs, and were originally grouped into A, M, P and T ( $\alpha$ ,  $\mu$ ,  $\pi$ , and  $\theta$  respectively) classes on the basis of their structure similarities (primary and tertiary), specificity (substrate and inhibitor) and immunological identity (Sheehan *et al.*, 2001; Board and Menon, 2013). But recent studies in humans showed that there seven major classes of soluble GST enzymes categorized according to their amino acid sequence: Alpha (A) class (5 members), Mu (M) class (5 members), Pi (P) class (1 member), Theta (T) class (2 members), Zeta (Z) class (1 member), Omega (O) class (2 members), and Sigma (S) (1 member) as shown in **Figure 2.2** (Wu and Dong, 2012).

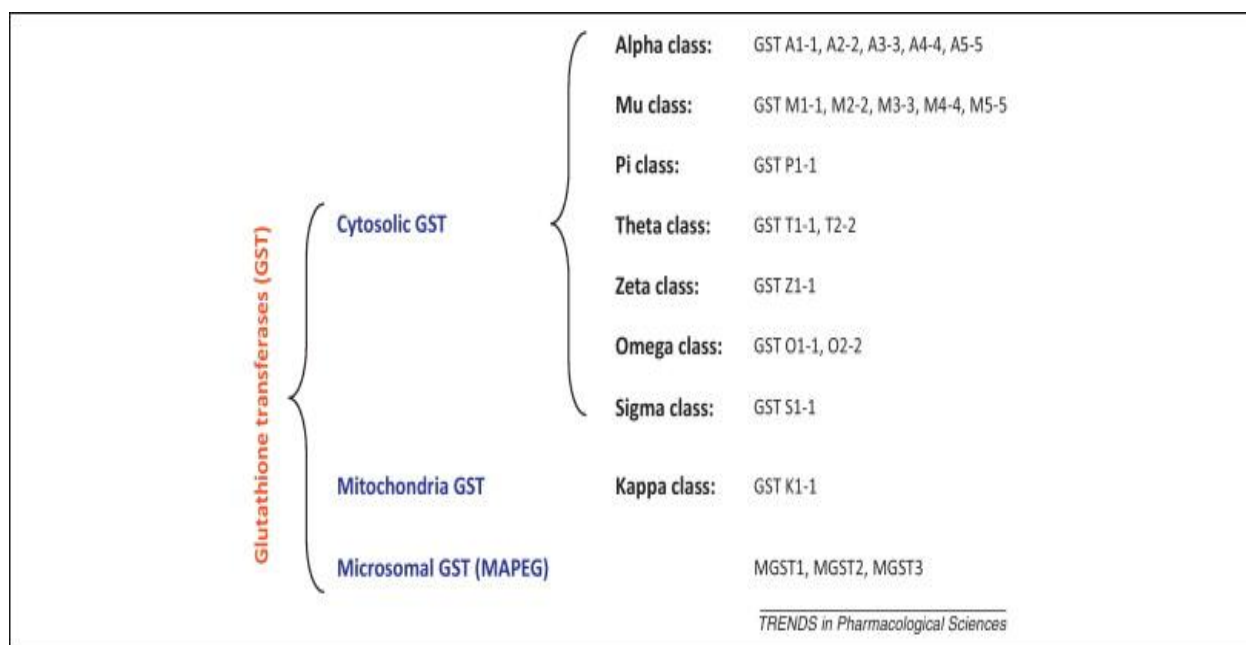


**Figure 2.2.** Classification of Human GSTs according to amino acid sequence relatedness (Wu and Dong, 2012).

## 2.5. Nomenclature

Systematically, GSTs are named “RX: glutathione R-transferase” (E.C. 2.5.1.18), and “glutathione transferase” (without the prefix “S”) as their trivial name, according to the recommendation of the Enzyme Commission (EC) of the International Union of Biochemistry and Molecular Biology (IUBMB) (Mannervik *et al.*, 2005). It has been noted that the commonly used name “glutathione S-transferase” could be misleading because actually, it is the glutathionyl group (GS-) that is transferred and not the sulfur atom *per se*, thus should be considered as “glutathionyl” (GS-) transferase (Mannervik *et al.*, 2005). Also, coupled with other function of the enzymes such as isomerase and peroxidase activities complicate issues, however, the abbreviation GSTs is still retained and commonly used as deliberation continues (Mannervik *et al.*, 2005; Board and Menon, 2013).

To ensure order, uniformity, and convenience in cataloging, an organized system of nomenclature of GSTs was necessary. According to Mannervik *et al.*, and Board and Menon, nomenclature of GSTs is according to their primary structure similarities and class designation, where they are assigned Greek letters names: alpha, mu, pi, and so on, abbreviated in Roman capitals as A, M, P and so on respectively. The Roman Capitals, instead of Greek characters, are commonly used because they matched computational bioinformatics tools well. Each class member is distinguished by an Arabic numeral, and then a numeric unit of the native dimeric protein structures based on the subunit composition. For example, the GSTA1-2 enzyme is in the Alpha class and composed of heterodimeric subunits 1 and 2. Homodimeric protein composing of two copies of subunits could occur too as in the Mu class GSTM1-1. When it comes to genes, they are named in the same way as enzymes but italicized. For example, *GSTM1* shows the gene for the Mu class subunit 1. Also, the need may arise to distinguish GSTs from different species. This is sorted by a prefix of the species initial added to the nomenclature. For example, rGST A1-1 and mGSTA1-1 shows GST enzymes from rat and mouse, respectively. Better, a three-letter prefix is used based on their Latin name instead of the one-letter: For example, Hsa for *Homo sapiens*, Mmu for *Mus musculus*, or Rno for *Rattus norvegicus* (Mannervik *et al.*, 2005; Board and Menon, 2013).

## 2.6. Structure of GSTs

There has been increased interest and studies in human GSTs due to their involvement in many vital biological processes such as prostaglandin and steroid biosynthesis, tyrosine catabolism, cell apoptosis and their overexpression in cancer resulting in drug resistance (Mannervik and Danielson, 1988; Prade *et al.*, 1997; Wu and Dong, 2012). Studies have revealed that cytosolic GSTs are typically dimeric proteins which are made up of about 22-30 kDa subunits (Board and Menon, 2013; Turk *et al.*, 2015). Each subunit comprise of two domains: the N-terminal  $\alpha/\beta$ -domain (or G domain for binding GSH) with a  $\beta\alpha\beta\alpha\beta\alpha$  topology that seems to have a thioredoxin-like ancestor, and the C-terminal all- $\alpha$ -helical domain (or H domain for binding electrophilic substrates) with no obvious evolutionary progenitor (Wu and Dong, 2012; Board and Menon, 2013). The dimeric structure of GSTs enhances their native protein stability and supply the active site with a proper orientation for efficient catalysis (Wu and Dong, 2012). The subunits associate to form an intrasubunit site for ligands binding that gives a resultant GSH-conjugate produced by one subunit to be sequestered by the adjacent subunit and thus preventing product inhibition (Singh, 2015). As shown in **Figure 2.3**, N-terminal domain contains a mixed four-stranded  $\beta$ -sheet ( $\beta_1$ ,  $\beta_2$ ,  $\beta_3$  and  $\beta_4$ ) having the third strand (strand 3) antiparallel to the others, and the C-terminal domain consisting of five major helices ( $\alpha_4$ -8) except in the alpha, theta, and omega classes of GSTs where they possess an extra helix  $\alpha_9$  bringing the number to six major helices ( $\alpha_4$ -9). While most members of the cytosolic GSTs are homodimers *in vivo*, however, heterodimers are known to exist among some classes, example GSTA1 and GSTA2 subunits in Alpha class or GSTM1 and GSTM2 subunits in Mu class (Board and Menon, 2013). The location of electrophile-binding sites (H-site) of mu class and pi class is not the same which explains the different substrate specificities for the two classes, that such kind of structural differences between GST classes can, therefore, be exploited in the development of novel anti-cancer drugs (Prade *et al.*, 1997).

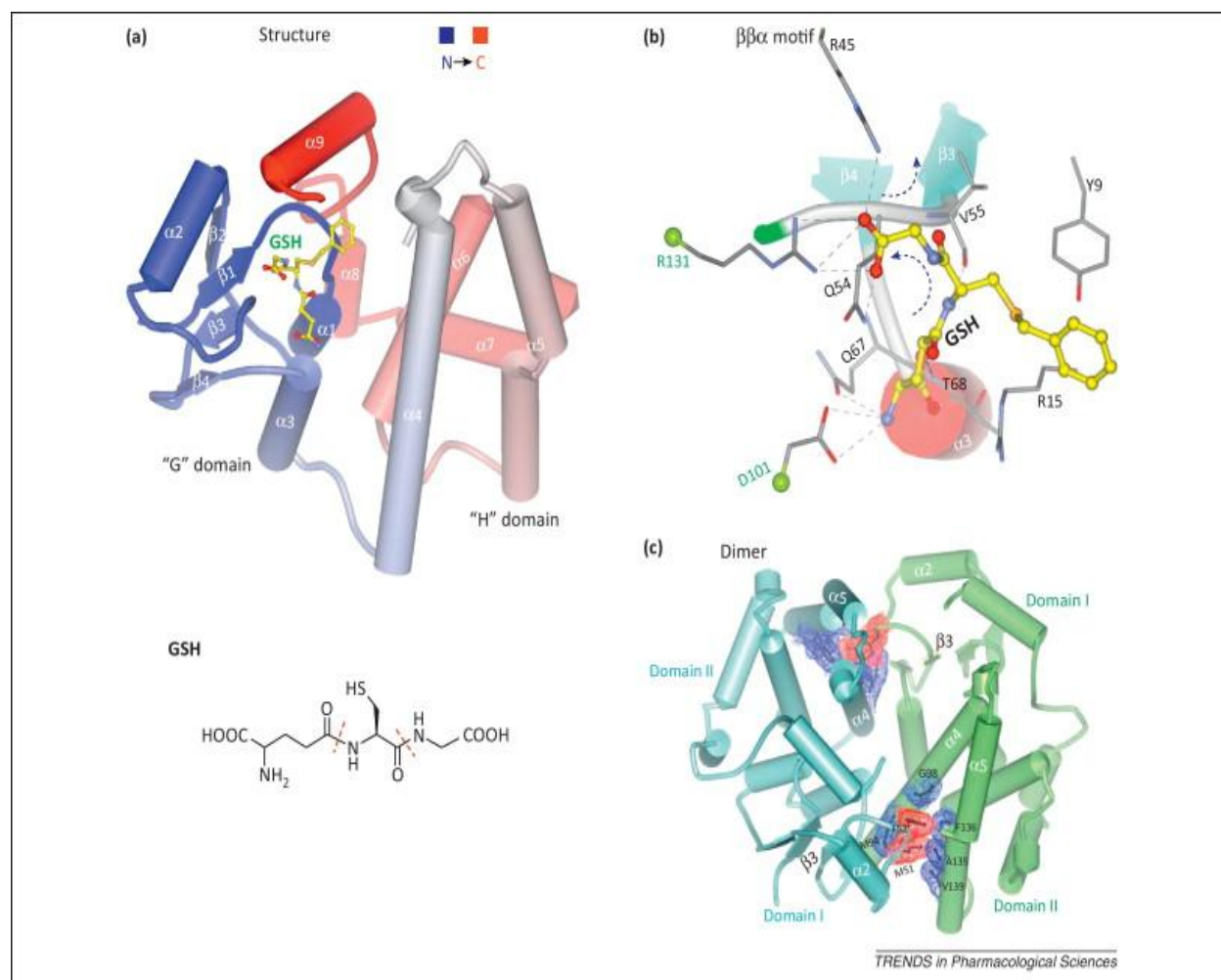


**Figure 2.3.** The Tertiary structure of a GST enzyme using GST A1-1 as an example (PDB code 1GUH) to depict the GSH-binding site and the overall fold of a GST structure: **(a)** shows the 3D structure of GST enzyme, comprising of the G domain for binding GSH and H domain for binding electrophilic substrates; **(b)** shows the conserved association of GSH with the GST  $\beta\beta\alpha$  motif residues. The Dashed lines show the hydrogen bonds. The Dashed arrows show the polypeptide direction of running; **(c)** shows Ball-and-socket association between GST monomers (subunits). The two monomers are shown in cyan and green, respectively. The ball and socket are shown by red and blue surfaces, respectively (Wu and Dong, 2012).

### 2.6.1. Active Sites of GSTs

Each of the GSTs subunits has its own active site which consists of a GSH-binding site (G-site) and an electrophilic substrate binding site (H-site) (Prade *et al.*, 1997). In a study of the crystal structures of soluble GSTs bound to substrates or products, it revealed a “canonical fold” with N-terminal  $\alpha/\beta$  domain that serves as GSH-binding site (“G-site”) and the second, a  $\alpha$ -helical domain that serves as the “H-site” which binds the xenobiotic (Josephy, 2010). The G-site is conserved and very specific for GSH, typically formed by the residues at the from the N-terminal domain of the GSTs subunits (Prade *et al.*, 1997; Zimriak, 2007; Board and Menon, 2013). In most soluble GSTs class, particularly Alpha, Mu, Pi and Sigma, the primary residue in the G-site (catalytic residue) was identified as tyrosine, but in Theta and Zeta classes was serine residue and in Omega class was cysteine residues shown in **Figure 2.4A, B** (Prade *et al.*, 1997; Sheehan, *et al.*, 2001; Wu and Dong, 2012; Board and Menon, 2013). The tyrosine residue has been shown to help in the stabilization of the glutathione thiolate anion (Prade *et al.*, 1997).

In contrast to the G-site, the H-site is not well conserved and has broad specificity to allow the acceptance of several kinds of xenobiotics (Prade *et al.*, 1997). They are largely formed by residues from the C-terminal domain (Board and Menon, 2013). This reflect the heterogeneity of different GST isoenzymes electrophilic substrates, that, while the G-site binding is very specific (specific to GSH, and not with other thiol like Dithiothreitol, 2-mercaptoethanol and cysteine), the requirement for binding with the H-site are not stringent, thus permitting the GST enzymes to metabolize quite a wide range of electrophilic substrates, even ones that has never been encountered in the past such as industrial pollutants and synthetic drugs (Zimriak, 2007; Board and Menon, 2013). At least three distinguishable interactions with the xenobiotic substrate have been identified in GSTP1-1 (Ralat and Colman, 2004). The H-site cleft of Alpha and mu-class GSTs are hydrophobic while that of the Pi class contain both hydrophobic and hydrophilic surfaces so as to facilitate recognition of substrates with both polar and apolar moieties (Ji *et al.*, 1994; Zimriak, 2007). H-site may even have double duty, for binding reaction substrates and noncatalytic ligand (Zimriak, 2007).

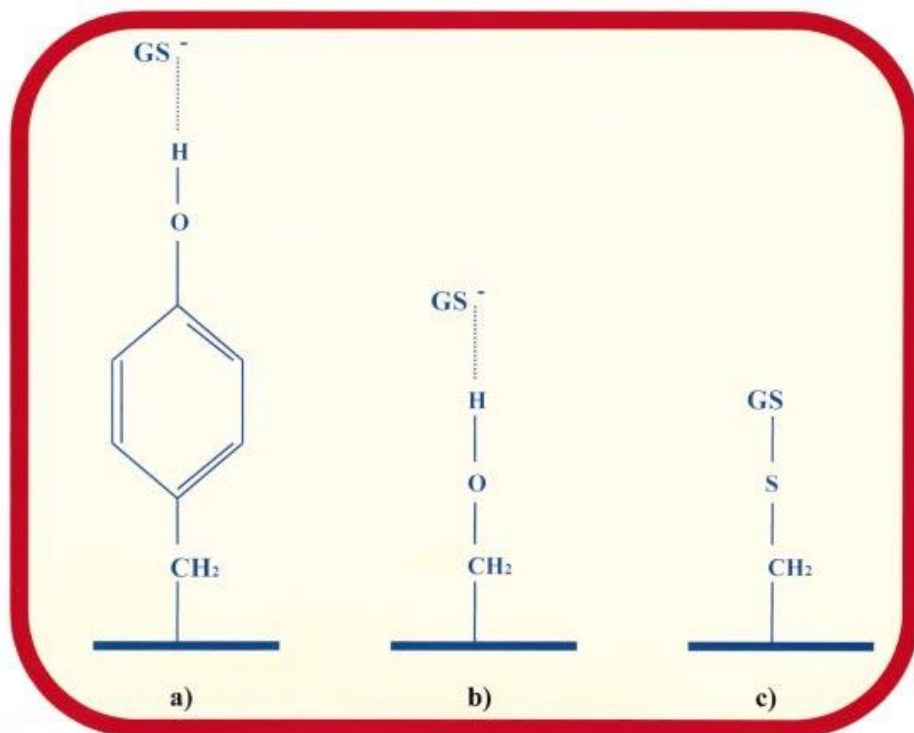


**Figure 2.4A.** Important residues in the active-site of GSTs. Most GST classes, they possess tyrosine residue in their N-terminal (**a**) which interacts with GSH to stabilize the thiolate anion, with a corresponding consequent decrease in  $\text{p}K_a$ . However, in the Theta class, and possibly Zeta classes, this role is carried out by a residue serine (**b**), while in the Omega and Beta classes a mixed disulfide is produced with a residue cysteine (**c**) (Sheehan *et al.*, 2001).

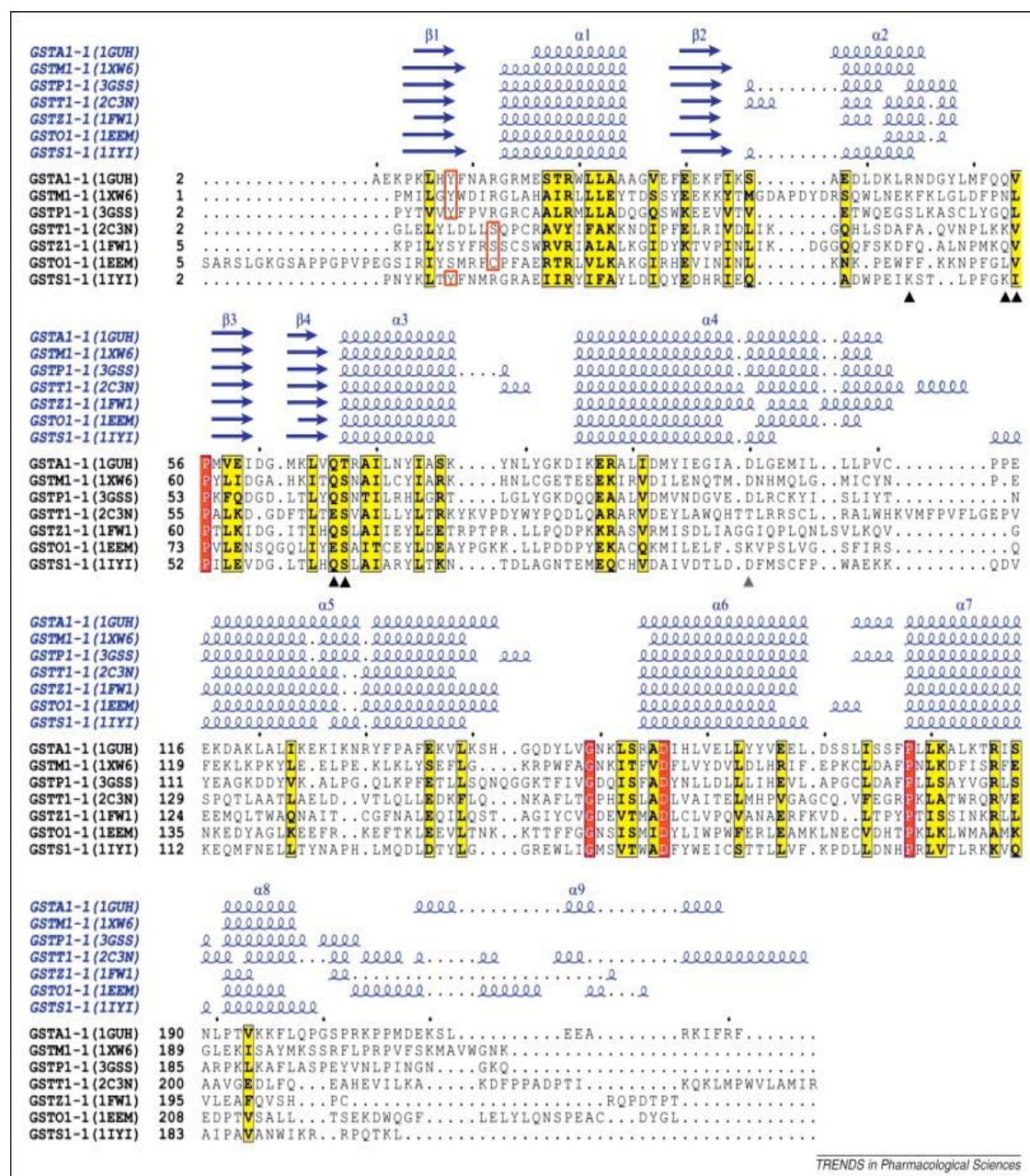


**Figure 2.4B.** Structure-base sequence alignment of some human GST enzymes (GST A1-1, GST M1-1, GST P1-1, GST T1-1, GST Z1-1, GST O1-1 and GST S1-1) produced using ENDscript; the conserved secondary structure elements are revealed above in the alignment. The residues that are conserved are highlighted in color. Protein data bank (PDB) codes for the structures are indicated in parentheses. The Red boxes indicate the catalytic residues. The triangles show the residues that interact with the glutathione (Du and Dong, 2012).

## 2.7. Reaction Mechanism of Canonical GSTs

The catalytic activity of the soluble canonical GSTs occur in two processes: the binding and activation of GSH which is common to all type of canonical GSTs and the binding of xenobiotics which occur based on the structure and chemical nature of the xenobiotics (Zimriak, 2007; Wu and Dong, 2012).

### 2.7.1. Binding and Activation of GSH

A common characteristic of GST-mediated reactions is the requirement of glutathione activation to the thiolate anion (GS<sup>-</sup>), which play a crucial role in the catalysis (Wu and Dong, 2012). The GSH is bound with the  $\gamma$ -glutamyl moiety protruding towards the protein core in an extended conformation at one end of the  $\beta$ -sheet and stabilized mainly by hydrogen bonding with the  $\beta 3\beta 4\alpha 3$  as shown in **Figure 2.3B** (Wu and Dong, 2012). Research has shown that the pKa of the sulfhydryl group of GSH, approximately 9.0 in aqueous solution, is brought down to between 6.2 and 6.5 in the GST enzyme-GSH complex (Parsons and Armstrong, 1996; Zimriak, 2007). Deprotonation of the Enzyme-bound GSH is great at physiological pH and thus activated for conjugation with an electrophilic substrate (Zimriak, 2007). Lowering pKa has been shown to promote the deprotonation and the formation of nucleophilic thiolate anion (Board and Menon, 2013). The thiolate anion is a strong nucleophile that attacks electrophilic substrates (Wu and Dong, 2012).

The thiolate ion of the glutathione bound to the enzyme, which is now ready for reaction with an electrophilic substrate, is stabilized by hydrogen bonding between the sulfur atom of the thiolate anion and the proton of the hydroxyl group of Tyr<sup>6</sup> in the protein active site of mu class (M1-1) isoenzyme from rat as illustrated in **Equation 2.7.1.1** (Parsons and Armstrong, 1996; Zimriak, 2007). In most GSTs, Tyr is the hydrogen-bond donor with just a few exceptions in the plant, specific insect GSTs classes, and in Theta-class GSTs, where a serine hydroxyl group carries out the function (Zimriak, 2007; Board and Menon, 2013). Two conserved water molecules were observed in the structure of the GST-glutathione complex, one of which formed hydrogen bonds directly to the glutathione sulfur atom and the other forms hydrogen bonds with residues around the G-site (Prade *et al.*, 1997).



In Pi-class GST particularly, there is an abnormally lowering of pKa of Tyr hydroxyl group that the tyrosinate anion act as a general base, drawing the proton from the Sulfhydryl (-SH) group as shown in **Equation 2.7.1.2** (Parsons and Armstrong, 1996). The catalytic Tyr residue in the Pi-class is Tyr7 (Oakley *et al.*, 1997; Prade *et al.*, 1997). The GSH binds initially in a pre-catalytic position and move subsequently to a catalytic position in a rate-limiting step such that the proton of sulfhydryl group is released and the thiolate ion is stabilized by the hydrogen bonding between the sulfur atom of the thiolate ion and the proton of the hydroxyl group in the active site of the protein provided by Tyr (Zimriak, 2007).



Wu and Dong (2012) reported that, first, as a result of the antiparallel running of the tripeptide GSH to the loop preceding strand  $\beta_3$  or the enzyme, a pair of hydrogen bonds between the central cysteine residue of the glutathione and the main chain of the protein (for example in GST A1-1, V55) is formed. Secondly, from the turn between  $\beta_4$  and  $\alpha_3$  of the protein, two residues (a glutamate or glutamine, and a threonine or serine) are linked by a hydrogen bond to the  $\gamma$ -glutamyl residue of the glutathione. Thirdly, there is also a hydrogen bond between a catalytic residue in the protein and the sulfur atom of the glutathione located at the N-terminal end of  $\alpha_1$  helix (Figure 2.3B).

### 2.7.2. Electrophilic Substrate Binding Site (H-site)

H-site, the region for binding electrophilic substrate, is adjacent to the G-site, and it is highly variable with distinct physicochemical features (size, shape, and hydrophobicity) and consists of three regions: the loop between the  $\alpha_1$  helix and  $\beta_1$ -strand,  $\alpha_4$  helix, and/or the tail of C-terminal (Wu and Dong, 2012). It accommodates different kinds of electrophiles, using the structural

elements from both the N-terminal and the C-terminal of the GST subunits to orient the substrate for nucleophilic attack by the thiolate of the GSH (Zimriak, 2007). This promiscuity is associated with its protein flexibility and active-site dynamics, including the C-terminal  $\alpha 9$  helix and the extended ends of  $\alpha 4$ - $\alpha 5$  helices as it has been shown that the  $\alpha 9$  helix, for example, may function as a mobile gate to the active-site cleft, regulating product liberation and substrate access being one of the distinguishing features between Alpha GSTs (having  $\alpha 9$  helix), and mu-class GSTs (having no  $\alpha 9$  helix) making the Mu-class able to catalyze bulkier electrophilic agents such as benzpyrenediols and aflatoxin B1-epoxides (Wu and Dong, 2012).

## 2.8. Catalytic Activity of GSTs

### 2.8.1. Glutathione Transferase activity

The GST transferase activity is generally based on the catalyzed reaction of GSH and electrophilic substrates to form thioether (Zimriak, 2007). There are several electrophilic substrates, some of them include epoxides, alkyl and aryl halides,  $\alpha, \beta$ -unsaturated aldehydes, and ketones, among others (Armstrong, 1991). GSTs, take advantage of the characteristic chemical behavior of electrophilic substrates, reacting more readily with thiolate anions than sulfhydryl groups to catalyze the nucleophilic attack of GSH on toxic electrophiles (Zimriak, 2007).

#### 2.8.1.1. Major Types of Glutathione Transferase Reaction

##### 2.8.1.1.1. Aromatic Nucleophilic Substitutional Reaction

The GST aromatic nucleophilic substitutional reaction is exemplified by the reaction of 1-chloro-2,4-dinitrobenzene (CDNB) and GSH, where the chloride is replaced by the glutathione (with identifiable Meisenheimer-complex intermediate) to form S-(2,4-dinitrophenyl)glutathione as shown in **Figure 2.5** (Zimriak, 2007). It has been shown that water molecules were absent from the structure of the Meisenheimer complex bound to GST, indicating that deprotonation of the cysteine happened during the formation of the ternary complex which involves removal of the inner bound water (Prade *et al.*, 1997).

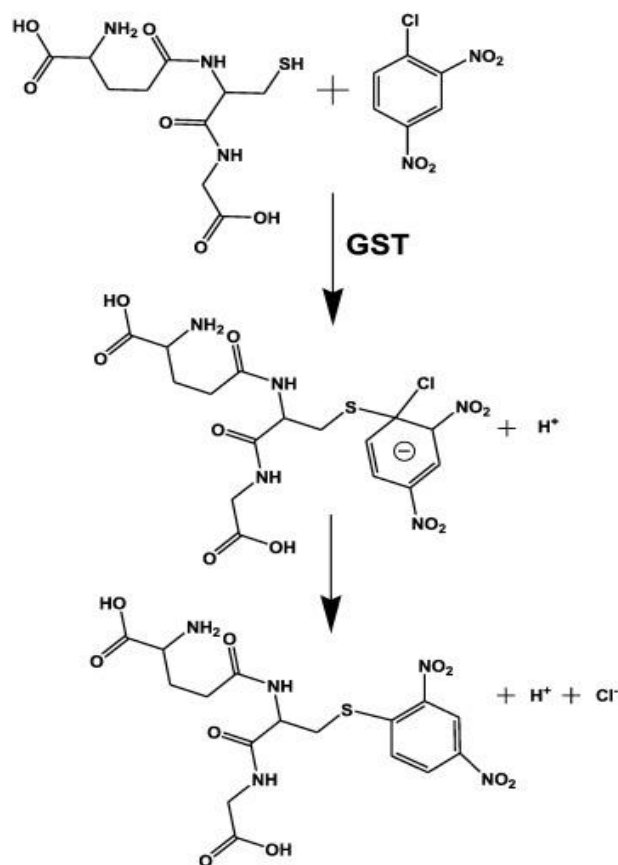


**Figure 2.5.** Conjugation reaction of GSH with CDNB catalyze by GST (Enache and Oliveira-Brett, 2014).

The GST activity is measured by following the increase in absorbance due to the conjugation of GSH to CDNB at 340nm (Habig and Jakoby, 1981; Wilce and Parker, 1994). CDNB is suitable for the broadest range of GST isozymes and it reacts readily (Dalmizrak *et al.*, 2016). This has been attributed to the small size of CDNB molecule when compared with the H-site cleft of most GSTs, thus, for this reason, the enzymes are placed with a few steric demands, making the artificial substrate able to bind with most GSTs that is almost universally accepted laboratory substrate for assaying GSTs (Zimriak, 2007). Even, CDNB reacts with nucleophilic substrates including thiolate anion of GSH in spontaneous noncatalytic reaction (Zimriak, 2007; Dalmizrak *et al.*, 2016). The mutagenesis studies and the crystal structure of GST M1-1 in complex with GS-DNB (**Figure 2.6**) revealed that H107 in helix  $\alpha$ 4 plays an important role in conjugation of

CDNB in which the polar association between the H107 and the CDNB *ortho*-nitro group orient the substrate in a productive conformation that the GSTs lacking H107-mediated interaction like the mu-class have weak activity with CDNB, and the ones having H107-mediated interaction have higher activity with CDNB, even though GST M1-1 shows a higher apparent affinity with 1-fluoro-2,4-dinitrobenzene (FDNB) compared to CDNB which authors suggest it could be due to smaller size of fluorine atom compared to chlorine permitting the *ortho*-nitro group of FDNB to associate and orient properly with Y115 (and H208) to promote binding and reaction (Wu and Dong, 2012).

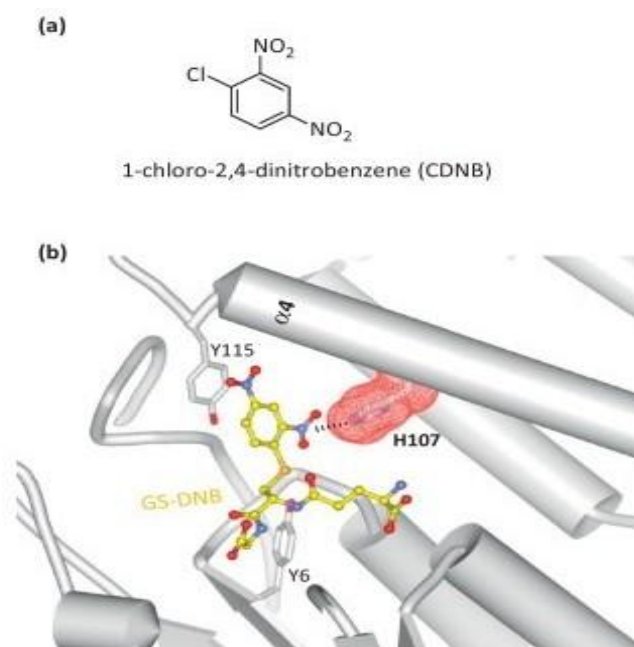


**Figure 2.6.** Molecular interactions between the artificial substrate CDNB molecules and the active sites of GSTM1-1: **(a)** Structure of 1-chloro-2,4-dinitrobenzene (CDNB). **(b)** Binding of CDNB to the active site of GST M1-1 (PDB code 1XWK) indicating the interaction of H107 with the CDNB *ortho*-nitro group (Wu and Dong, 2012).

### **2.8.1.1.2. Nucleophilic Additional Reaction to Double Bond**

In addition to the aromatic nucleophilic substitutional reaction, some GSTs also catalyze nucleophilic addition reaction by adding GSH to double bond in  $\alpha,\beta$ -unsaturated carbonyl compounds known as the Michael acceptor (Zimriak, 2007). This is exemplified in the conjugation of ethacrynic acid (EA) to GSH catalyzed by alpha- and pi-class GSTs, although the reaction is much more efficient in pi-class owing to the fact that the EA is attached in the deep location of the H-site where the Y108, and N204 possibly (the equivalent tyrosine is replaced by a valine in alpha-class) are hydrogen bonded with EA ketone oxygen either directly or indirectly thereby increasing the electrophilicity of the EA  $\beta$ -alkene carbon and resulting in nucleophilic attack (the selective bonding of the nucleophile electron to the electrophile) on the EA  $\beta$ -alkene carbon that enhances much more efficient Michael addition (Wu and Dong, 2012).

### **2.8.1.1.3. Opening of Oxirane (Epoxide) Ring**

The third major type of transferase reaction of canonical GSTs is opening of the strained oxirane (epoxide) ring, where the thiolate anion of the glutathione attacks the electrophilic center of the target molecule (Zimriak, 2007). One of the substrates in this category is (+)-anti-7,8-dihydroxy-9,10-oxo-7,8,9,10-tetrahydrobenzo[a]pyrene (+)-anti-BPDE, a carcinogen produced from polycyclic aromatic hydrocarbon benzo[a]pyrene which main clearance pathway is GST P1-1-catalyzed conjugation to GSH (Wu and Dong, 2012). This shows how GST reaction plays a crucial protective role against the carcinogenicity of polycyclic aromatic hydrocarbons such as benzo[a]pyrene (Zimriak, 2007).

## **2.9. GSTs and Bioactivation of Toxins**

Glutathione conjugation reaction of GSTs in the majority of cases results to detoxification of target xenobiotic, however, in some cases, the product of the reaction has rather increased toxicity than decreased toxicity. This phenomenon is referred to as bioactivation of toxins (Zimriak, 2007). Zimriak reported that a good example of GST bioactivation reaction is the glutathione conjugation of dichloromethane in which the product formed is unstable, giving rise to toxic formaldehyde.

### 2.10. GST Peroxidase Activity

The Alpha-class GSTs, particularly, account for most of the glutathione peroxidase activity in cells by utilizing GSH as a reductant to convert organic hydroperoxide (not  $H_2O_2$ ) to alcohol, the reaction that helps to reduced phospholipid hydroperoxides without the need for its prior hydrolysis to oxidized fatty acid (Zimriak, 2007).

### 2.11. GST Isomerase activity

The isomerization step in the synthesis of steroid hormones such as progesterone and testosterone where  $\Delta^5$ -3-ketosteroid is converted to a  $\Delta^4$ -3-ketosteroid is catalyzed by GSTs (Zimriak, 2007) as shown in **Figure 2.7**. Alpha-class GSTs hGSTA3-3 has been identified as the most efficient members with steroid isomerase activity (Wu and Dong, 2012). The steroid  $\Delta^5$ -3-ketosteroids such as  $\Delta^5$ -pregnane-3,20-dione and  $\Delta^5$ -androstene-3,17-dione are converted to the immediate precursors of testosterone and progesterone  $\Delta^4$ -pregnane-3,20-dione and  $\Delta^4$ -androstene-3,17-dione respectively (Board and Menon, 2013).

In a study using hGSTA3-3 to catalyze the formation of  $\Delta^4$ -androstene-3,17-dione from  $\Delta^5$ -androstene-3,17-dione, the reaction mechanism for the double-bond isomerization showed that the thiolate anion of the glutathione stabilized by Tyr-9 draws proton from carbon 4 of the steroid nucleus and transferred to carbon 6 of the same molecule through a proton conducting-wire, involving glutathione and Tyr-9 thus, for complete isomerization as shown in **Figure 2.8** (Zimriak, 2007; Board and Menon, 2013). Deficiency of enzymes along this degradation pathway has been shown to result in serious diseases such as hereditary tyrosinemia type I, alkaptonuria and phenylketonuria (Wu and Dong, 2012).

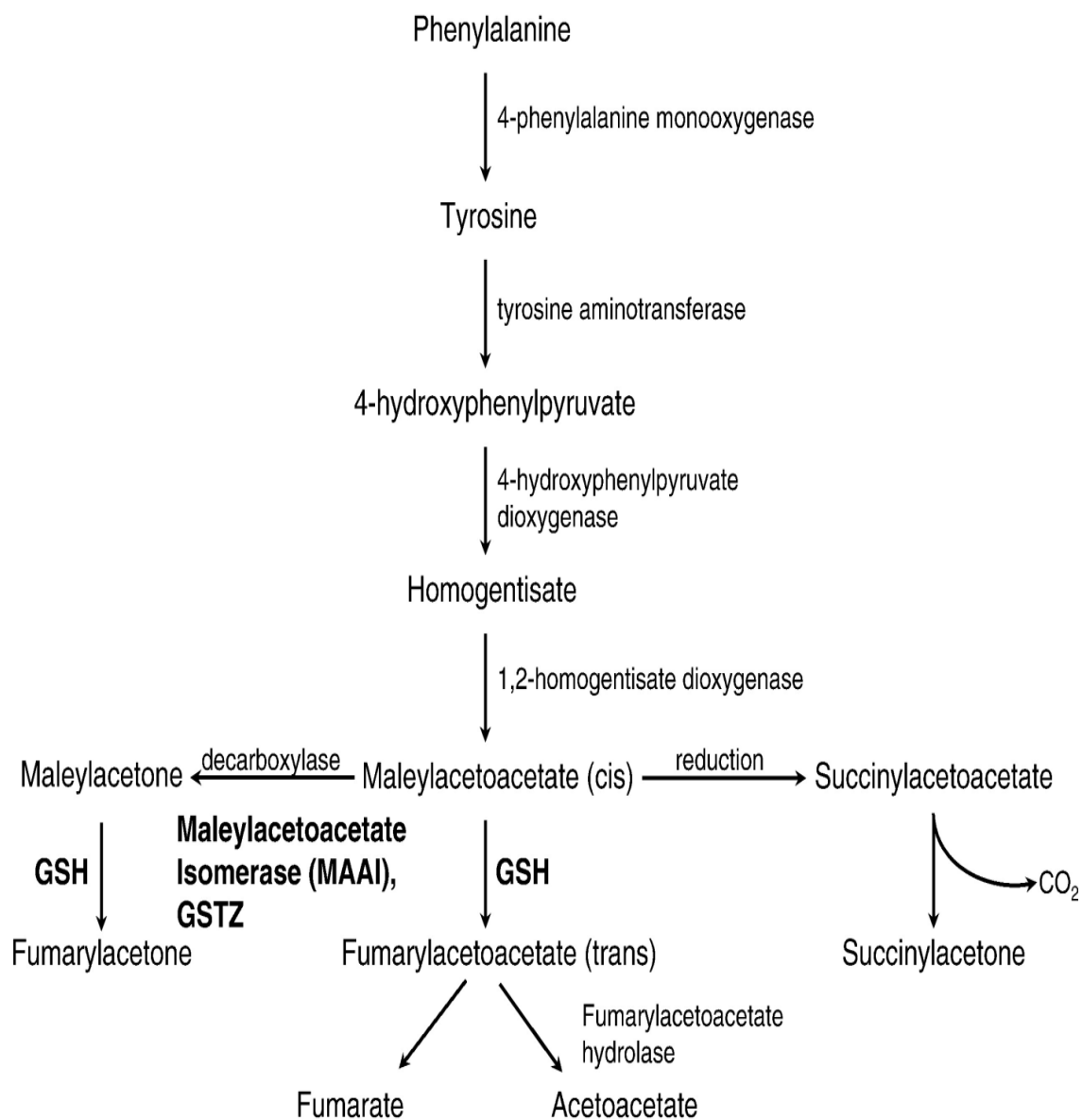


**Figure 2.7.** The isomerization steps and intermediates in the phenylalanine–tyrosine degradation pathway. (Board and Menon, 2013).

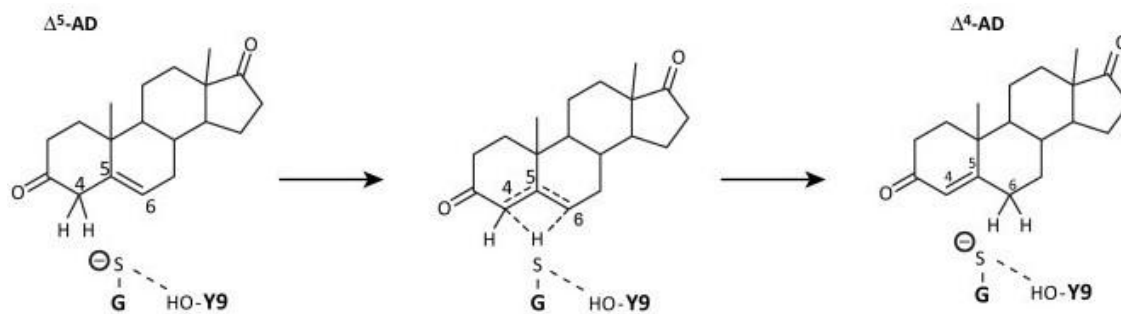


**Figure 2.8.** The Proposed reaction mechanism for GSH-assisted conversion of  $\Delta^5$ -androsten-3,17-dione ( $\Delta^5$ -AD) to  $\Delta^4$ -androsten-3,17-dione ( $\Delta^4$ -AD) (Wu and Dong, 2012).

The Zeta-class GSTs also, particularly GSTZ1-1 (also known as maleylacetoacetate isomerase), have been shown to catalyze the physiologically *cis-trans* isomerization reaction of maleylacetoacetate to fumarylacetoacetate, a second-to-last step in a pathway regulating the catabolism of phenylalanine and tyrosine as shown in **Figure 2.7** (Jowsey *et al.*, 2003; Zimriak, 2007; Wu and Dong, 2012; Board and Menon, 2013). The conversion of the 13-*cis*-retinoic acid to the isomeric form all-*trans*-retinoic acid is catalyzed by a number of Pi-class GST, hGSTP1-1, and to a lesser extent by hGSTA1-1 and hGSTM1-1 (Zimriak, 2007).

## 2.12. GSTs in the Metabolism of Eicosanoids

Eicosanoids, such as leukotrienes and prostaglandins, are synthesized from arachidonic acid. It has been shown that GSTs participate in several aspects of prostaglandin metabolism (Board and Menon, 2013). One of the two prostaglandin D<sub>2</sub> synthase enzymes which catalyze the conversion of the PGH<sub>2</sub> precursor to various products (among them PGD<sub>2</sub>) is the only mammalian sigma-class GST (Zimriak, 2007; Board and Menon, 2013). Also, the isomerization of PGH<sub>2</sub> to PGE<sub>2</sub> has been shown in humans to be catalyzed by GSTM2-2 and GSTM3-3 but not GSTM4-4 suggesting their possible role in sleep-wake and temperature regulation (Board and Menon, 2013). Due to the important biological role of GSTs such as GSTS1-1 responsible for the production of prostaglandin D<sub>2</sub> (a mediator of allergy and inflammation), they have been shown to have promise for anti-allergy and anti-inflammation actions when inhibited thus they are

targets for drug development (Wu and Dong, 2012). The precursor PGH<sub>2</sub> has been shown to have another fate when converted by canonical mu-class GSTM2-2 and GSTM3-3 or by MAPEG enzyme (PGE synthase) (Zimriak, 2007). The inhibitors PGA2 and PGJ2 of cellular proliferation are substrates for Many GSTs such as GSTA1-1, GSTA2-2, GSTM1-1 and GSTP1-1 with stereoselectivity that varies (Board and Menon, 2013).

## **2.13. Noncatalytic Activities of GSTs**

### **2.13.1. Ligandin function**

In addition to their enzymatic function, GSTs have the ability to bind a wide range of noncatalytic hydrophobic molecules or ligands (both apolar and hydrophobic) which otherwise could interfere with the normal function of the cell (Prade *et al.*, 1997; Zimriak, 2007). This physiological role is known as the so-called ligandin function of GSTs, where they serve as transport proteins binding to many noncatalytic ligand molecules including bile acid, steroid, heme, bilirubin, drugs, wide range of organic dyes and other xenobiotics (Zimriak, 2007; Dalmizrak *et al.*, 2012; Wu and Dong, 2012).

### **2.13.2. Buffering**

Buffering is another noncatalytic function of GSTs. Here, GSTs buffer or provide a form of sequestration or storage for compounds intracellularly much as albumin does in circulation, there by stopping a bioactive ligand or signal molecule action and modulating cellular response (Zimriak, 2007). This is seen in the ability of many GSTs to bind to 15-deoxy- $\Delta$ 12,14-prostaglandin J2 or its glutathione conjugate, which act as Peroxisome proliferator-activated receptor gamma (PPAR $\gamma$ ) ligand in the nucleus, to sequester it so as to inhibit PPAR $\gamma$  activation and prevent nuclear translocation (Zimriak, 2007; Wu and Dong, 2012).

## **2.14. Role of GST in Cellular Survival and Apoptosis**

In humans, GSTP1-1 is the single functional gene which maps to chromosome 11q13 (Board and Menon, 2013). It is expressed widely in the cytosol and has been implicated in several cancers

and proposed as potential diagnostic and/or prognostic marker protein (Tuna *et al.*, 2010; Board and Menon, 2013; Erkmen *et al.*, 2013). The increased concentration of GSTP1-1 due to overexpression in tumors whether the drug is its substrate or not has been associated with drug resistance (Tuna *et al.*, 2010; Erkmen *et al.*, 2013). It was thought that the observed drug resistance is as a result of the ability of GSTP1-1 to regulate kinase signaling pathways (Board and Menon, 2013). GST P1-1 defend tumor cells through conjugation to chemotherapeutics such as chlorambucil and ethacrynic acid and inhibiting apoptosis through its interaction with JNK kinase thus presenting the enzyme as a promising target for inhibition in cancer therapy (Wu and Dong, 2012). However, in a recent study on prostate cancer, it was demonstrated that GSTP1-1 overexpression interferes with Motility and Viability of the Prostate Cancer by interacting with MYC and shutting down the MEK/ERK1/2 Pathways (Wang *et al.*, 2017). Signaling molecules like JNK, TRAF2, and ASK1 has been shown to interact with GSTP1-1 through protein-protein interactions, thereby inhibiting the activation of JNK and p38 induced apoptotic signaling, hindering the interaction of TRAF2 with ASK1 and impeding TRAF2-ASK-1 induced downstream pro-apoptotic signaling (**Figure 2.9**). The observed upregulation of GSTP1-1 in tumors inactivates JNK thus resulting in the suppression of the apoptotic signaling pathways and bestowing resistance to drug-induced cell death (Board and Menon, 2013). JNK in particular (an important protein in the signaling pathway), has been implicated in apoptosis and cell survival (Erkmen *et al.*, 2013). Under physiological conditions, a fraction of GSTP1-1 is bound to JNK (Board and Menon, 2013). However, under stress induced by H<sub>2</sub>O<sub>2</sub> or UV-irradiation, JNK oligomerizes thus causing dissociation of GSTP1-1-JNK complex, leading to apoptosis (Adler *et al.*, 1999; Tuna *et al.*, 2010). The dissociated GSTP1-1 accumulates in the cytosol in the form of dimmers and the released of JNK triggers a cascade of signaling events, first by activating Jun-c through phosphorylation and subsequently resulting in apoptosis (Board and Menon, 2013). By inhibiting JNK, GSTP1-1 regulates cell survival and apoptosis through maintaining JNK in an inactive form and protecting the cells against hydrogen peroxide and UV-irradiation induced cell death (Adler *et al.*, 1999; Sheehan *et al.*, 2001; Zimriak, 2007; Dalmizrak *et al.*, 2016).

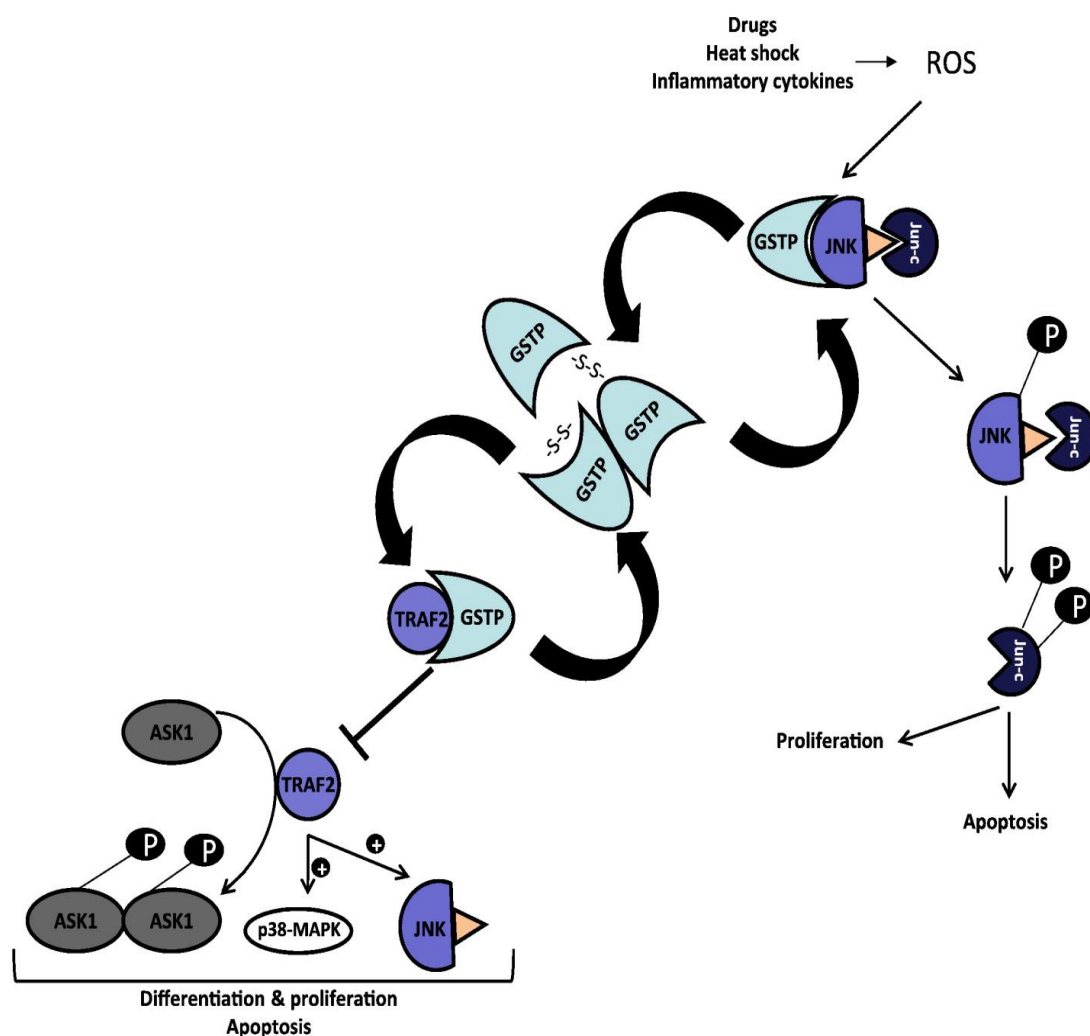


**Figure 2.9.** The role of GSTP1-1 in Cellular Survival and Apoptosis. Under the physiological non-stressed state, Jun-c and JNK are kept in an inactive form, complexed with GSTP1-1. When the cell is exposed to a range of stresses changing the redox potential in the cell environment, oligomerization of GSTP1-1 and dissociation of the complex occur. Thus JNK is then phosphorylated, which leads to the activation of downstream kinases. Similar interactions between GSTP1-1 and TRAF2 can inhibit the downstream actions of ASK1, JNK, and p38-MAPK. Activation or proliferation can occur even with brief low-level oxidative stress. High level and prolonged oxidative stress can result in apoptosis (Board and Menon, 2013).

### **2.15. GST Inhibitors**

Zimriak reported that although GSTs can be inhibited by their own reaction product due to the ability of such product to recognize the G-site and H-site with the requirement of effective and efficient transport and further metabolism of the conjugates, however, so far three broad of GST inhibitor groups have been identified. According to the report, the first group consist of the nonsubstrate ligands that bind to the noncatalytic sites on the GSTs (it lacks specificity and potency), while the other two groups are analogue of glutathione that bind to the G-site or a hydrophobic compounds that bind to the H-site of the enzymes (Zimriak, 2007).

### **2.16. Pesticides**

Pesticides have been used widely in agriculture and in public health to control disease vectors but unfortunately have been highly toxic to humans and represent a major concern for human health (Hernández *et al*, 2013). Pesticides production in the world increased to about twentyfold from 1960 to 2000 and has risen from 1.0 billion tons to 1.7 billion tons from 2002 to 2007 (Hu *et al.*, 2015). People are exposed to pesticides from food, water, and air, either at home, farm or occupation (Alavanja *et al.*, 2004; Hernández *et al*, 2013). Reports have shown that the mechanism of toxicity of various pesticides is majorly by oxidative stress (Hernández *et al*, 2013). Many diseases are implications of pesticides exposure including cancer, neurodegenerative diseases, disorders of protein, lipid, and carbohydrate metabolism, defects in blood cells, liver, pancreas, muscles and many other health disorders (Steenland *et al.*, 2000; Alavanja *et al.*, 2004; Bassil *et al.*, 2007; Karami-Mohajeri and Abdollahi, 2011; Parrón *et al.*, 2011; Hu *et al.*, 2015). Also, there has been an ugly statistics of death. Reports have shown that about 220,000 people die each year in the world from organophosphate (OP) pesticides exposure (Ekinici and Beydemir, 2009).

### **2.17. Deltamethrin (DEL)**

The effects of organochlorine as a result of their bioaccumulation and organophosphates high toxicity especially to non-target organisms have made pyrethroids potential alternative (Yekeen and Adeboye, 2013). Pyrethroids, of which DEL is one of the members, are the only class of

insecticides recommended by both the Centre for Disease Control and Prevention (CDC) and the World Health Organization (WHO) to treat nets for the control of malaria (Pennetier *et al.*, 2008). Mosquito nets impregnated in DEL have been used successfully all over the world to control malaria (Joshi *et al.*, 2003). DEL is a common name for a synthetic dibromo-pyrethroid insecticide. Its IUPAC name is [ $\alpha$ -cyano-3-phenoxybenzyl-(1R,S)-cis,trans-3-(2,2-dibromovinyl)-2,2-dimethylcyclopropane carboxylate] (Figure 2.10A,B)(Chargui *et al.*, 2012).

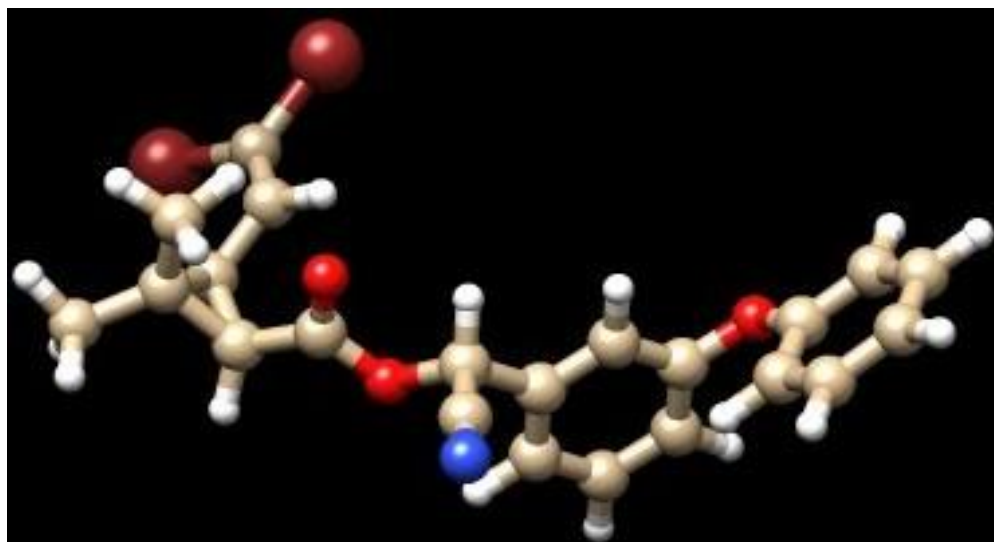
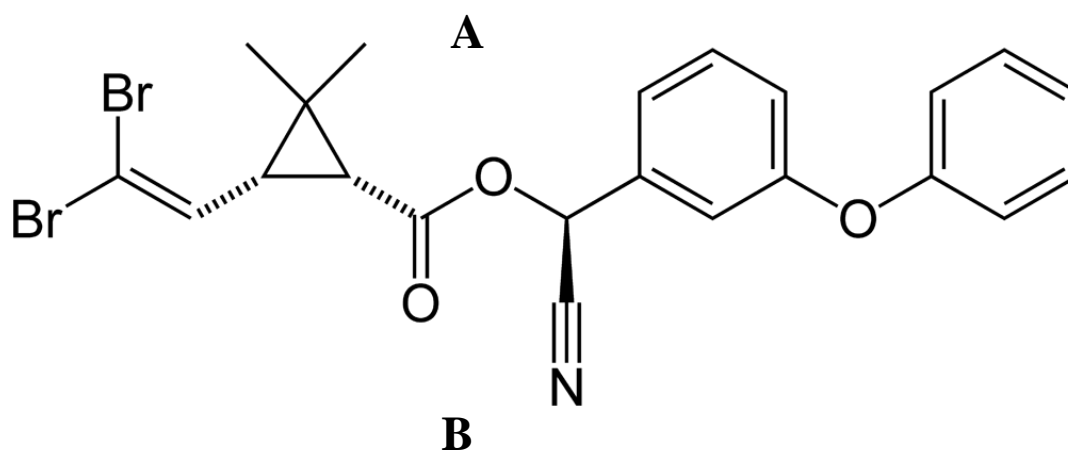


**Figure 2.10.** The structure of Deltamethrin.**A.**2D structure (Saoudi *et al.*, 2011).**B.** 3D structure (ball and stick) generated using CORINA Classic.

Aside from being used extensively in agriculture, pyrethroids have found application in public health in reducing the morbidity and mortality of malaria (Hougard *et al.*, 2002; Pennetier *et al.*, 2008) due to its high potency on a large number of pests having three times power than some other pyrethroids (Chargui *et al.*, 2012; Yekeen and Adeboye, 2013) and owing to the fact that it has rapid metabolism and low toxicity to other non-target organisms including humans (Chargui *et al.*, 2012). Although pyrethroids, particularly DEL have been considered to be safe (Rehman *et al.*, 2014), however, reports have shown that low dose of DEL has harmful effects in pubescent female rats by causing DNA damage and disrupting renal and hepatic function (Chargui *et al.*, 2012).

Specifically, the early stage of fetus and neonate development are critical periods in the development stages that is uniquely sensitive to toxic chemical substances to which it is exposed *in utero*, with effect and damage shown to modify ontogeny of the enzyme involved in its clearance of toxins (Johri *et al.*, 2006). Researchers suggest that early life insult during the season of birth could cause permanent damage to the developing immune system thus leading to premature deaths (Ofordile *et al.*, 2005). In a study by the Columbia Center for Children's Environmental Health (CCCEH), it was shown that fetal and childhood exposure to pesticides can adversely affect neurodevelopment (Tapia *et al.*, 2012).

Pyrethroids have been shown to cross the placenta and are secreted into milk (Ofordile *et al.*, 2005). The placenta functions as the interface between the maternal and fetal circulations and controls the transfer of nutrients, oxygen, and waste products, but when xenobiotics are present in maternal circulation, the degree of exposure and effect is determined by biotransformation processes and transport system in the placental barrier (Al-Enazy *et al.*, 2016). The enterohepatic clearance system of the fetus is immature (Beath, 2003; Dalmizrak *et al.*, 2016), thus this can cause a threat in the event of maternal exposure to xenobiotics. There is need therefore for more information about the toxic effects of DEL in order to assess its impact, especially on the fetus. Authorities have shown concern that fetuses and babies represent a group greatly endangered by pesticides than adults (Martínez *et al.*, 1993). Evidence of pesticides metabolites and compounds have been detected in placenta, fat and body fluids, umbilical cord blood, fetal organs and subcutaneous fat tissues (Martínez *et al.*, 1993; Waliszewski *et al.*, 2000; Perera *et al.*, 2004; Souza *et al.*, 2005).

The aim of this study, therefore, was to elucidate the interaction of human placental GSTP1-1 with DEL. It was thought that appropriate monitoring of biomarkers changes during antenatal is pivotal in the fight against congenital anomalies and deformities. And the placental GSTP1-1, as one of the most important detoxification enzymes, possesses great potential as a marker protein for monitoring deregulation in redox homeostasis, especially during fetal development. Due to the role of human placental GSTP1-1 in fetal enterohepatic clearance of toxic agents, its interaction with DEL pesticide needs to be studied. This is because in a case where there is an inhibition of this enzyme, aside from other cellular effects, detoxification of reactive electrophiles would not be possible. This, therefore, would result in accumulation and persistence of these electrophilic substrates in the cell, thereby bringing deleterious interactions with essential cellular components such as nucleic acids, lipids, and proteins. This study is hoped to provide findings that would help to reinforce placental GSTP1-1 as an enzyme with good diagnostic value for the identification of safety liabilities reliable during stages of fetal development, with promise for its integration and use as routine clinical biomarkers in health surveillance and monitoring programs for early diagnosis of low-dose pesticides exposure that could be a potential threat particularly to fetus.

### 3. MATERIALS AND METHODS

#### 3.1. Chemicals

Glutathione Transferase P1-1 (GSTP1-1) from Human Placenta has obtained the Sigma-Aldrich United Kingdom. Potassium phosphate (monobasic and dibasic), L-Glutathione reduced and 2-mercaptoethanol (2-ME) were obtained from Sigma-Aldrich Japan. Ethylenediaminetetraacetic acid (EDTA) purchased from AppliChem Germany. Ethanol was obtained from Riedel-de Haen Germany. Ammonium persulfate, Formaldehyde Trizma base, glycine, 1-chloro-2,4-dinitrobenzene (CDNB), sodium thiosulfate, silver nitrate, and bromophenol blue was obtained from Sigma, St. Louis, MO, USA. Coomassie Brilliant Blue R-250 from Fluka Analytical United Kingdom. Acrylamide, N,N,N',N'-tetramethylethylenediamine (TEMED), N,N'-methylene bisacrylamide and were obtained from Sigma China. Acetic acid, sodium azide, sodium carbonate and glycerol were obtained from Sigma Germany. Methanol was obtained from Sigma France. Roti-mark standard was purchased from Carl Roth GmbH Germany. Deltamethrin (DEL) was obtained from Agrobrest Grup Izmir Turkey.

#### 3.2. Methods

##### 3.2.1 Enzyme Preparation

The *hp*GSTP1-1 enzyme was prepared by dissolving 1 mg (48 U mg<sup>-1</sup> solid) in 1 mL of 100 mM potassium phosphate buffer, pH 6.5, containing 1 mM EDTA. This was aliquot and kept in -20 °C.

##### 3.2.2. Native-Polyacrylamide Gel Electrophoresis (Native-PAGE) and Sodium Dodecyl Sulfate-polyacrylamide Gel Electrophoresis (SDS-PAGE)

The Purity and relative molecular mass ( $M_r$ ) of the *hp*GSTP1-1 were determined by discontinuous native-PAGE and SDS-PAGE (Laemmli, 1970). Coomassie Brilliant Blue (CBB) R-250 and silver staining methods were performed to visualize protein bands (Blum *et al.*, 1987; Hames, 1998). In the native PAGE, the gel concentrations for separating and stacking were 7 and 4 percent, respectively. In SDS-PAGE, the separating gel concentration increased to 15% while

the stacking gel concentration retained as 4 percent. Native and SDS-PAGE gels were stained with both staining methods; CBB and silver staining (Blum *et al.*, 1987; Hames, 1998).

All reagents prepared were according to Laemmli protocol (Laemmli, 1970) with slight modifications. The acrylamide solution prepared was 30%, containing 29.4 g acrylamide and 0.6 g N,N'-methylene-bis-acrylamide dissolved in 100 mL of distilled water. The solution was then filtered using 0.45  $\mu\text{m}$  pore size filter and kept at +4 °C in the dark.

The separator gel buffer was made up of 1.5 M Tris/HCl, pH 8.8. In the preparation, Tris base (27.23 g) was dissolved in 80 mL of distilled water and its pH was adjusted to 8.8 using 12 M HCl. Its volume was then made up to 150 mL with the distilled water and stored at +4 °C.

The stacking gel buffer contained 0.5 M Tris/HCl, pH 6.8. In the preparation, 6 g of Tris base was dissolved in 60 mL distilled water and its pH was adjusted to 6.8 using 12 M HCl. Its volume was made up to 100 mL with distilled water and stored at +4 °C.

Five times concentrated (5x) electrode (running) buffer was prepared. Tris base (15 g) and glycine (72 g) was dissolved in 1 liter of distilled water and its pH was adjusted to 8.3 using 12 M HCl. The stock solution was diluted five times with distilled water before use. The same buffer was used for SDS-PAGE, but in that, 1 g of sodium dodecyl sulfate (SDS) per liter of the diluted buffer was added. To prevent bacterial growth 0.02% sodium azide ( $\text{NaN}_3$ ) was added to the stock buffer and this made possible to use the same electrode buffer 4-5 times.

Sample preparation buffer for native-PAGE was prepared by mixing 2 mL of 0.5 M Tris/HCl pH 6.8, 1.6 mL glycerol, 0.4 mL bromophenol blue (from 0.05% stock prepared in distilled water), 0.8 mL 2-mercaptoethanol (2-ME) from stock and the total volume was made up to 10 mL with distilled water. Due to the high viscosity of glycerol, it was not pipette, it was weighed. The weight was calculated by multiplying volume with its density. In the sample preparation for SDS-PAGE, all the components were the same as in the native-PAGE preparation buffer except 1 mL of 10% SDS was added to the solution so that the final concentration of the SDS in the solution was 1%. The 10% SDS was prepared by dissolving 10 g SDS in 100 mL distilled water and was filtered using 0.45  $\mu\text{m}$  pore size filter and then stored at +20 °C.

The Ammonium persulfate (10%) solution was prepared by dissolving 100 mg in 1 mL distilled water. The solution was daily prepared fresh.

**Table 3.1.** The volumes used in the preparation of the gel for native-PAGE

<b>Components</b>	<b>Separator Gel (7%)</b>	<b>Stacking gel (4%)</b>
30% Acrylamide/Bisacrylamide	2.335 mL	1.3 mL
1.5 M Tris/HCl, pH 8.8	2.5 mL	-
0.5 M Tris/HCl, pH 6.8	-	2.5 mL
Distilled Water	5.115 mL	6.14 mL
10% APS	0.050 mL	0.050 mL
TEMED	0.005 mL	0.01 mL
Total	10.005 mL	10.000 mL

**Table 3.2.** The volumes used in the preparation of the gel for SDS-PAGE

<b>Components</b>	<b>Separator Gel (15%)</b>	<b>Stacking gel (4%)</b>
30% Acrylamide/Bisacrylamide	5 mL	1.3 mL
1.5 M Tris/HCl, pH 8.8	2.5 mL	-
0.5 M Tris/HCl, pH 6.8	-	2.5 mL
Distilled Water	2.35 mL	6.04 mL
10% SDS	0.10 mL	0.10 mL
10% APS	0.050 mL	0.05 mL
TEMED	0.005 mL	0.01 mL
Total	10.005 mL	10.000 mL

### 3.2.3. Casting of Gels for Native-PAGE and SDS-PAGE

Using the casting stand, the spacer (1.5 mm) and the plain glasses were placed and clamped vertically. About 1-2 mL of distilled water was poured into the glass and allowed for some minutes to ensure no leaking was experienced when the gel would be loaded. The water was then drained using a long specialized tissue paper. The next thing was loading of the separator gel mixture (**Tables 3.1** and **3.2**). After pouring the acrylamide mixture between the glasses, immediately distilled water was layered on top of the gel in order to smooth the surface at the gel top. The gel was allowed for 1 hour to polymerize. After the time elapsed, the excess water was drained using tissue paper and the stacking gel was cast on top of the separator gel. A 10-well comb was immediately placed in the stacking gel and allowed for 1 hour 30 minutes for complete polymerization. The glasses carrying the gels were carefully removed from the casting stand and placed in the electrophoresis assembly and transferred into the electrophoresis tank. The tank was filled with electrode (running) buffer and the 10-well combs removed. Each well was washed with the running buffer before the sample was loaded.

### 3.2.4. Sample Preparation for Native and SDS-PAGE

In accordance with the staining method, two different sample preparations were employed. The sample preparation buffer (SPB) was added to a portion of the stock enzyme ( $2 \text{ mg mL}^{-1}$ ) so that the final enzyme concentration in each well was adjusted to 2, 3, 4, 5, and 6  $\mu\text{g}$  for CBB staining, and 0.4, 0.6, 0.8, 1, and 1.2  $\mu\text{g}$  for silver staining, in native-PAGE. For the SDS-PAGE, the protein concentrations were 2, 4, and 8  $\mu\text{g}$  for CBB staining and 0.4, 0.8 and 1.6  $\mu\text{g}$  and for silver staining.

#### 3.2.4.1. Sample Preparation for CBB Staining (Native-PAGE)

- 2  $\mu\text{L}$  stock enzyme + 8  $\mu\text{L}$  0.1 M Tris/HCl, pH 6.8 +10  $\mu\text{L}$  of SPB
- 3  $\mu\text{L}$  stock enzyme + 7  $\mu\text{L}$  0.1 M Tris/HCl, pH 6.8 +10  $\mu\text{L}$  of SPB
- 4  $\mu\text{L}$  stock enzyme + 6  $\mu\text{L}$  0.1 M Tris/HCl, pH 6.8 +10  $\mu\text{L}$  of SPB
- 5  $\mu\text{L}$  stock enzyme + 5  $\mu\text{L}$  0.1 M Tris/HCl, pH 6.8 +10  $\mu\text{L}$  of SPB

In each case, 10  $\mu\text{L}$  of the sample was loaded into the wells.

#### **3.2.4.2. Sample Preparation for Silver Staining (Native-PAGE)**

From the remaining sample after loading 10  $\mu\text{L}$  in the CBB staining (native-PAGE) above, 2  $\mu\text{L}$  was pipette and loaded into the wells for silver staining. Thus, the final concentrations of the protein in the wells, for silver staining were 0.4, 0.6, 0.8, and 1  $\mu\text{g}$ .

#### **3.2.4.3. Sample Preparation for CBB Staining (SDS-PAGE)**

- 2  $\mu\text{L}$  stock enzyme + 7  $\mu\text{L}$  0.1 M Tris/HCl, pH 6.8 + 1  $\mu\text{L}$  10% SDS + 10  $\mu\text{L}$  SPB
- 4  $\mu\text{L}$  stock enzyme + 7  $\mu\text{L}$  0.1 M Tris/HCl, pH 6.8 + 1  $\mu\text{L}$  10% SDS + 10  $\mu\text{L}$  SPB
- 8  $\mu\text{L}$  stock enzyme + 6  $\mu\text{L}$  0.1 M Tris/HCl, pH 6.8 + 1  $\mu\text{L}$  10% SDS + 10  $\mu\text{L}$  SPB

Before the sample preparation buffer was added, the samples (containing enzyme stock, 0.1 M Tris/HCl, pH 6.8 and 10% SDS) were incubated at 95  $^{\circ}\text{C}$  for 5 min and cooled to room temperature. Roti-mark protein molecular weight marker was used as a standard.

#### **3.2.4.4. Sample Preparation for Silver Staining (SDS-PAGE)**

From the remaining sample left after loading 10  $\mu\text{L}$  in the CBB staining (SDS-PAGE) above, 2  $\mu\text{L}$  was pipette and loaded into the wells for silver staining. Thus, the final concentrations of the protein in the wells, for silver staining were 0.4, 0.6, 0.8, and 1  $\mu\text{g}$ .

#### **3.2.5. Performing the Electrophoresis**

Bio-Rad Miniprotein Tetra Cell electrophoresis system was used in performing the electrophoresis. First, the electrophoresis was initiated with 120 V so that the sample migrated gradually and concentrated at the top of the separator gel. Then, the voltage was increased to 150 V or 200 V. The electrophoresis was stopped when the bromophenol blue dye reached about 1 cm to the end of the gel. The gels were transferred into Petri dishes for staining processes.

### 3.2.6. Coomassie Brilliant Blue (CBB) Staining and Destaining

CBB staining was carried out to visualize the protein bands on the gel after the native- and SDS-PAGE was completed. The CBB staining solution contained 0.1% Coomassie Brilliant Blue R-250, 40% methanol and 10% acetic acid. After native- and SDS-PAGE, gels were incubated in staining solution for 30 minutes and then transferred into destaining solution. The destaining solution was made up of 40% methanol and 10% acetic acid and was replaced about every 30 minutes until the background was clear and the protein bands became visible. The gels were kept at 4 °C in 5% acetic acid.

### 3.2.7. Silver Staining

Silver staining was carried out, with just some slight modifications, in the method described by Blum *et al.*, (Blum *et al.*, 1987). First, the gels were fixed with 50% methanol, 12% glacial acetic acid and 0.005% formalin solution for 2 hours. The fixation solution was thrown away and the gels were washed three times with 50% ethanol for 20 minutes. Then the gels were sensitized with 0.02% sodium thiosulfate ( $\text{Na}_2\text{S}_2\text{O}_3$ ) for 2 minutes and then washed with distilled water three times for 20 seconds. The gels were stained with a solution containing 0.2% silver nitrate ( $\text{AgNO}_3$ ) and 0.076% formalin for 20 minutes. After staining, the gels were washed twice with distilled water for 20 seconds. Then the gels were impregnated with sodium carbonate ( $\text{Na}_2\text{CO}_3$ ), 0.05 formalin and 0.0004% sodium thiosulfate solution until the bands were visible. When the bands were clearly seen, the gels were washed with distilled water twice for 2 minutes and the staining was finalized by the addition of solution for 20 minutes of a stop solution containing 40% methanol, 10% glacial acetic acid. The gels were kept at +4 °C in 1% glacial acetic acid solution after the completion of the staining procedure.

### 3.2.8. Reaction Mixture for the *hpGSTP1-1* kinetics

The reaction mixture (total volume 500  $\mu\text{L}$ ) consisted of 100 mM potassium phosphate buffer, pH 6.5, 1 mM EDTA, 1 mM CDNB, 1 mM GSH, and the appropriate amount of the *hpGSTP1-1* enzyme (Dalmizrak *et al.*, 2016). CDNB was dissolved in ethanol and GSH was dissolved in

distilled water. In all the experiments, the enzyme ( $1 \text{ mg mL}^{-1}$  or  $48 \text{ U mg}^{-1}$  solid) was diluted five times with  $100 \text{ mM}$  potassium phosphate buffer, pH 6.5, containing  $1 \text{ mM}$  EDTA, before use.

### 3.2.9. Determination of the *hp*GSTP1-1 Enzyme Activity

The activity of *hp*GSTP1-1 was assayed according to the method of Habig and Jakoby (Habig and Jakoby, 1981) with slight modifications using a Perkin Elmer LAMBDA 25 UV/VIS Spectrophotometer. The activity of *hp*GSTP1-1 was determined by following the increase in absorbance due to the conjugation of the natural substrate L-glutathione reduced (GSH) to artificial substrate CDNB at  $340 \text{ nm}$  for 20 seconds (Habig and Jakoby, 1981; Wilce and Parker, 1994). The conjugation is shown below:



The *hp*GSTP1-1 enzyme catalyzes the conjugation of GSH to CDNB via the thiol group of the GSH. The rate increase in absorption by GS-DNB Conjugate (the product of the reaction) is directly proportional to the GST activity (Habig and Jakoby, 1981; Wilce and Parker, 1994). The initiation of the reaction was done by the addition of CDNB which is suitable for the broadest range of GST isozymes (Dalmizrak *et al.*, 2016). A non-enzymatic reaction was run, containing the mixture all constituents of the reaction mixture above excluding the *hp*GSTP1-1 enzyme. The value obtained by the non-enzymatic reaction was deducted from the value for the enzymatic reaction. All measurements were taken at  $37 \text{ }^\circ\text{C}$  and in triplicates.

Average activity ( $\text{U mL}^{-1}$ ) values were converted to as specific activity ( $\text{U mg}^{-1}$  protein) and were used to depict Michaelis-Menten, Lineweaver-Burk and other plots (Segel 1975). One unit of the *hp*GSTP1-1 activity was defined as the amount of the enzyme that catalyzes the formation of  $1 \text{ } \mu\text{mol}$  of product per minute at pH 6.5 and  $37^\circ\text{C}$ . The Formula used for the calculation of the enzyme activity is shown below.

Specific Activity ( $\text{U mg}^{-1}$  protein):

$$\frac{\Delta\text{Abs}_{340}/\text{min} \times V_t}{9.6 \times V_s \times [\text{protein}]}$$

Where,

$\Delta\text{Abs}_{340}/\text{min}$  = Absorbance change per minute at 340 nm

$V_t$  = Total volume of the reaction mixture (500  $\mu\text{L}$ )

$V_s$  = Sample volume ( $\mu\text{L}$ ) used to measure enzyme activity

9.6 = Extinction coefficient of GS-DNB conjugate

### 3.2.10 Determination of Optimum pH

The optimum pH of *hpGSTP1-1* was determined using seven selected pH values (ranging from 5.0-8.0) for the experiment. Potassium phosphate buffer (200 mM, with 2 mM EDTA) was prepared, and pH was adjusted to 5.0, 5.5, 6.0, 6.5, 7.0, 7.5 and 8.0. Enzyme activity for each pH was measured in triplicates at 340 nm for 20 seconds at 37 °C. The change in absorbance ( $\Delta A \text{ min}^{-1}$ ) was taken as a measure of the enzyme activity in each case and was converted to a specific activity, ( $\text{U mg}^{-1}$  Protein). The specific activity ( $\text{U mg}^{-1}$  Protein) versus pH graph was plotted.

### 3.2.11. Determination of Optimum Temperature

The determination of the optimum temperature of *hpGSTP1-1* was done by measuring the enzyme activity at a different temperature. First, the reaction mixture was incubated at different temperatures (20, 25, 30, 35, 40, and 45 °C). In each case, measurement was taken in triplicate and the specific activity ( $\text{U mg}^{-1}$  protein) was calculated. A graph of the specific activity ( $\text{U mg}^{-1}$  protein) against temperature (°C) was plotted and the optimum temperature was determined from

the graph. The same data was used to plot  $1/\text{specific activity}$  versus  $1/T$  in degrees Kelvin was plotted to calculate activation energy,  $E_a$ , and temperature coefficient,  $Q_{10}$ .

### 3.2.12. Effect of DEL on *hp*GSTP1-1 and the Determination of $IC_{50}$

The inhibition of *hp*GSTP1-1 was measured by the addition of the reaction mixture above at a different concentration of DEL (ranging from 0.5  $\mu\text{M}$  to 15  $\mu\text{M}$ ). DEL was dissolved in absolute ethanol. The data were obtained in triplicates for each DEL concentration. The percentage (%) remaining activity was plotted against the concentration of DEL to determine the  $IC_{50}$  value (Segel, 1975).

### 3.2.13. Confirmation of the reversible inhibition of *hp*GSTP1-1 by DEL

The activities of six selected concentrations of *hp*GSTP1-1 (0.2, 0.4, 0.8, 1.6, 3.2, 4.8  $\mu\text{g mL}^{-1}$ ) were measured in the presence and absence of 6  $\mu\text{M}$  DEL. The reaction mixture (total volume 500  $\mu\text{L}$ ) contained 100 mM potassium phosphate buffer (pH 6.8), 1 mM EDTA, 1 mM CDNB, 1 mM GSH, 6  $\mu\text{M}$  DEL and the appropriate enzyme. The data obtained were measured in triplicates for each enzyme concentration. The enzyme activity ( $\text{U mL}^{-1}$ ) was plotted against the different enzyme concentrations ( $\mu\text{g mL}^{-1}$ ).

### 3.2.14. Inhibitory Kinetic Experiments with DEL

Inhibitory kinetic studies were conducted in the absence and presence of DEL. Appropriate amounts of DEL dissolved in absolute ethanol were added to the reaction mixture and incubated, bringing the different inhibitor concentrations to 0.0 (control), 0.5, 1.0, 2.0, 4.0 and 8.0  $\mu\text{M}$  in the reaction mixture. The final concentration of ethanol was always kept at 7% (v/v) both in the reaction mixture and controls. Here, the reaction mixture consisted of 100 mM potassium phosphate buffer (pH 6.5) with 1 mM EDTA, different concentrations of DEL (mentioned above), 1 mM  $[\text{CDNB}]_f - [\text{GSH}]_v$ , or 1 mM  $[\text{GSH}]_f - [\text{CDNB}]_v$ . The concentration of the varied GSH and CDNB were 0.1, 0.2, 0.4, 0.8 and 1.6 mM in the reaction mixture in each case. The remaining volume was made up with distilled water. The increase in the absorbance due to the

formation of the GS-DNB conjugate was followed at 340 nm for 20 seconds. The data obtained with and without DEL were calculated and evaluated with different kinetic models (Segel, 1975).

### **3.2.15. Statistical Analysis**

STATISTICA '99 for Windows (StatSoft, Tulsa, OK) was used in addition to different kinetic models (Segel, 1975) for the evaluation of the data obtained, calculations of kinetic parameters and estimation of the inhibition type.

### **3.2.16. Molecular Docking of the GSTP1-1 Enzyme Inhibitor, DEL**

The molecular docking was used for evaluating the interaction of DEL with the GSTP1-1 enzyme to find the best geometrical arrangement or preferred orientation and predict the strength of association or binding affinity between the enzyme and inhibitor. The crystal structure of dimeric GSTP1-1 complexed with 1-(S-glutathionyl)-2,4-dinitrobenzene (GS-DNB) and 2-(N-morpholino)-ethane sulfonic acid (MES) at a resolution of 1.9 Å was downloaded from the Protein Data Bank (PDB ID: 18GS). Water molecules and MES molecules were deleted from the crystal structure to prepare the structure for docking using a Molecular graphics and visualization System, PyMOL Version 1.8.6.2 (Schrödinger, LLC, Portland, OR, USA). Predicted, ready-to-dock three-dimensional structure of DEL was generated by a docking algorithm (CORINA Classic, version 4.0) using the 'canonical SMILES' obtained from PubChem (a database for chemical molecules). A Structure-Complementarity Base molecular docking algorithm, PatchDock Version Beta 1.3 was used to conduct a blind docking (Duhovny *et al.*, 2002; Duhovny *et al.*, 2005) with receptor and ligand molecules inputs in PDB file format. In the docking input form, the set complex type was enzyme–inhibitor and the clustering RMSD was 1.5 Å. According to the geometric score rank, the best one hundred docking solutions were downloaded and viewed in the UCSF Chimera, a Molecular Graphics System version 1.11.2 (Pettersen *et al.*, 2004).

## 4. RESULTS

### 4.1. Characterization of Human Placental Glutathione Transferase P1-1 (*hpGSTP1-1*)

The *hpGSTP1-1* purity and relative molecular mass ( $M_r$ ) were determined by discontinuous native and SDS-PAGE. CBB R-250 staining and silver staining was performed to view the protein bands. The visualization of single protein bands on native polyacrylamide gels (either CBB-stained or silver-stained) confirmed the purity of the enzyme (**Figure 4.1A** and **4.1B**).

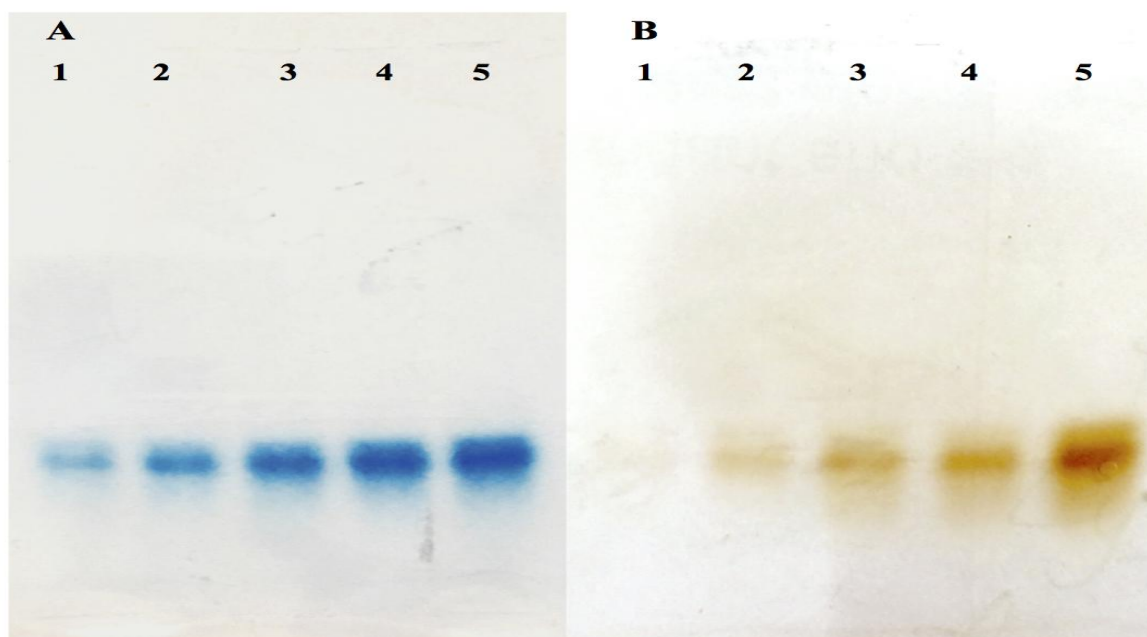


**Figure 4.1.** *hpGSTP1-1* on discontinuous native polyacrylamide gels. Separator gel was 7% and the stacking gel 4%. **A.** CBB R-250 staining. Protein concentration: Lane #1, 2 $\mu$ g; Lane #2, 3 $\mu$ g; Lane #3, 4 $\mu$ g; Lane #4, 5 $\mu$ g; and Lane #5, 6 $\mu$ g. **B.** Silver staining. Protein concentration: Lane #1, 0.4 $\mu$ g; Lane #2, 0.6 $\mu$ g; Lane #3, 0.8 $\mu$ g; Lane #4, 1 $\mu$ g; and Lane #5, 1.2 $\mu$ g.

The molecular mass of the subunit of *hpGSTP1-1* was determined by SDS-PAGE. After staining the gels with both CBB (not shown) and silver staining (**Figure 4.2A**), the protein bands were identified and the relative molecular mass ( $M_r$ ) was calculated to be 21,380 Da from the graph plotted using the logarithm of  $M_r$  versus the relative migration distance ( $R_F$ ) (**Figure 4.2B**).  $R_F$  was obtained by dividing protein migration distance by bromophenol blue migration distance (**Figure 4.2A and 4.2B**).

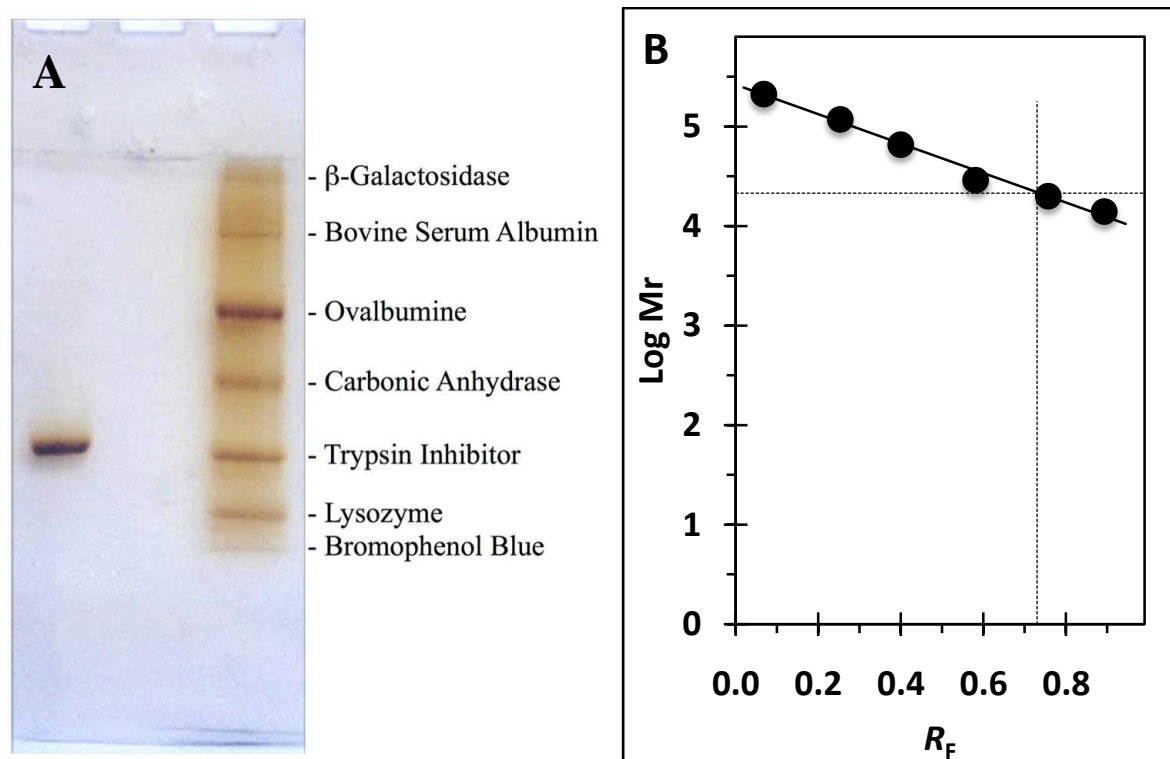


**Figure 4.2.** Determination of the relative molecular mass of *hpGSTP1-1*. **A.** *hpGSTP1-1* on discontinuous SDS-PAGE, Silver staining. The separator gel was 15% and stacking gel 4%. The concentration of the *hpGSTP1-1* in the well was 8 $\mu$ g. Amount Loaded into the well for the Protein marker was 10  $\mu$ L. The proteins and corresponding  $M_r$  are 212 kDa: myosin; 118k Da:  $\beta$ -galactosidase; 66 kDa: serumalbumin; 43 kDa: ovalbumin; 29 kDa: carbonic anhydrase; 20 kDa: trypsin inhibitor; and 14 kDa: lysozyme. **B.** The logarithm of relative molecular mass ( $M_r$ ) vs the relative migration distance of the protein divided by the relative migration distance of bromophenol blue ( $R_F$ ) plot.

#### 4.2. Determination of Optimum pH

The pH values (ranging from 5.0 to 8.0), were experimented to find the optimum pH of *hpGSTP1-1*. Potassium phosphate buffer (200 mM, with 2 mM EDTA) was prepared, and pH was adjusted to 5.0, 5.5, 6.0, 6.5, 7.0, 7.5, or 8.0. Enzyme activity at each pH value was measured in triplicates at 340 nm for 20 s at 37 °C. The change in absorbance ( $\Delta A_{\text{min}}^{-1}$ ) was taken as a measure of the enzyme activity in each case and was converted to a specific activity, ( $\text{U mg}^{-1}$  protein). The specific activity was plotted against pH. Accordingly, the optimum pH value for *hpGSTP1-1* was found to be 6.62 (**Figure 4.3**).

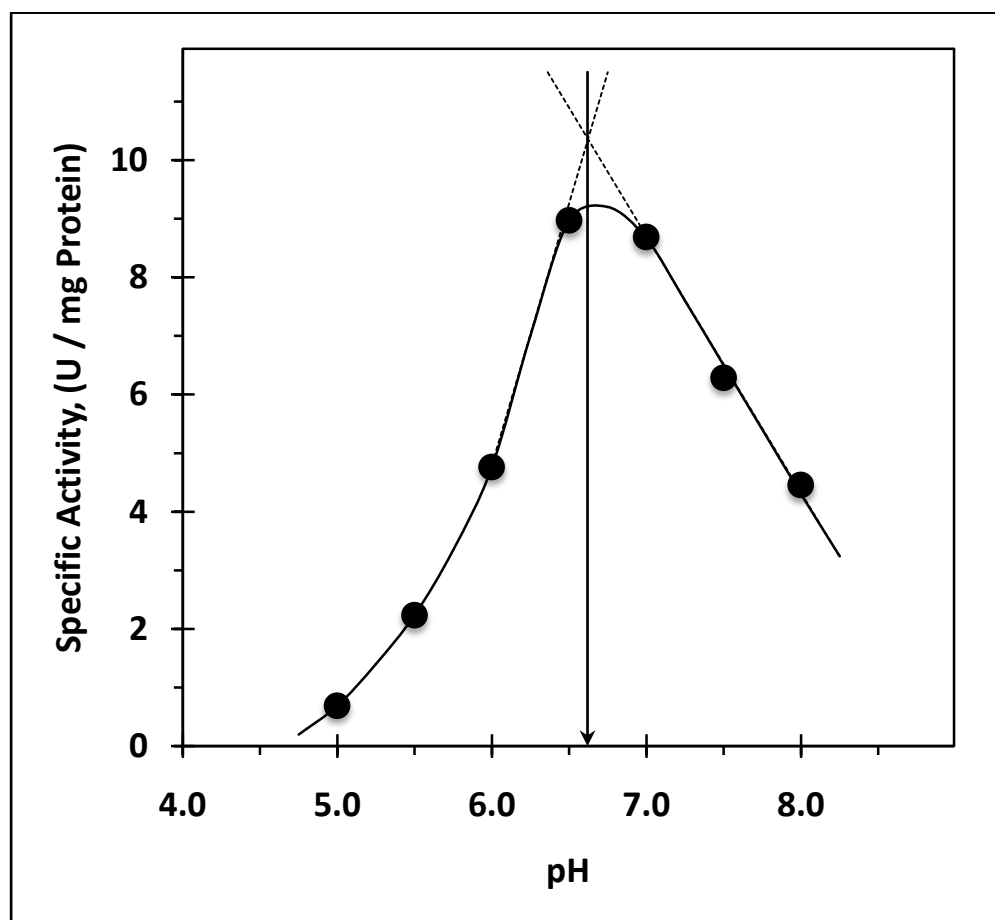


**Figure 4.3.** Specific activity ( $\text{U mg}^{-1}$  protein) vs. pH plot

### 4.3. Determination of Optimum Temperature

The optimum temperature of the *hpGSTP1-1* enzyme was determined by incubating the reaction mixture at different temperatures (20 °C, 25 °C, 30 °C, 35 °C, 40 °C, and 45 °C). In each case, measurements were taken in triplicates, and the specific activity was calculated. A graph of the specific activity against temperature was plotted (**Figure 4.4A**), and the optimum temperature was determined to be 35.4 °C (Segel, 1975).

For the activation energy ( $E_a$ ), it was determined by plotting the logarithms of specific activity versus the inverse of the temperature in degrees Kelvin (**Figure 4.4.B**) (Segel, 1975). The  $E_a$  and the temperature coefficient ( $Q_{10}$ ) were calculated to be 7,623 cal mol<sup>-1</sup> and 1.52, respectively, as shown below (Segel, 1975).

$$-\text{Slope} = -E_a/2.3R$$

$$E_a = 2.3RT_1T_2 \log Q_{10}/10$$

$E_a$ : activation energy

R: gas constant

$Q_{10}$ : temperature coefficient

$T_1$  and  $T_2$ : temperatures in Kelvin

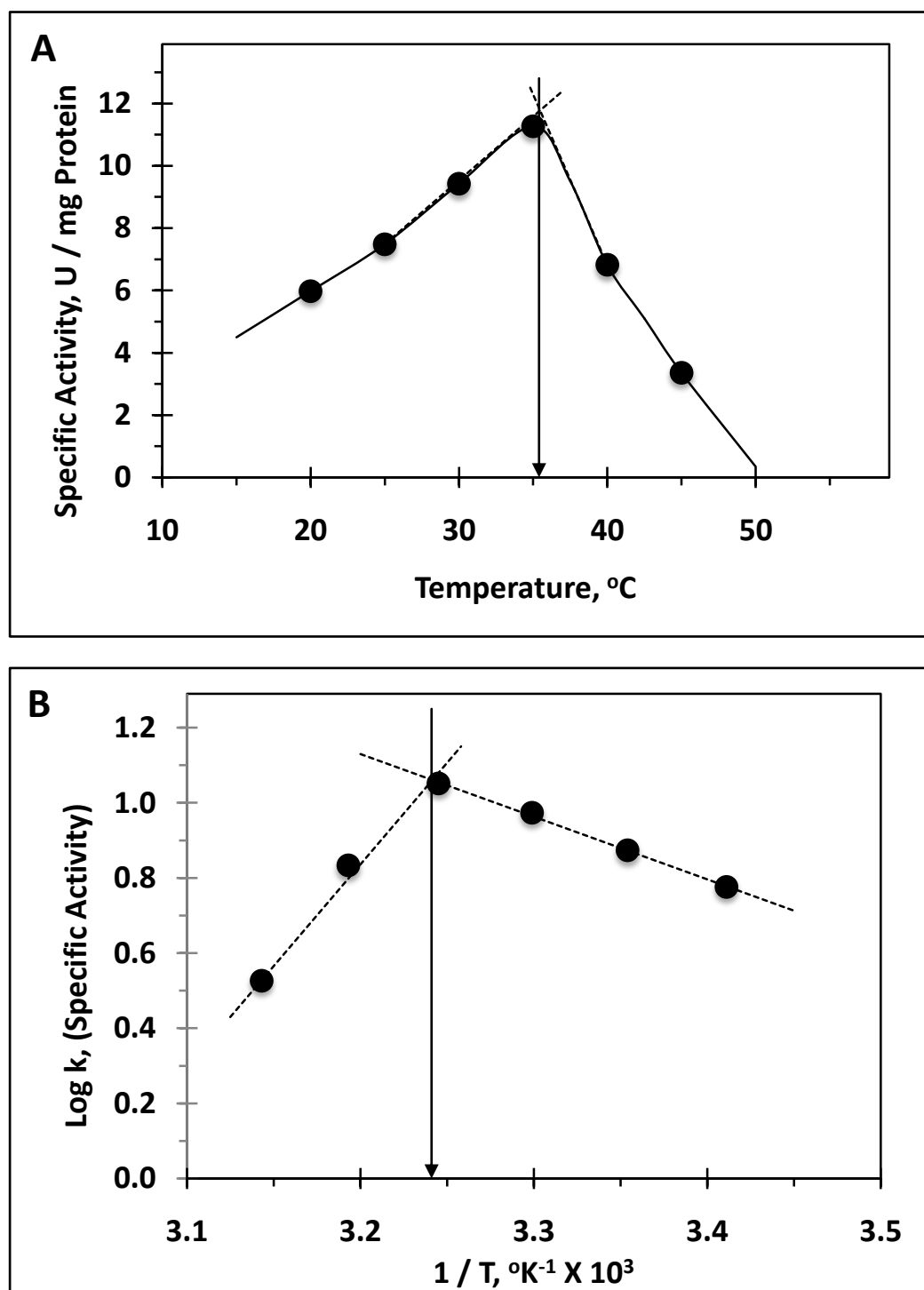


**Figure 4.4.** Plots for temperature optimum, the energy of activation and temperature coefficient. **A.** Specific activity ( $\text{U mg}^{-1}$  protein) vs. temperature ( $^{\circ}\text{C}$ ). **B.** The logarithm of specific activity ( $\text{U mg}^{-1}$  protein) vs.  $1/T$  plot.

#### 4.4. Inhibitory Kinetic Interaction of *hp*GSTP1-1 with DEL

The effect of DEL on *hp*GSTP1-1 was studied by the addition, to the reaction mixture different concentration of DEL (ranging from 0.5  $\mu\text{M}$  to 15  $\mu\text{M}$ ). The reaction mixture (500  $\mu\text{L}$  total volume) was made up of 100 mM potassium phosphate buffer with 1 mM EDTA, pH 6.5, 1 mM CDNB, 1 mM GSH, deionized  $\text{H}_2\text{O}$  and appropriate *hp*GSTP1-1 enzyme. The data were obtained in triplicates for each DEL concentration. The specific activity ( $\text{U mg}^{-1}$  protein) was plotted against concentrations of DEL which  $IC_{50}$  value was determined to be 6.2  $\mu\text{M}$  (**Figure 4.6.A**). The same value was obtained from the inhibitory Hill plot (**Figure 4.6.B**). The activities of six selected concentrations of *hp*GSTP1-1 (0.2, 0.4, 0.8, 1.6, 3.2, 4.8  $\mu\text{g mL}^{-1}$ ) were measured in the presence and absence of 6  $\mu\text{M}$  DEL to confirm the reversible inhibition of *hp*GSTP1-1 by DEL. In the plot of activity ( $\text{U mL}^{-1}$ ) versus the enzyme concentration ( $\mu\text{g mL}^{-1}$ ), the inhibition of *hp*GSTP1-1 by DEL was confirmed to be reversible (**Figure 4.5**). As shown, the graph lines representing the control and noncompetitive inhibition pass through the origin, but the lines have different slopes (**Figure 4.5**).

In the inhibitory kinetic studies, five selected concentrations of DEL (0.5, 1.0, 2.0, 4.0 and 8.0  $\mu\text{M}$ ) were used. The inhibitory kinetic studies were conducted to determine  $K_m$  and  $V_m$  in the absence and presence of DEL. In the experiments, the reaction mixture comprised of 100 mM potassium phosphate buffer (pH 6.5) with 1 mM EDTA, the different concentrations of DEL, 1 mM  $[\text{CDNB}]_f\text{--}[\text{GSH}]_v$  or 1 mM  $[\text{GSH}]_f\text{--}[\text{CDNB}]_v$ , deionized  $\text{H}_2\text{O}$  and appropriated enzyme. The concentration of the varied GSH and CDNB were 0.1, 0.2, 0.4, 0.8 and 1.6 mM in the reaction mixture in each case. The increase in the absorbance due to the formation of the GS-DNB complex at 340 nm was followed for 20 seconds. The data obtained were evaluated using STATISTICA '99 for Windows to obtain different kinetic parameters and they were also used to depict different plots such as Michaelis–Menten (**Figures 4.7 and 4.10**), Lineweaver–Burk (**Figures 4.8 and 4.11**) and secondary plots (**Figures 4.9 and 4.12**). The  $V_m$  at  $[\text{CDNB}]_f\text{--}[\text{GSH}]_v$ , and  $[\text{GSH}]_f\text{--}[\text{CDNB}]_v$  were  $10.4 \pm 0.22$  and  $8.7 \pm 0.33$   $\text{U mg}^{-1}$  protein, respectively. On the other hand, the  $K_m$  at  $[\text{CDNB}]_f\text{--}[\text{GSH}]_v$ , and  $[\text{GSH}]_f\text{--}[\text{CDNB}]_v$  were and  $0.31 \pm 0.02$  and  $0.30 \pm 0.03$  mM, respectively. The inhibition types with respect to both substrates were non-competitive with the  $K_i$  values of  $5.61 \pm 0.32$  and  $7.96 \pm 0.97$   $\mu\text{M}$ , respectively (**Figures 4.8, 4.9, 4.11, and 4.12**).

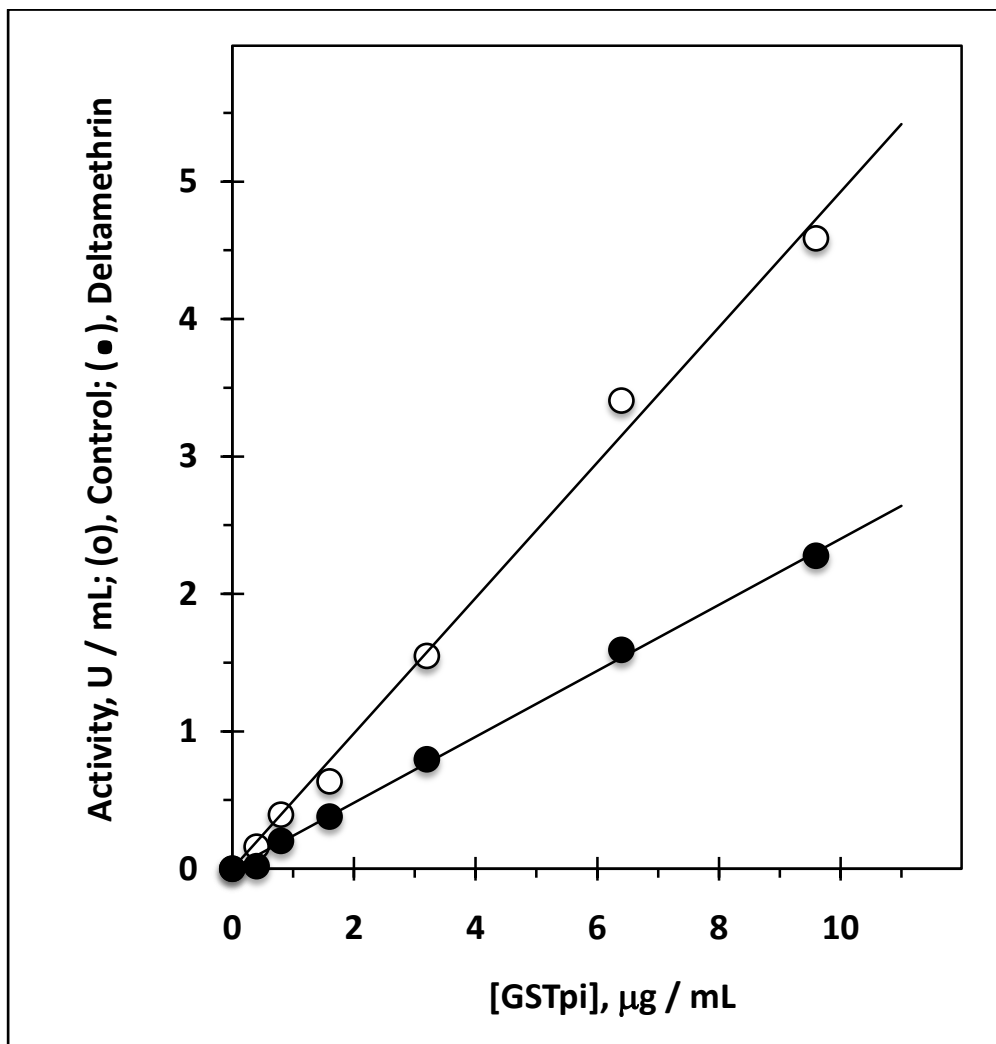
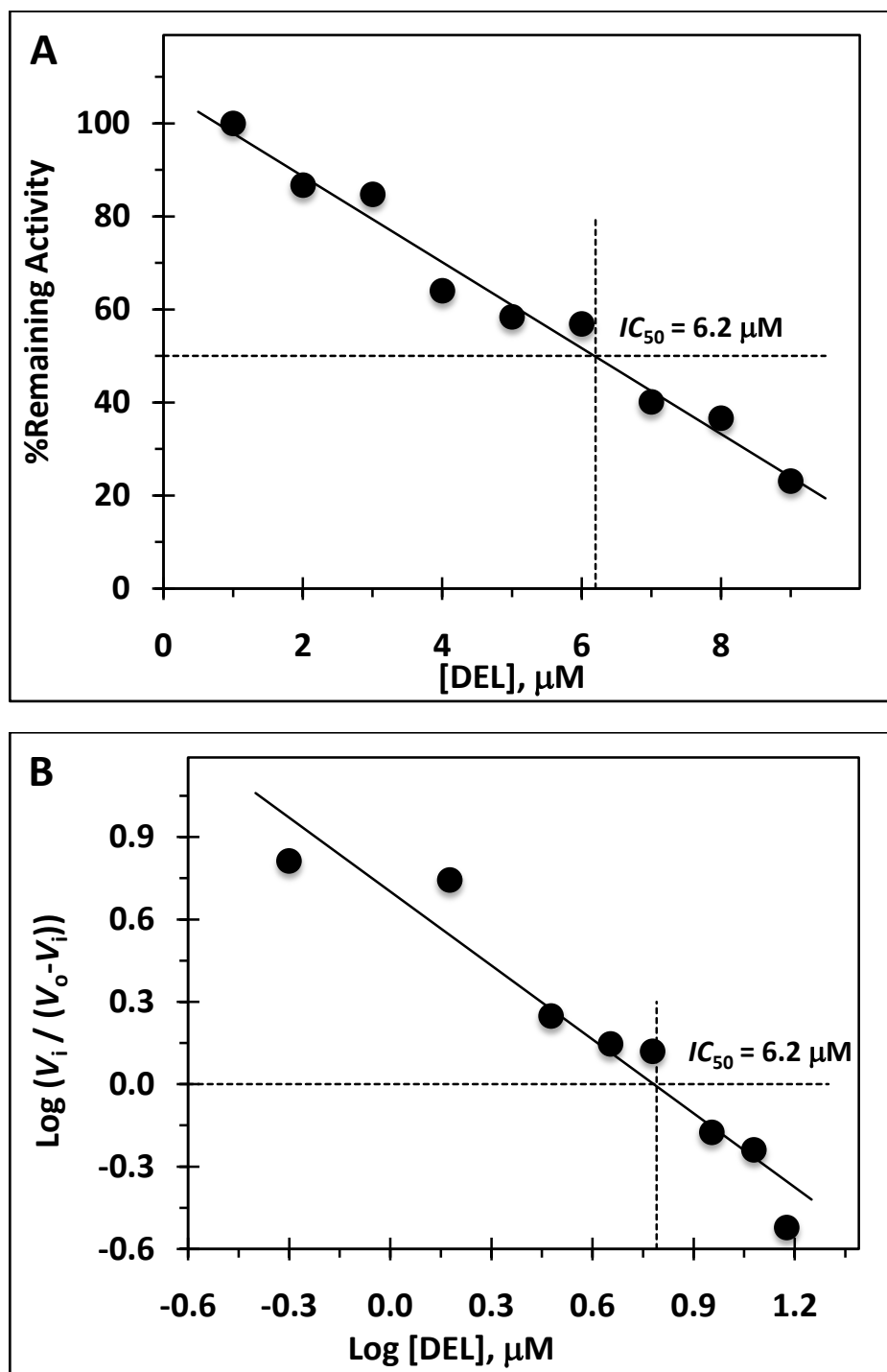
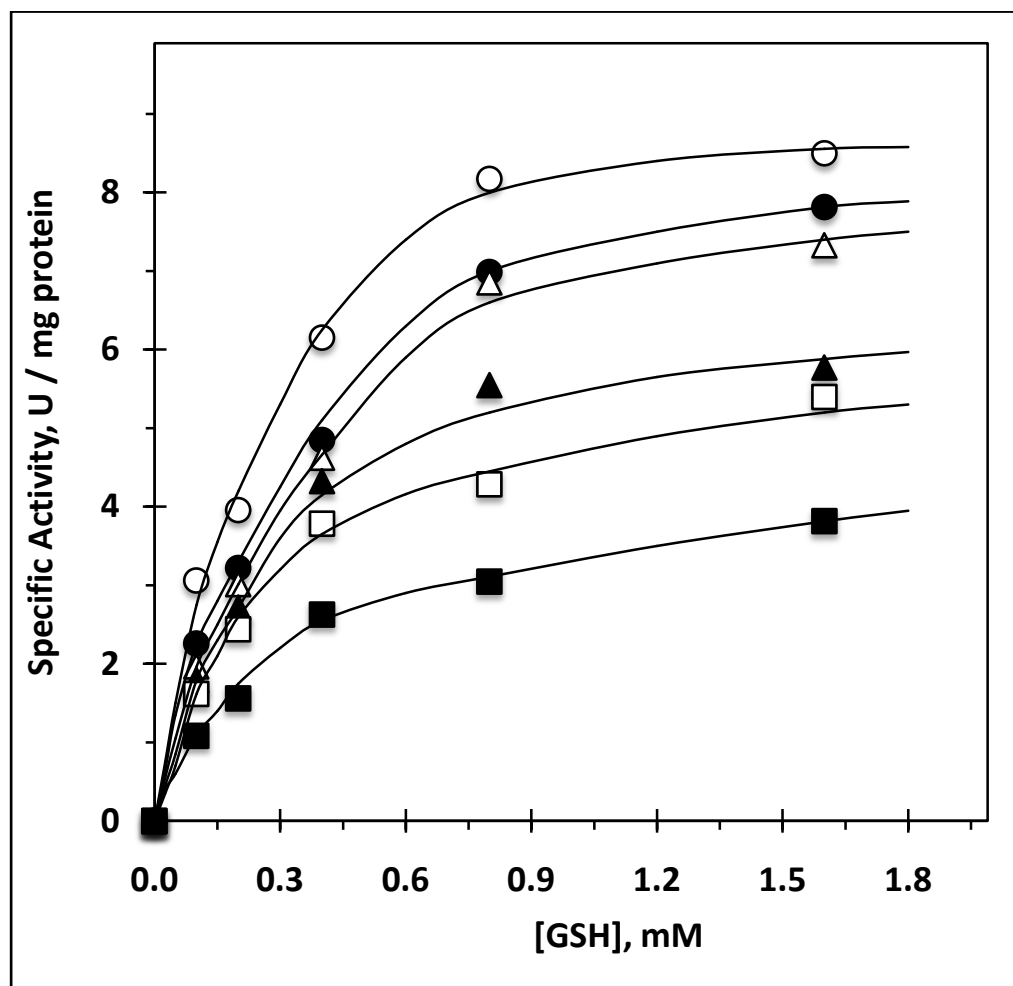


Figure 4.5. Confirmation of the reversibility of hpGSTP1-1inhibition by DEL



**Figure 4.6.** Inhibition of *hpGSTP1-1* by DEL. **A.** Dose-dependent inhibition of *hpGSTP1-1* by DEL; % remaining activity versus [DEL]. **B.** Inhibitory Hill plot of DEL.  $[CDNB]_f = 1 \text{ mM}$ ;  $[GSH]_f = 1 \text{ mM}$ ;  $[DEL] = 0.5, 1.5, 3, 4.5, 6, 9, 12$  and  $15 \text{ } \mu\text{M}$ .



**Figure 4.7.** Michaelis–Menten plot for *hpGSTP1-1* enzyme with different concentrations of DEL at 1 mM [CDNB]<sub>f</sub> and [GSH]<sub>v</sub>: 0.1, 0.2, 0.4, 0.8 and 1.6 mM. [DEL]: (○), 0; (●), 0.5; (△), 1; (▲), 2; (□), 4; (■), 8 μM.

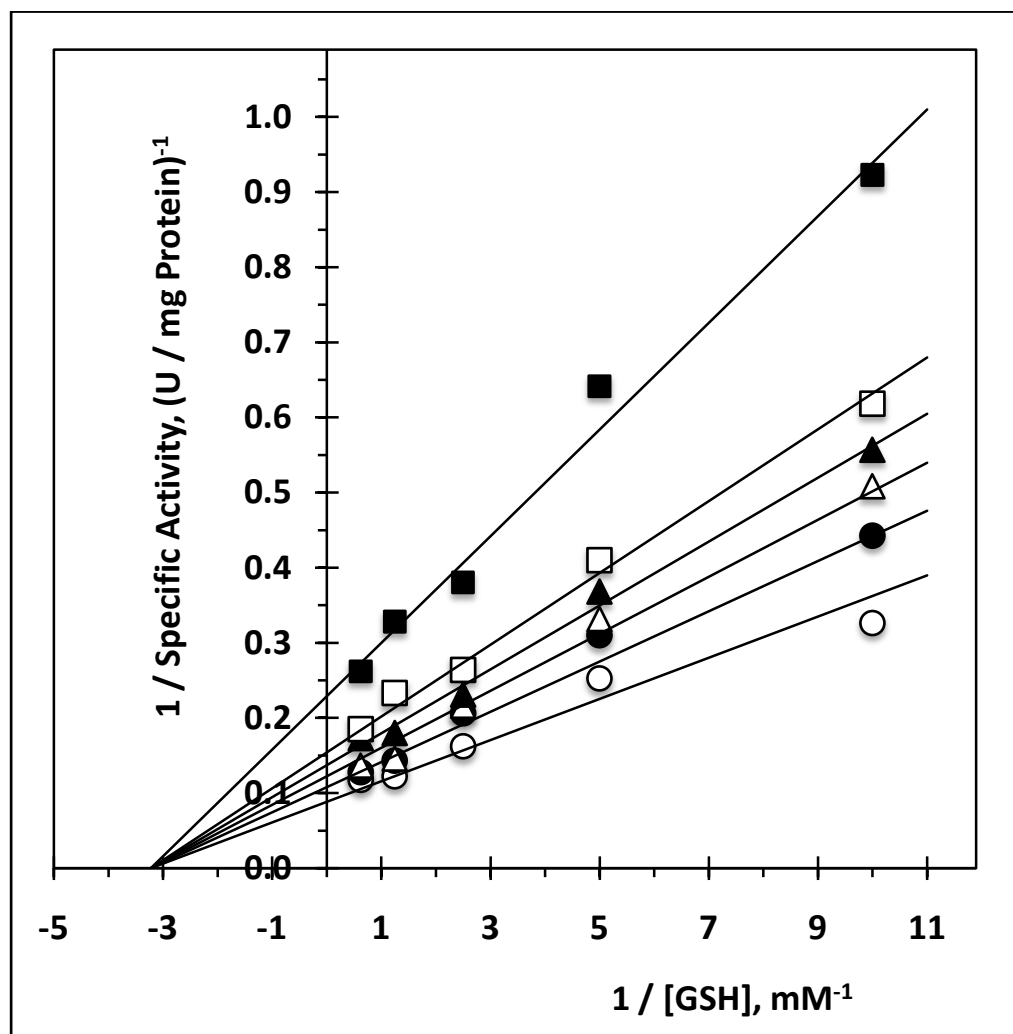


**Figure 4.8.** Lineweaver–Burk plot for *hpGSTP1-1* enzyme with different concentration of DEL at 1 mM [CDNB]<sub>f</sub> and [GSH]<sub>v</sub>: 0.1, 0.2, 0.4, 0.8 and 1.6 mM. [DEL]: (○), 0; (●), 0.5; (Δ), 1; (▲), 2; (□), 4; (■), 8 μM.

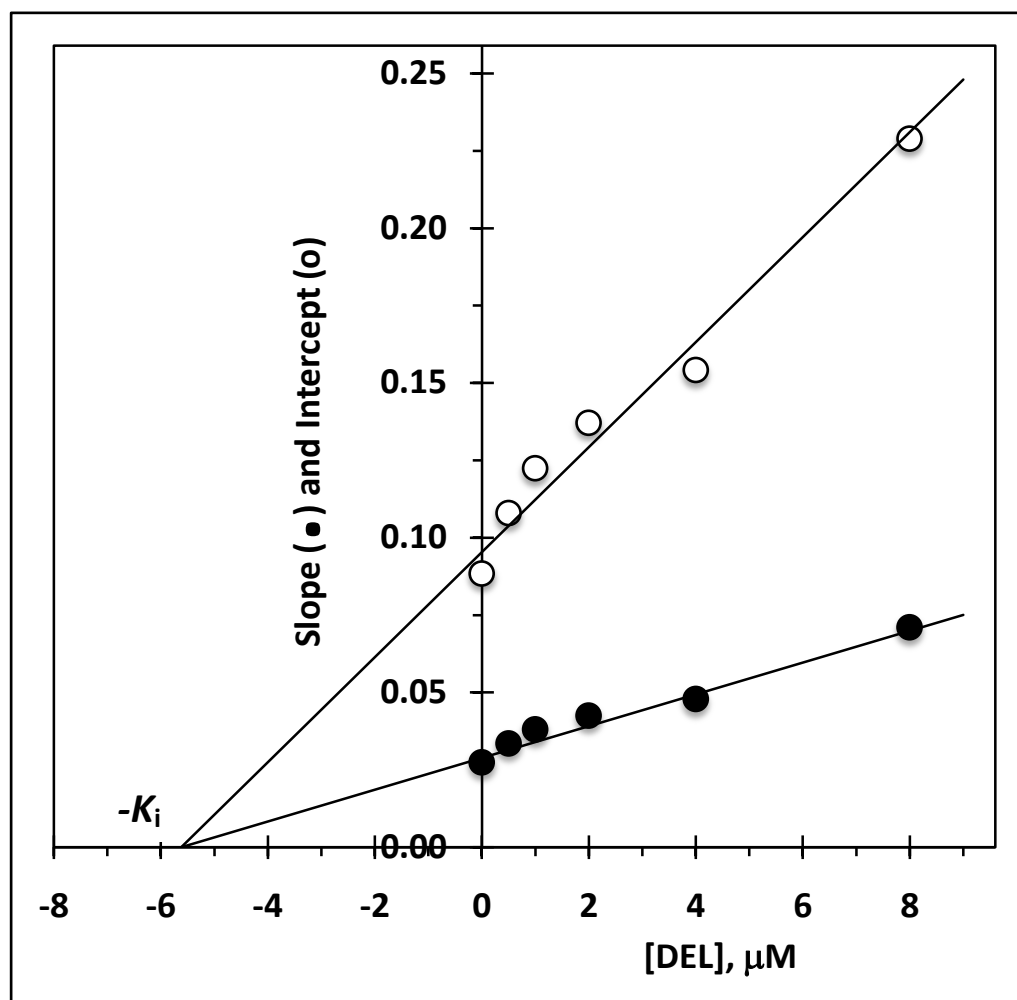
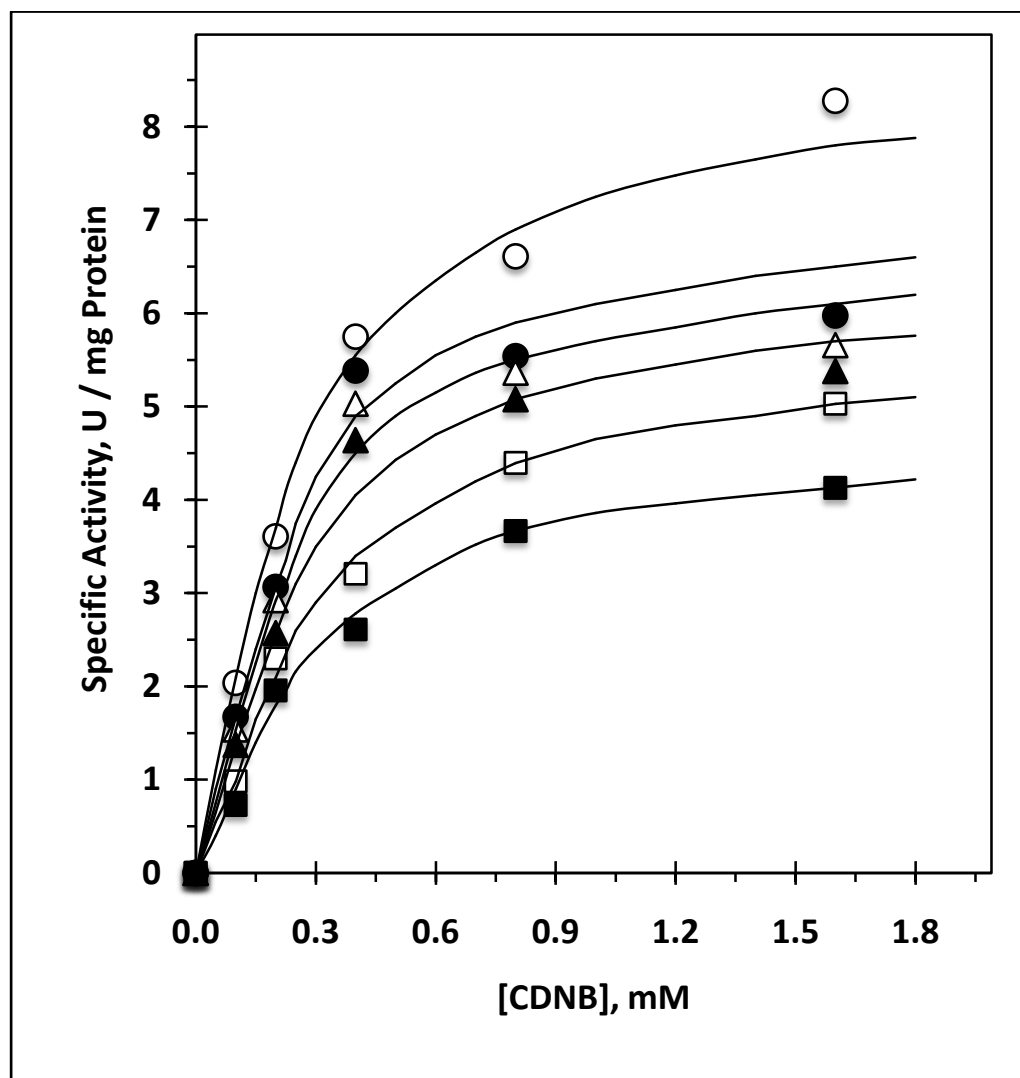
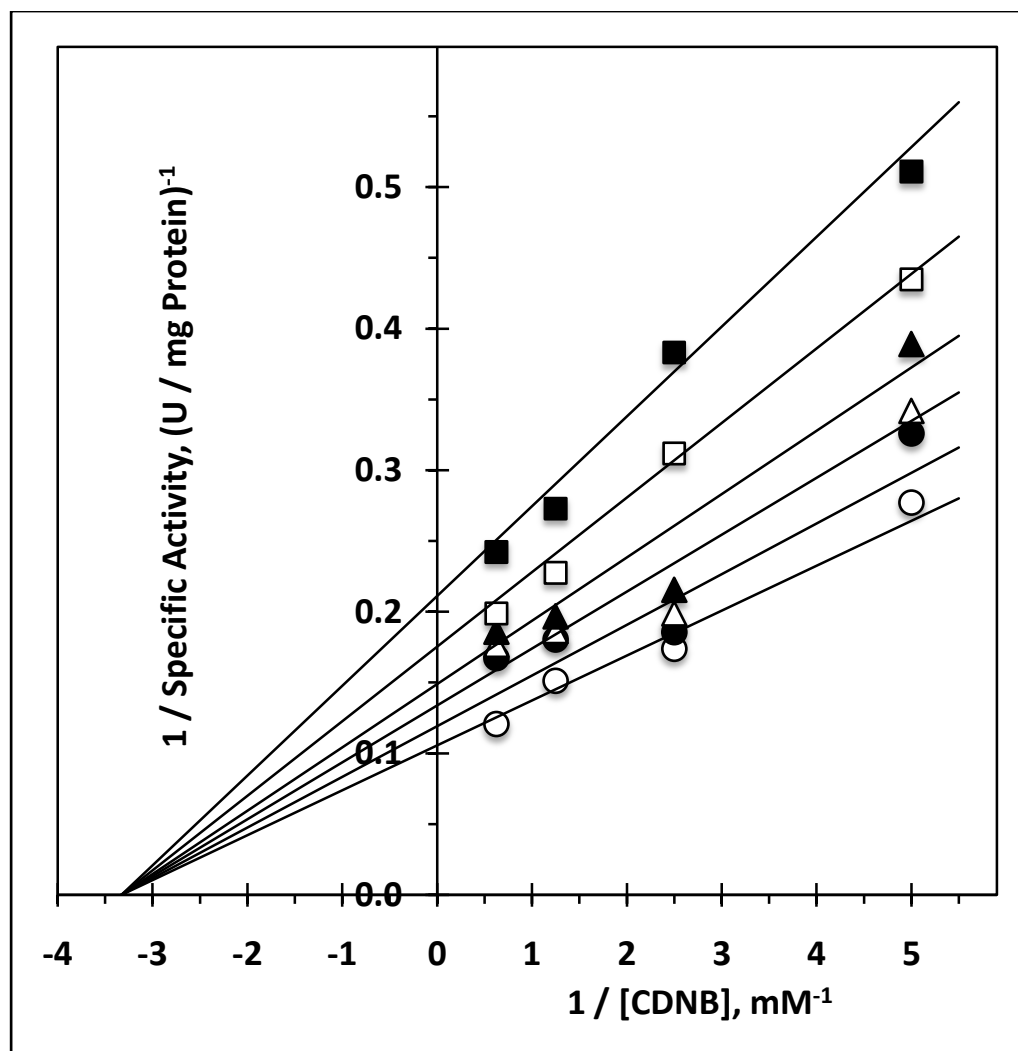


Figure 4.9. Slope (●) and intercept (○) vs. [DEL] plot at 1 mM [CDNB]<sub>f</sub> and [GSH]<sub>v</sub>.



**Figure 4.10.** Michaelis–Menten plot for the *hpGSTP1-1* enzyme with different concentrations of DEL at 1 mM [GSH]<sub>f</sub> and [CDNB]<sub>v</sub>: 0.1, 0.2, 0.4, 0.8 and 1.6 mM. [DEL]: (○), 0; (●), 0.5; (Δ), 1; (▲), 2; (□), 4; (■), 8 μM.



**Figure 4.11.** Lineweaver–Burk plot for the *hpGSTP1-1* enzyme with different concentrations of DEL at 1 mM [GSH]<sub>f</sub> and [CDNB]<sub>v</sub>: 0.1, 0.2, 0.4, 0.8 and 1.6 mM. [DEL]: (○), 0; (●), 0.5; (Δ), 1; (▲), 2; (□), 4; (■), 8 μM.

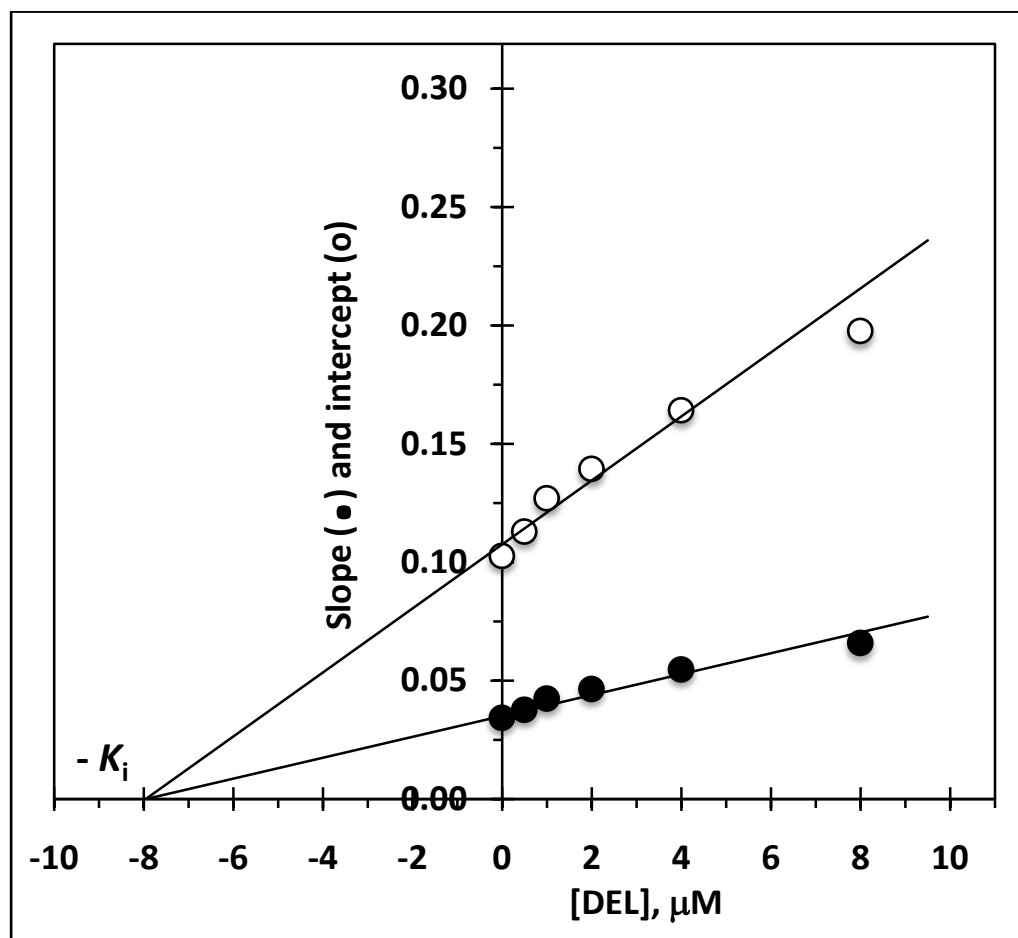


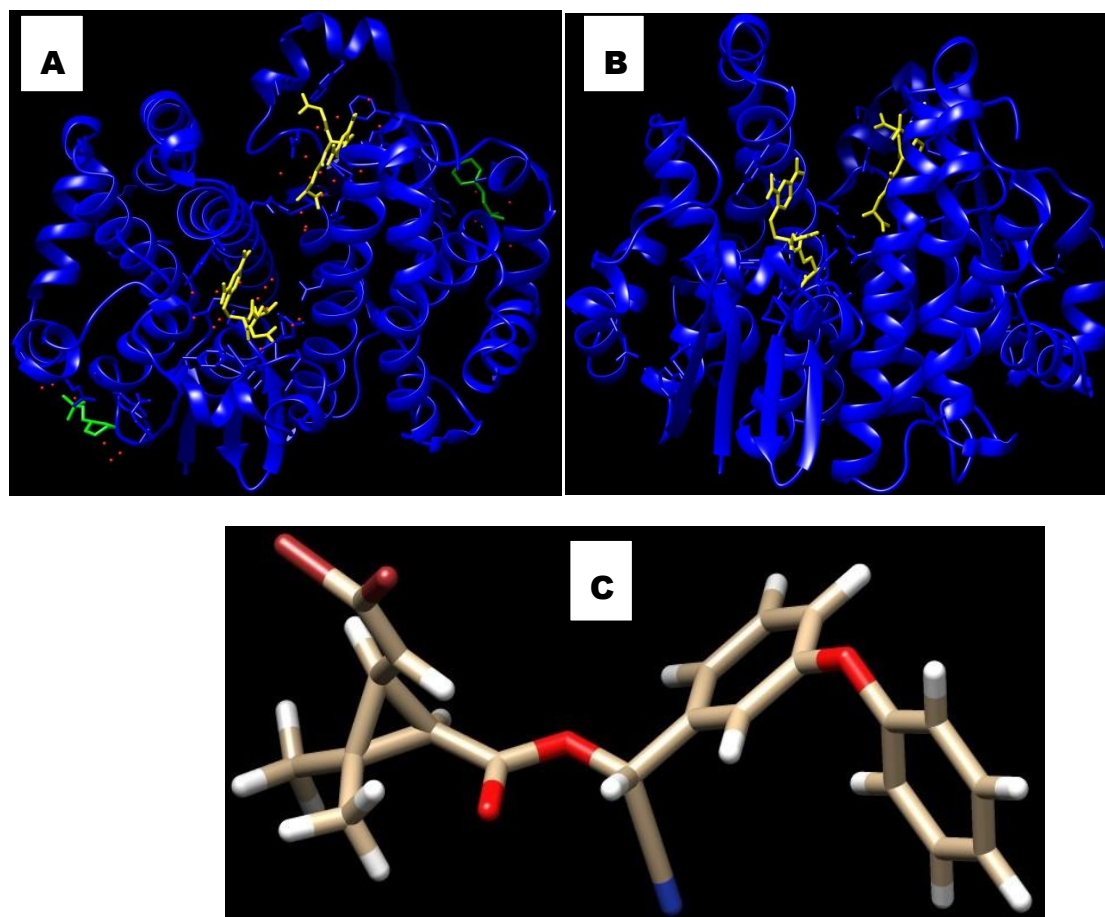
**Figure 4.12.** Slope (●) and intercept (○) vs. [DEL] plot at 1 mM [GSH]<sub>f</sub> and [CDNB]<sub>v</sub>

**Table 4.1.** Kinetic Parameters of *hp*GSTP1-1 Inhibition by DEL

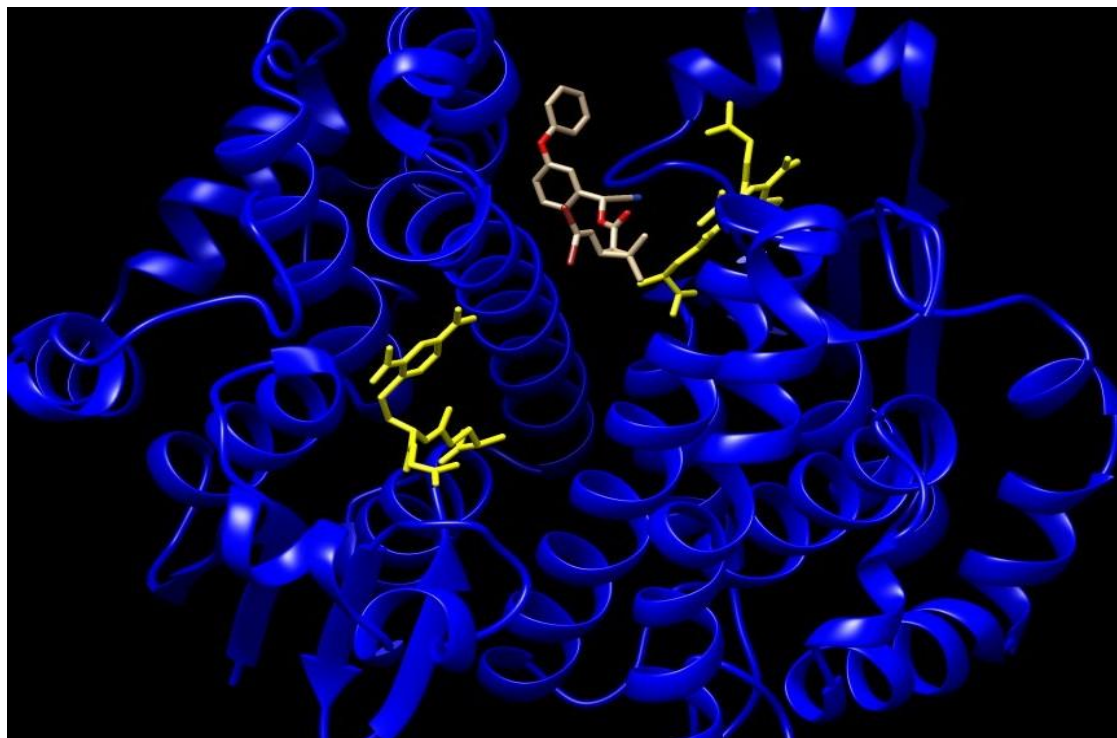
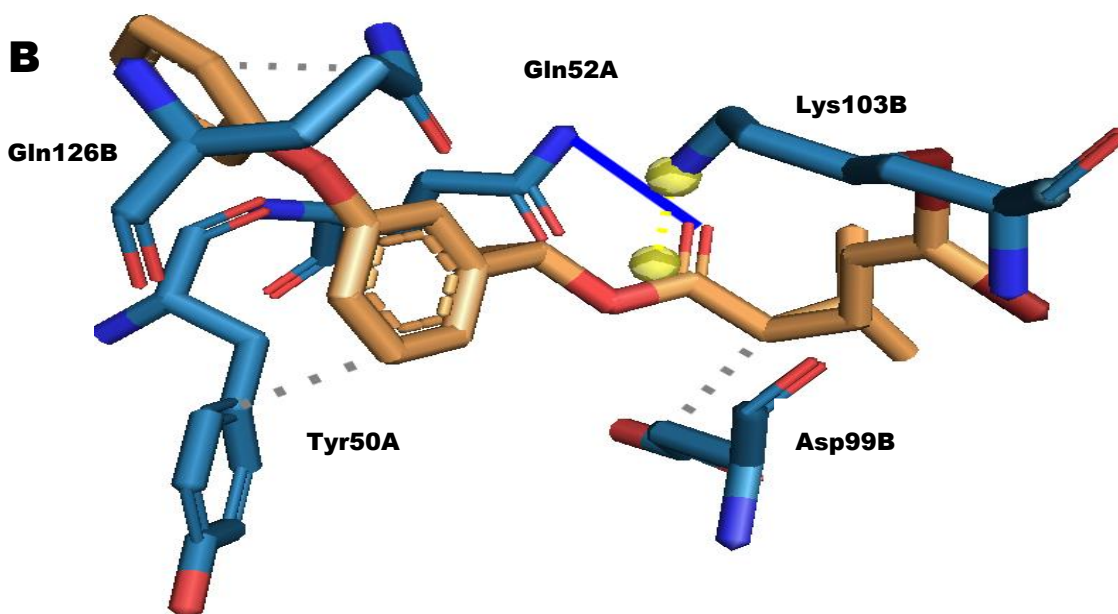
Parameters	[CDNB] <sub>f</sub> - [GSH] <sub>v</sub>	[GSH] <sub>f</sub> - [CDNB] <sub>v</sub>	Half-Inhibition
$IC_{50}$ , $\mu\text{M}$	-	-	6.2
Inhibition type	Non-competitive	Non-competitive	-
$V_m$ , $\text{U mg}^{-1}$ protein	$10.4 \pm 0.22$	$8.7 \pm 0.33$	-
$K_m$ , mM	$0.31 \pm 0.02$	$0.30 \pm 0.03$	-
$K_i$ , $\mu\text{M}$	$5.61 \pm 0.32$	$7.96 \pm 0.97$	-

#### 4.5. Molecular Docking of the GSTP1-1 Enzyme Inhibitor, DEL

The molecular docking was carried out to evaluate the interaction of DEL with the GSTP1-1 enzyme. This was to find the best geometrical arrangement or preferred orientation and predict the strength of association or binding affinity between the enzyme and the inhibitor pesticide.



**Figure 4.13.** Three-dimensional structures of GSTP1-1 and DEL. **A.** Crystal structure of GSTP1-1 (blue cartoon) complexed with GS-DNB (yellow sticks) and MES (green sticks) (PDB ID: 18GS). Water molecules are shown in red dots. **B.** Template structure of GSTP1-1 (blue cartoon) complexed with GS-DNB (yellow sticks) prepared for docking. Water and MES molecules have been deleted from the crystal structure. **C.** Predicted, ready-to-dock three-dimensional structure of DEL.

**A****B**

**Figure 4.14.** Noncovalent interactions between DEL and GSTP1-1. **A.** GSTP1-1 (blue Cartoon) complexed with GS-DNB (Yellow sticks) with docked DEL (tan sticks). **B.** Interaction of GSTP1-1 amino acid residues (blue sticks) with DEL (tan sticks). Hydrophobic Interactions are represented as dim-gray dashed lines; hydrogen bond is shown in blue solid line, and the salt bridge is indicated in yellow dashed lines.

**Table 4.2.** Interactions between GSTP1-1 and DEL

<b>Index</b>	<b>Residue position</b>	<b>Residue name</b>	<b>Distance between the two interacting atoms (Å)</b>
<b>Hydrophobic interactions</b>			
1	50A	Tyr	3.45
2	99B	Asp	3.57
3	126B	Gln	3.60
<b>Hydrogen bond</b>			
4	52A	Gln <sup>*</sup>	3.36
<b>Salt bridge</b>			
5	103B	Lys <sup>**</sup>	3.35

\* Interacts with the carbonyl oxygen of the DEL molecule

\*\* Provides the positive charge for the interaction with the carbonyl group of DEL

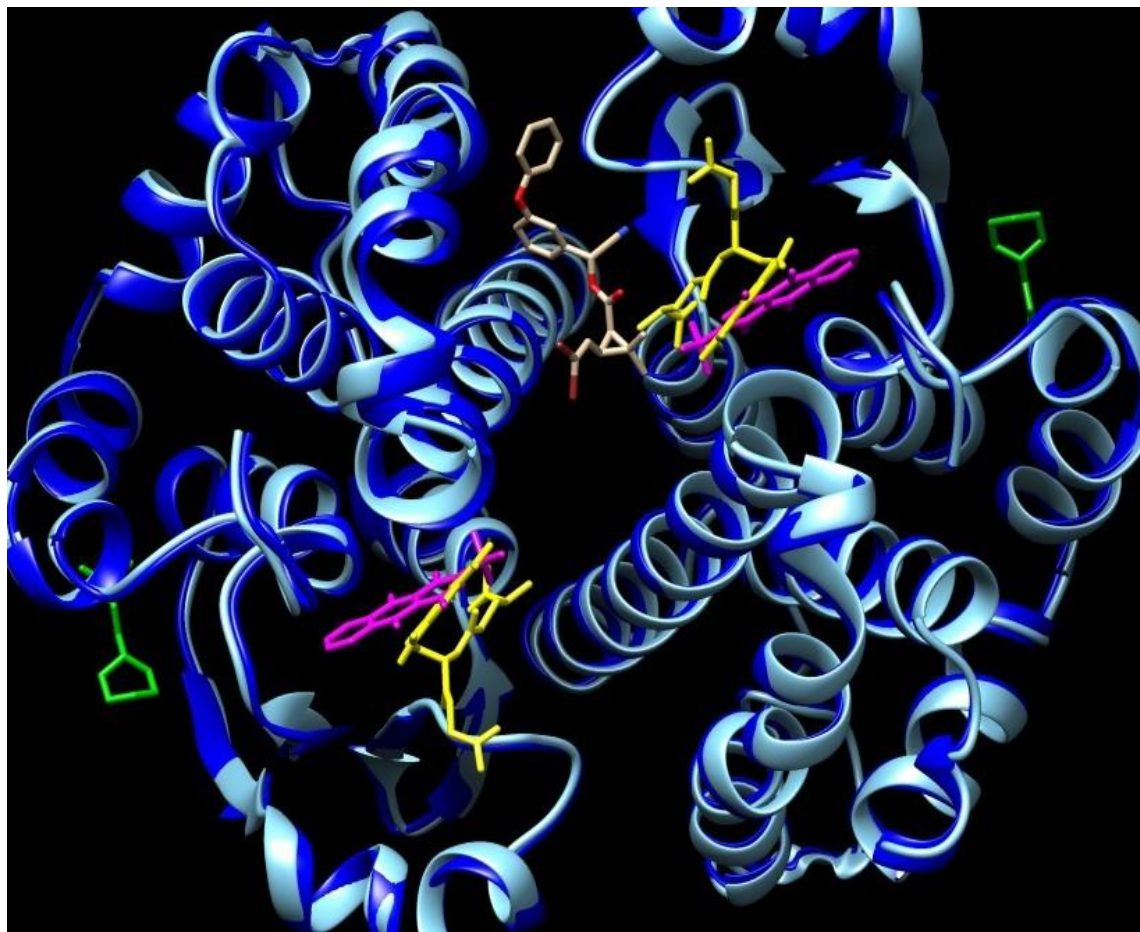


**Figure 4.15.** Comparison of the binding sites of GSTP1-1 derived by the superimposition of the docking result in this study and the crystal structures of GSTP1-1 (cornflower blue cartoon) in complex with Cibacron blue (magenta sticks) and MES (green sticks) (PDB ID: 20GS). The protein crystal structures used in this study is indicated by the blue cartoon (PDB ID: 18GS) complexed with GS-DNB (yellow sticks) and DEL (tan sticks).

## 5. DISCUSSION

Concerns have been generated by relevant authorities with regard to the ugly statistics of health disorders and deaths caused from pesticides exposure. Reports have shown that about 220,000 people die worldwide each year from organophosphate (OP) pesticides exposure alone (Ekinci and Beydemir, 2009). Many diseases and disorders have been linked to pesticides exposure including cancer, neurodegenerative diseases, disorders of protein, lipid, and carbohydrate metabolism, defects in blood cells, liver, pancreas, muscles and many others (Steenland *et al.*, 2000; Alavanja *et al.*, 2004; Bassil *et al.*, 2007; Karami-Mohajeri and Abdollahi, 2011; Parrón *et al.*, 2011; Hu *et al.*, 2015). This exposure has been chiefly through food, water, and air, either at home, farm or occupation (Alavanja *et al.*, 2004; Hernández *et al.*, 2013) with the mechanism of toxicity shown to be mainly by oxidative stress (Hernández *et al.*, 2013), and consequences more on fetus and babies than adult (Tapia *et al.*, 2012). Owing to this fact, alternative less toxic pesticides have been proposed. In recent years, a group of pesticides called pyrethroid has received attention as a potential alternative to the high toxicity and complications resulting from organophosphates exposure especially to non-target organisms, and the effects of organochlorine as a result of their bioaccumulation (Yekeen and Adeboye, 2013; Rehman *et al.*, 2014). These pyrethroids, of which DEL is a member, are the only class of insecticides recommended by both the Centre for Disease Control and Prevention (CDC) and the World Health Organization (WHO) to treat nets for the control of malaria (Pennetier *et al.*, 2008). However, reports have shown that low dose of DEL has harmful effects in pubescent female rats by causing DNA damage and disrupting renal and hepatic function (Chargui *et al.*, 2012). Since pyrethroids, of which DEL is a member, can cross the placental barrier (Ofordile *et al.*, 2005), they may accumulate in the fetus and interfere with the essential processes that could be deleterious to the development of the cargo *in utero* in the case of maternal exposure. Therefore, owing to the role of *hpGSTP1-1* in fetal detoxification (Dalmizrak *et al.*, 2011; Dalmizrak *et al.*, 2012; Dalmizrak *et al.*, 2016), its interaction with the DEL needs to be studied. The aim of this study was to investigate the interaction of *hpGSTP1-1* with DEL. To my knowledge, this study is the first evaluation of the effect of DEL on the *hpGSTP1-1* enzyme.

In this study, the *hpGSTP1-1* enzyme was obtained commercially. The purity and relative molecular mass ( $M_r$ ) of the enzyme was evaluated by discontinuous native and SDS-PAGE. CBB

R-250 staining and silver staining was used to view the protein bands. The visualization of single protein bands on native polyacrylamide gels (both CBB-stained and silver-stained) confirmed the purity of the enzyme (**Figures 4.1A** and **4.1B**). The molecular mass of a single *hpGSTP1-1* subunit was determined by SDS-PAGE. After staining the SDS-polyacrylamide gels with both CBB and silver, the protein bands were identified and the molecular mass of *hpGSTP1-1* was calculated from the plot depicted logarithm of  $M_r$  versus the relative migration distances of marker proteins to bromophenol blue ( $R_F$ ) as 21.4 kDa (**Figures 4.2A** and **4.2B**). This value, however, was slightly lower than the one declared (23.5 kDa) by the commercial company from which the enzyme was purchased. This slight difference may have come by the slightly unpredictable behavior of small natural proteins in an electric field (Roth, 2017) that protein band may sometimes display a slight positional change than usual. The concentration of the gel used may have also contributed to this phenomenon. The commercial company recommended the use of a 10% gel on a 0.75 mm thick spacer with 5  $\mu$ L loading volume for Coomassie staining and 1  $\mu$ L for silver staining (Roth, 2017). After employing this specification, the protein bands could not be seen clearly on the gel. The spacer available in this study was twice in thickness than the one recommended by the commercial company. The spacer used in this study was 1.5 mm and obtained from Bio-Rad Miniprotein Tetra Cell electrophoresis system. Because of these alterations, the volume loaded into the well was increased to 10  $\mu$ L and the gel percentage to 12%. A better resolution and visibility was obtained with the 12% gel, but they were much better in the presence of a 15% gel (**Figure 4.2A**). However, using the 15% gel, one of the protein markers, myosin (**Appendix I**), was possibly stuck at the border between the stacking gel and separator gel and washed off during staining/destaining procedure; thus, the band corresponding to myosin was not visible (**Figure 4.2A**). The 15% gel must have had smaller pores that could not filter the protein easily at the permitted time during electrophoresis. The next protein marker after myosin was  $\beta$ -galactosidase (**Appendix I**); its migration position on the 15% gel indicated that the protein was very close to the border between the stacking gel and the separator gel (**Figure 4.2A**), confirming that myosin must have stacked at the border. Generally, the GST family of enzymes consists of a number of isoenzymes with subunits ranging in size from 17 to 28 kDa (Aliya *et al.*, 2003). Many studies of different isoenzymes corroborate this finding (Guthenberg *et al.*, 1981; Dalmizrak *et al.*, 2011; Board and Menon, 2013; Tuna *et al.*, 2010; Turk, *et al.*, 2015). This variation is an indication of their broad substrate specificities, occurrence in different

organisms, grouping, inhibitor sensitivity, the sequence of amino acids, and immunological relatedness (Aliya *et al.*, 2003). The approximate value for the molecular mass obtained in this study was not in disagreement with what many studies have revealed for *hpGSTP1-1* from different sources (Guthenberg *et al.*, 1981; Singh *et al.*, 1987; Tahir *et al.*, 1988; Ozer *et al.*, 1990; Dalmizrak *et al.*, 2011, Turk *et al.*, 2015).

To determine the optimum pH, the activity of *hpGSTP1-1* was measured at seven selected pH values (5.0, 5.5, 6.0, 6.5, 7.0, 7.5, and 8.0). The buffer used was potassium phosphate buffer (200 mM) containing 2 mM EDTA. The optimum pH value for *hpGSTP1-1* was found to be 6.62 (**Figure 4.3**), which is in good correlation with the optimum pH of 7, reported for recombinant GSTP1-1 (Kolm *et al.*, 1992). The isoelectric point, pI, was found to be 4.8, which is also in good correlation with the reported pI values in literature (Guthenberg *et al.*, 1981; Singh *et al.*, 1987; Tahir *et al.*, 1988; Ozer *et al.*, 1990; Dalmizrak *et al.*, 2011, Turk *et al.*, 2015).

For the determination of optimum temperature ( $T_{op}$ ), the energy of activation ( $E_a$ ) and temperature coefficient ( $Q_{10}$ ) of the enzyme, the activity of the enzyme was measured at five selected temperatures (20 °C, 25 °C, 30 °C, 35 °C, 40 °C, and 45 °C). Different plots were depicted by processing the same data (**Figures 4.4A** and **4.4B**). From the graph of the specific activity ( $U\ mg^{-1}\ protein$ ) versus temperature (°C) (**Figure 4.4A**), the optimum temperature was determined to be 35.4 °C. The activation energy ( $E_a$ ) was obtained from the graph plotted between the logarithms of specific activities at different temperatures and the reciprocal of the temperature in degrees Kelvin (**Figure 4.4B**). The activation energy ( $E_a$ ) and the temperature coefficient ( $Q_{10}$ ) were calculated to be 7,623  $cal\ mol^{-1}$  and 1.52, respectively.

In kinetic studies, which were carried out at fixed 1 mM [CDNB] and 1 mM [GSH], the *hpGSTP1-1* was inhibited by DEL in a concentration-dependent manner with an  $IC_{50}$  value of 6.2  $\mu M$  (**Figure 4.6A**). The same value was also obtained from the inhibitory Hill plot (**Figure 4.6B**) (Segel, 1975). From the concentrations studied (ranging from 0.5 to 15  $\mu M$ ), the inhibition did not reach zero although the enzyme activity decreased as the DEL concentration was increased. By extrapolation, total inhibition is expected when the concentration of DEL is about twice the  $IC_{50}$  (**Figure 4.6A**). Recently, the interaction of *hpGSTP1-1* with some antidepressants was elucidated (Dalmizrak *et al.*, 2011; Dalmizrak *et al.*, 2016). From the results obtained, DEL seems to be a more potent inhibitor of *hpGSTP1-1* than the antidepressants studied.

GSTs are generally a significant large family of enzymes, primarily responsible for the phase II detoxification of endogenous and exogenous noxious chemical compounds by catalyzing their conjugation to the nucleophile reduced glutathione (GSH) (Whalen and Boyer, 1998; Sheehan *et al.*, 2001). Other reported functions of GSTs include isomerase and peroxidase activities, regulation of signaling cascades through protein–protein interaction, synthesis of steroids, synthesis and degradation of eicosanoids, degradation of aromatic amino acids, and ability to bind a wide range of non-catalytically ligands such as heme, bilirubin and steroid hormones (Sheehan *et al.*, 2001; Tuna *et al.*, 2010; Dalmizrak *et al.*, 2016). Undoubtedly, there will be a compromise of the body defense system and complications of other systems when the integrity of GST enzymes is affected. Four types of GST enzymes have been identified: the soluble canonical GSTs, kappa-class mitochondrial GSTs, MAPEG (membrane-associated proteins in eicosanoid and glutathione metabolism) or otherwise known as microsomal GSTs, and fosfomycin resistance protein from bacteria (Morgenstern *et al.*, 1982; Armstrong, 1991; Sheehan *et al.*, 2001; Bernat *et al.*, 2004; Ladner *et al.*, 2004; Josephy, 2010). Particularly, the soluble canonical GSTs (sometimes called cytosolic GSTs) have been well characterized than other types of GSTs, and were originally grouped into A, M, P, and T ( $\alpha$ ,  $\mu$ ,  $\pi$ , and  $\theta$ , respectively) classes on the basis of their structural similarities (primary and tertiary), specificity (to substrate and inhibitor) and immunological identity (Mannervik and Danielson, 1988; Sheehan *et al.*, 2001). GSTP1-1, a member of the cytosolic GSTs, regulates cell survival and apoptosis by interacting with C-Jun-N terminal kinase-1 (JNK-1), maintaining it in an inactive form, thereby protecting the cells against hydrogen peroxide-induced cell death (Sheehan *et al.*, 2001; Zimriak, 2007; Dalmizrak *et al.*, 2016). A recent study revealed that GSTP1-1 overexpression interferes with prostate cancer motility and viability by interacting with MYC and shutting down the MEK/ERK1/2 Pathways (Wang *et al.*, 2017).

The inhibition of *hp*GSTP1-1 by DEL in the micromolar concentration range (**Figure 4.6 A, B**) indicates that the pesticide is a potent inhibitor. From the inhibitory kinetic studies using five selected concentrations of DEL (0.5, 1.0, 2.0, 4.0, and 8.0  $\mu\text{M}$ ) with *hp*GSTP1-1, the  $V_m$  at  $[\text{CDNB}]_f - [\text{GSH}]_v$ , and  $[\text{GSH}]_f - [\text{CDNB}]_v$  were  $10.4 \pm 0.22 \text{ U mg}^{-1} \text{ protein}$  and  $8.7 \pm 0.33 \text{ U mg}^{-1} \text{ protein}$ , respectively (**Figure 4.8 and 4.11**; **Table 4.1**). The results show no significant difference between the  $V_m$  values at  $[\text{CDNB}]_f - [\text{GSH}]_v$ , and  $[\text{GSH}]_f - [\text{CDNB}]_v$  suggesting that, at the

concentrations used, the rate of reactions and turn over are similar. On the other hand, the  $K_m$  at  $[\text{CDNB}]_f$  -  $[\text{GSH}]_v$ , and  $[\text{GSH}]_f$  -  $[\text{CDNB}]_v$  were  $0.31 \pm 0.02$  mM and  $0.30 \pm 0.03$  mM, respectively (**Figure 4.8** and **4.11**; **Table 4.1**). These results indicate that the affinity of the enzyme for both substrates is the same. CDNB is an artificial electrophilic substrate generally suitable for the broadest range of GST isozymes, and it reacts readily with the GSH in the presence of GSTs (Dalmizrak *et al.*, 2016). This has been attributed to its small size in relation to the H-site cleft of most GSTs; therefore, the enzymes are placed with a few steric demands, making the artificial substrate able to bind with most GSTs that makes it popular and almost universally accepted laboratory substrate for assaying GSTs (Zimriak, 2007). Even in spontaneous noncatalytic reactions, CDNB reacts with nucleophilic substrates including thiolate anion of GSH (Zimriak, 2007; Dalmizrak *et al.*, 2016). This was why during the experiment, in addition to the enzymatic reaction, a non-enzymatic reaction was carried out, which contain in the reaction mixture all constituents of the reaction excluding the *hp*GSTP1-1 enzyme. The reading obtained from the nonenzymatic reaction was deducted from the reading for the enzymatic reaction.

The *hp*GSTP1-1 enzyme has been shown to possess two substrate-binding sites in each of its subunits: the “G-site” which is GSH-binding site and the “H-site” which is an electrophilic substrate-binding site (Josephy, 2010). The G-site is conserved and very specific for GSH only (Prade *et al.*, 1997; Zimriak, 2007; Board and Menon, 2013). The Tyr7 residue has been shown to be a catalytic residue in human GSTP1-1 and it helps in the stabilization of the glutathione thiolate anion (Oakley *et al.*, 1997; Prade *et al.*, 1997). Different from the G-site, the H-site is not well conserved and has broad specificity to permit the binding of a wide range of xenobiotics or electrophiles (Prade *et al.*, 1997).

This study showed that the inhibition types at both  $[\text{CDNB}]_f$  -  $[\text{GSH}]_v$ , and  $[\text{GSH}]_f$  -  $[\text{CDNB}]_v$  were non-competitive (**Figures 4.8** and **4.11**) with the  $K_i$  values of  $5.61 \pm 0.32$   $\mu\text{M}$  and  $7.96 \pm 0.97$   $\mu\text{M}$ , respectively (**Figures 4.9** and **4.12**; **Table 4.1**). The inhibition was confirmed to be reversible, as the graph lines representing the control and noncompetitive inhibition pass through the origin (**Figure 4.5**). From the statistical analysis, the  $K_i$  values obtained (**Table 4.1**) were in good agreement with the  $K_i$  values obtained from the graphical analysis (**Figures 4.9** and **4.12**). The inhibition type indicates that DEL may have bound to a site other than the CDNB or GSH-

binding site to inhibit the *hp*GSTP1-1 noncompetitively. This finding is in agreement with a long-established characteristic non-substrate binding of ligands to GST enzymes characterized by a noncompetitive mode of inhibition in the presence of CDNB and GSH as substrates (Ketley *et al.*, 1975). The binding of DEL to *hp*GSTP1-1 in this study must have caused conformational changes particularly to the substrate-binding sites of the enzyme such that the enzyme was not able to bind and catalyze the two substrates (GSH and CDNB) effectively, thus resulting in the observed inhibition mode. The results from the molecular docking studies corroborate this finding (**Figures 4.14A** and **4.14B**). Molecular docking was carried out to evaluate the interaction of DEL with the GSTP1-1 enzyme, which would ultimately pave the way to find the best geometrical arrangement or preferred orientation and predict the strength of association or binding affinity between the enzyme and the inhibitor pesticide. First, the 3D structure of GSTP1-1 was retrieved from Protein Data Bank (PDB ID: 18GS). The retrieved structure was already complexed with GS-DNB and MES and surrounded by water molecules (**Figure 4.13A**). Using a molecular visualization system, PyMOL Version 1.8.6.2 (Schrödinger, LLC, Portland, OR, USA), the enzyme structure was prepared and set for docking. With the knowledge of the inhibition type from the *in vitro* study (*i.e.*, non-competitive) already, there was no need to delete the GS-DNB molecule from the enzyme structure. A non-competitive mode of inhibition means the inhibitor binds to a binding site other than the substrate-binding site. However, the buffer MES and water molecules were removed because they could interfere with the docking since the DEL was expected to bind to a binding site on the surface of the protein other than the substrate-binding sites (G-site and H-site). Earlier studies have suggested the buffer-binding site (BBS) of HEPES (Ji *et al.*, 1997) and MES near Trp28 (Prade *et al.*, 1997) as the L-site for GSTP1-1. All these necessitated the removal of MES and water molecules from the retrieved GSTP1-1 crystal structure. After the deletion of MES and water molecules, the enzyme was only left complexed with GS-DNB (**Figure 4.13B**). To conduct molecular docking, the 3D structure of DEL had to be predicted first (**Figure 4.13C**). Using a docking algorithm, CORINA Classic version 4.0, for generating 3D structures of small- and medium-sized molecules particularly of drug-like type, the 3D structure of DEL was generated using the 'canonical SMILES' obtained from PubChem (a database for chemical molecules) and prepared by PyMOL prior to the docking approach. DEL was then docked on the GSTP1-1 protein complexed with GS-DNB (**Figure 4.14A**) using the molecular docking algorithm PatchDock (version Beta 1.3) (Duhovny *et al.*, 2002; Duhovny *et*

*al.*, 2005). The docking was carried out with receptor and ligand molecules inputted in PDB file format. In the request form for the docking, the complex type was enzyme–inhibitor and the clustering RMSD was 1.5 Å. According to the geometric score rank, the best one hundred docking solutions were downloaded and viewed in the Molecular Graphics System, UCSF Chimera (version 1.11.2) (Pettersen *et al.*, 2004). The number 1 docking solution was selected because it had the highest geometric score (5194) and, distance-wise, showed possible interactions with the key functional groups (cyano, ether, ester) of the DEL molecule reported to have the highest reactivity tendency (Taillebois *et al.*, 2015). Using Protein–Ligand Interaction Profiler (PLIP), a Web service that analyzes and visualizes noncovalent interactions between a protein and its ligand, the association between DEL and the GSTP1-1 enzyme was assessed. From the outcome, it was found that DEL bound to a binding site on the surface of the enzyme between the monomers different from the CDNB and GSH-binding sites (**Figure 4.14A**). GSTs have been originally named ligandins because of their capacity to bind large ligand molecules (of molecular weight >400 Da) (Oakley *et al.*, 1999). Usually, the non-substrate binding site (ligandin-binding site) for GSTs has been shown to be either overlapped with the H-site (Oakley *et al.*, 1999) or situated adjacent to the G-site (McTigue *et al.*, 1995; Ji *et al.*, 1996), or located at the buffer binding site (BBS) (Ji *et al.*, 1997; Prade *et al.*, 1997) depending on the kind of ligand molecules. At least three separate binding sites have been reported for xenobiotics within the H-site; only one is for CDNB (Ralat and Colman, 2004). However, the noncompetitive inhibition of *hp*GSTP1-1 by DEL observed in this study could not have been by the interaction of DEL with the GSH-binding site or the CDNB-binding site, and also, not even with the L-site within the H-site (Oakley *et al.*, 1999) or BBS (Ji *et al.*, 1997; Prade *et al.*, 1997) but with a binding site on the surface of the enzyme situated adjacent to the G-site of chain-A (**Figure 4.14A**). The L-site of GST enzymes generally has been established to be different from the G-site and H-site (Oakley *et al.*, 1999). The position of the binding site for DEL in this study is in agreement with this finding (**Figure 4.14A**). Studies have suggested that the L-site is located at the intermonomer space of the GST in *Schistosoma japonica* mu class (McTigue *et al.*, 1995) and about 14 Å to the G-site in squid sigma class (Ji *et al.*, 1996). For human GSTP1-1, the L-site has been proposed to be at the HEPES BBS (Ji *et al.*, 1997) or MES BBS near to Trp28 (Prade *et al.*, 1997). This has been questioned because the small BBS may not accommodate the large ligand molecules (molecular weight >400 Da) that bind to L-site with high affinity, and its distance from the G-site makes it

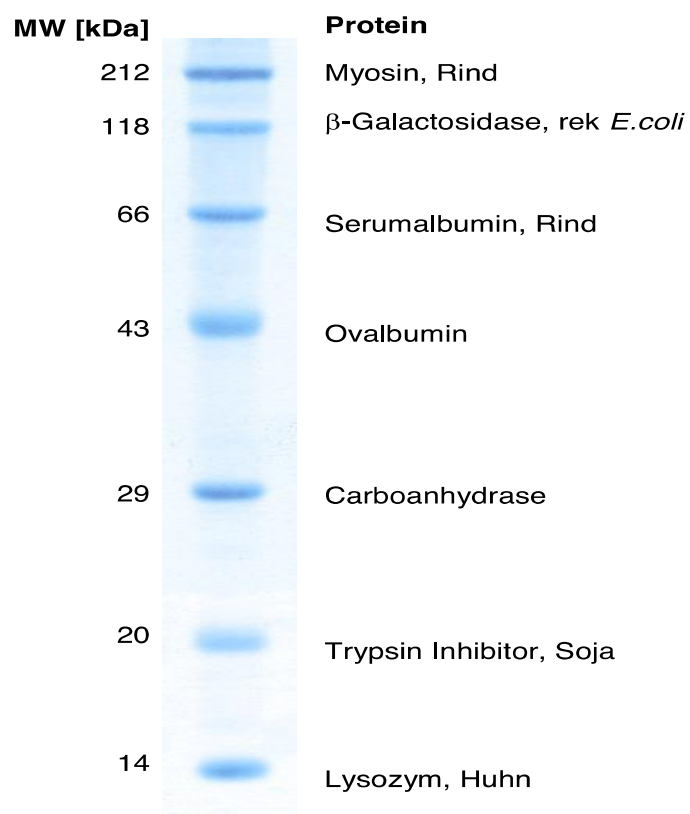
hard to explain the characterized noncompetitive mode of inhibition of ligand molecules bound to the L-site (Oakley *et al.*, 1999). A Comparison of the DEL binding site and the reported GSTP1-1 L-sites by the superimposition of the docking result in this study and GSTP1-1 crystal structures complexed with Cibacron blue (CB) and MES (PDB ID: 20GS) (**Figure 4.15**) demonstrated that the binding site of DEL is different from the L-site reported for CB and MES (Prade *et al.*, 1997; Oakley *et al.*, 1999). The molecular weight of DEL is approximately 505 Da. This large size ligand molecule and with the corresponding result from this study further support the argument (Oakley *et al.*, 1999) that the BBS may not likely be the L-site of GSTP1-1. However, the binding site occupied by DEL within the interface of *hp*GSTP1-1 dimer as observed in this study may suggest a novel non-substrate site for the GSTP1-1 enzyme. In total, DEL makes three different interactions with the protein subunits (A and B) (hydrophobic contacts, hydrogen bonding, and an ionic interaction). The two ring structures of the DEL molecule make hydrophobic contacts with Tyr50A, Asp99B and Gln126B (all  $<4\text{\AA}$ ) (**Table 4.2**). The hydrogen bonding interaction is between the amide group of Gln52A and the carbonyl group of the DEL molecule ( $3.36\text{\AA}$ ), and a salt bridge between the  $\epsilon$ -amino Lys102B and the carbonyl group of the DEL molecule (**Figure 4.14B**). This finding is in line with previously reported molecular electrostatic potential values ( $\text{kJ mol}^{-1}$ ) located on the cyano, ether, ester and bromine moieties of DEL that showed a qualitative ranking of the possible molecular interaction of the fragments (Taillebois *et al.*, 2015). The study showed that the main interacting functional groups in order of reactivity are the nitrile group, followed by the carbonyl group, and oxygens of the ether groups. The bromine atoms of the DEL molecule also hold the potential of donating halogen-bonds (Taillebois *et al.*, 2015).

The micromolar range  $K_i$  values  $5.61 \pm 0.32$  and  $7.96 \pm 0.97$   $\mu\text{M}$  obtained at both  $[\text{CDNB}]_f$ - $[\text{GSH}]_v$ , and  $[\text{GSH}]_f$ - $[\text{CDNB}]_v$  respectively (**Table 4.1**) seem to make DEL a potent inhibitor of *hp*GSTP1-1. The roles of *hp*GSTP1-1 especially in fetuses suggest there could be severe and multiple consequences in developing babies in the event where the enzyme is inhibited. When a fetus encounters extended exposure to DEL from maternal circulation and *hp*GSTP1-1 is inhibited, the fetus, therefore, is left defenseless to even other electrophiles which may result in multiple and severe complications. The stages of fetus and neonate development are critical periods that is uniquely sensitive and vulnerable to noxious chemical substances (Johri *et al.*,

2006). The early life insult, particularly during the period of development *in utero* and birth, could cause permanent damage to the developing immune system, thus leading to premature deaths (Ofordile *et al.*, 2005). In a study conducted by the Columbia Center for Children's Environmental Health (CCCEH), it was revealed that fetal and childhood exposure to pesticides can adversely affect neurodevelopment (Tapia *et al.*, 2012). The placenta functions as the interface between the maternal and fetal circulations and controls the transfer of nutrients, oxygen, and waste products, but when xenobiotics are present in maternal circulation, the degree of exposure and effect is determined by biotransformation processes and transport system in the placental barrier (Al-Enazy *et al.*, 2016). Due to the immature enterohepatic clearance system of the fetus (Beath, 2003; Dalmizrak *et al.*, 2016), the xenobiotics that a mother can tolerate could become deleterious to the developing fetus *in utero*. Already, residues of pesticides in placenta, fetal organs, subcutaneous fat tissues, umbilical cord blood and body fluids have been reported (Martínez *et al.*, 1993; Waliszewski *et al.*, 2000; Perera *et al.* 2004; Souza *et al.*, 2005). These residues can accumulate and result in severe complications. Maternal health is crucial, thus monitoring of alterations in redox homeostasis during antenatal is thought to be pivotal in the fight against congenital anomalies and deformities. Human placental GSTP1-1, therefore, could be a potential marker protein for monitoring deregulation the in redox homeostasis. There have been compelling pieces of evidence supporting this. It has been demonstrated that, although other GST enzymes such as GSTA1, GSTA2, and GSTM1 are expressed during developmental stages, GSTP1-1 expression in all embryonic and fetal organs is outstandingly higher, only goes down at the end of prenatal period (Raijmakers *et al.*, 2001).

## 6. CONCLUSION

In this study, the interaction of the *hp*GSTP1-1 isoenzyme with the DEL was studied. It was shown that at  $[\text{CDNB}]_f$ -  $[\text{GSH}]_v$  and  $[\text{GSH}]_f$  -  $[\text{CDNB}]_v$  the inhibition type was non-competitive, with the  $K_i$  values of  $5.61 \pm 0.32 \mu\text{M}$  and  $7.96 \pm 0.97 \mu\text{M}$ , respectively. Also, the  $V_m$  and  $K_m$  at  $[\text{CDNB}]_f$ -  $[\text{GSH}]_v$  and  $[\text{GSH}]_f$  -  $[\text{CDNB}]_v$  were  $10.4 \pm 0.22 \text{ U mg}^{-1}$  protein and  $8.7 \pm 0.33 \text{ U mg}^{-1}$  protein, and  $0.31 \pm 0.02 \text{ mM}$  and  $0.30 \pm 0.03 \text{ mM}$ , respectively. The  $IC_{50}$  was  $6.2 \mu\text{M}$ , and the pH optimum, temperature optimum ( $T_{op}$ ), activation energy ( $E_a$ ) and temperature coefficient ( $Q_{10}$ ) were found to be 6.62,  $35.4^\circ\text{C}$ ,  $7.6 \text{ kcal mol}^{-1}$  and 1.52, respectively. The molecular docking results suggest that DEL binds to a site located at the intermonomer space of *hp*GSTP1-1 using its two ring structures to make hydrophobic contacts with Tyr50A, Asp99B, and Gln126B (all  $<4\text{\AA}$ ) and its carbonyl group to make a hydrogen bonding interaction with Gln52A ( $3.36\text{\AA}$ ) and a salt bridge with Lys102B. The binding may have caused an alteration in the conformation of the substrate-binding sites (G-site and H-site) of the enzyme to cause the noncompetitive mode of inhibition observed in the *in vitro* study. Also noted was that the binding site was distinct from the site suggested to be the L-site for GSTP1-1 (Oakley *et al.*, 1999), which may suggest a novel non-substrate binding site. Furthermore, the inhibition of *hp*GSTP1-1 at micromolar concentrations indicates that the DEL is a potent inhibitor. However, its effect on fetuses may be severe than on adults because the enterohepatic clearance system of fetuses are not as matured as that of adults (Beath, 2003; Dalmizrak *et al.*, 2016), more so owing to the fact that pyrethroids, of which DEL is a member, can cross the placental barrier (Ofordile *et al.*, 2005). For this reasons, in the incidence of maternal exposure to DEL, it may accumulate in the developing baby and result to congenital complications. This finding, therefore, presents *hp*GSTP1-1 as potential marker protein that could be employed during antenatal for monitoring deregulation in redox equilibrium in the case of maternal exposure to noxious chemicals, mutagens, carcinogens, drugs and pharmacologically active agents which may otherwise unknowingly harm the cargo *in utero*.

**APPENDIX****Appendix I**

Roti®-Mark Standard Protein-molecular weight marker on SDS-PAGE, 10% separator gel, 0.75 mm thick. Amount Loaded in the well, 5  $\mu$ L Coomassie-staining.

## Appendix II

<b>Amino Acid Sequence of Human Glutathione Transferase P1-1 Subunit</b>					
<b>Source</b>	<a href="http://www.uniprot.org/uniprot/P09211">http://www.uniprot.org/uniprot/P09211</a>				
<b>Identity in PDB</b>	18GS				
<b>Number of Amino Acids</b>	210				
<b>Amino Acid Sequences</b>	10	20	30	40	50
	MPPYTVVYFP	VRGRCAALRM	LLADQGQSWK	EEVVTVETWQ	EGSLKASCLY
	60	70	80	90	100
	GQLPKFQDGD	LTLYQSNTIL	RHLGRTLGLY	GKDQQEAAALV	DMVNDGVEDL
	110	120	130	140	150
	RCKYISLIYT	NYEAGKDDYV	KALPGQLKPF	ETLLSQNQGG	KTFIVGDQIS
	160	170	180	190	200
	FADYNLLDLL	LIHEVLAPGC	LDAFPLLSAY	VGRLSARPKL	KAFSLASPEYV
	210				
	NLPINGNGKQ				

## REFERENCES

- Abdollahi, M., Ranjbar, A., Shadnia, S., Nikfar, S. and Rezaiee, A. (2004) Pesticides and oxidative stress: a review. *Medical Science Monitor*.10, 141-147.
- Adler, V., Yin, Z., Fuchs, S.Y., Benezra, M., Rosario, L., Tew, K. D., Pincus, M. R., Sardana, M., Henderson, C.J., Wolf, C.R., Davis, R.J. and Zonai, Z. (1999) Regulation of JNK signaling by GSTP. *EMBO Journal*.18 (5), 1321-1334.
- Alavanja, M. C., Hoppin, J. A. and Kamel, F. (2004) Health effects of chronic pesticide exposure: cancer and neurotoxicity. *Annual Review of Public Health*.25, 155-197.
- Al-Enazy, S., Ali, S., Albekairi, N., El-Tawil, M. &Rytting, E. (2016) Placental control of drug delivery. *Advance Drug Delivery Review*. xxx, 1-10.
- Aliya, S. Reddanna, P. and Thyagaraja, K. (2003) Does glutathione S-transferase Pi (GST-Pi) a marker protein for cancer? *Molecular and Cellular Biochemistry*.253,319-327.
- Angelucci, F., Baiocco, P., Brunori, M., Gourlay, L., Morea, V. and Bellelli, A. (2005) Insights into the Catalytic Mechanism of Glutathione S-Transferase: The Lesson from *Schistosoma haematobium*. *Structure*.13(9),1241–1246.
- Armstrong, R.N. (1991) Glutathione S-transferase: Reaction Mechanism, Structure, and Function. *Chemical Research in Toxicology*.4 (2), 131-140.
- Armstrong, R.N. (1997) Structure, catalytic mechanism, and evolution of glutathione transferase. *Chemical Research in Toxicology*.10 (1), 2-18.
- Bassil, K.L., Vakil, C., Sanborn, M., Cole, D.C., Kaur, J.S. and Kerr, K.J. (2007) Cancer health effects of pesticides: a systematic review. *Canadian Family Physician*. 53, 1704-1711.
- Beath, S.V. (2003) Hepatic function and physiology in the newborn. *Seminars in Neonatology*.8, 337-346.
- Bernat, A.B., Laughlin, T.L. and Armstrong N.R. (1997) Fosfomycin resistance protein (FosA) is a manganese Metallo-glutathione transferase related to glyoxalase I and the estradiol dioxygenases. *Biochemistry*. 36 (11), 3050.

Board, P.G. and Menon D. (2013) Glutathione transferases, regulators of cellular metabolism and Physiology. *Biochimica et Biophysica Acta*.1830, 3267-3288.

Cao, T.T., Ma, L., Kandpal, G., Warren, L., Hess, F. J. and Seabrook, R.G. (2005) Increased nuclear factor-erythroid 2 p45-related factor 2 activity protects SH-SY5Y cells against oxidative damage. *Journal of Neurochemistry*. 95, 406-417.

Carlberg, I. And Mannervik, B. (1975) Purification and Characterization of the Flavoenzyme Glutathione Reductase from Rat Liver. *The journal of biological chemistry*. 250 (14), 575-580.

Chargui, I., Grissa, I., Bensassi, F., Hrira, M.Y., Haouem, S., Haouas, Z. and Bencheikh, H. (2012) Oxidative stress, biochemical and histopathological alterations in the liver and kidney of female rats exposed to low doses of deltamethrin (DM): A molecular assessment. *Biomedical Environmental Science*. 25 (6), 672-683.

Dalmizrak, O., Erkmen, K.G. and Ozer, N. (2011) The inhibition characteristics of human placental glutathioneS-transferase-p by tricyclic antidepressants: amitriptyline and clomipramine. *Molecular and Cellular Biochemistry*. 355, 223-231.

Dalmizrak, O., Erkmen, K.G. and Ozer, N. (2012) Evaluation of the in vitro Inhibitory Impact of Hypericin on Placental Glutathione S-Transferase pi. *The Protein Journal*. 31,544-549.

Dalmizrak, O., Kulaksiz-Erkmen, G., and Ozer, N., (2016) Fluoxetine-induced toxicity results in human placental glutathione S-transferase-n (GST-n) dysfunction. *Drug and Chemical Toxicology*. 39 (4), 439–444.

Duhovny, D., Nussinov, R. and Wolfson, H.J. (2002) Efficient Unbound Docking of Rigid Molecules. In Gusfield et al., Ed. Proceedings of the 2'nd Workshop on Algorithms in Bioinformatics (WABI) Rome, Italy, Lecture Notes in Computer Science 2452, pp. 185-200, Springer Verlag.

Ekinci, D. and Beydemir, S. (2009) Evaluation of the Impact of antibiotics drugs on PON 1; a major bio-scavenger against cardiovascular disease. *Europeans Journal of Pharmacology*. 617, 84-89.

Enache, A. T. and Oliveira-Brett, A. M. (2015) Electrochemical evaluation of Glutathione S-transferase kinetic parameters. *Bioelectrochemistry* 101, 46–51.

Erkmen, K.G., Dalmizrak, O., Tuna, D.G., Dogan, A., Hamdi O. I., and Ozer, N. (2013) Amitriptyline may have a supportive role in cancer treatment by inhibiting glutathione S-transferase pi (GST- $\pi$ ) and alpha (GST- $\alpha$ ). *Journal of Enzyme Inhibition and Medicinal Chemistry*. 28 (1), 131-136.

Grijalva, J., Vakili, K. (2013) Neonatal liver physiology. *Seminars in Pediatric Surgery*. 22, 185-189.

Guthenberg, C., and Mannervik, B. (1981) Glutathione S-transferase (transferase pi) from human placenta is identical or closely related to glutathione S-transferase (transferase rho) from erythrocytes. *Biochim Biophys Acta*. 661 (2), 255-260.

Habig, W.H. and Jakoby, W.B. (1981) Assays for differentiation of glutathione S-transferases. *Methods in Enzymology*. 77, 398-405.

Hames, B.D. (1998) Gel Electrophoresis of protein: a practical approach, 3<sup>rd</sup> Edition. Oxford University Press; New York.

Hernández, F.A., Lacasaña, M., Gil, F., Rodríguez-Barranco, M., Pla, A. and López-Guarnido, O. (2013) Evaluation of pesticide-induced oxidative stress from a gene-environment interaction perspective. *Toxicology*. 307, 95-102.

Hougaard, J.M., Duchon, S., Zaim, M. and Guillet P. (2002) Bifenthrin: A Useful Pyrethroid Insecticide for Treatment of Mosquito Nets. *Journal of Medical Entomology*. 39(3), 526-533.

Hu, R., Huang, X., Huang, J., Li, Y., Zhang, C., Yin, Y., et al. (2015) Long- and Short-Term Health Effects of Pesticide Exposure: A Cohort Study from China. *PLoS ONE*. 10 (6), 1-13.

Ji, X., Johnson, W.W., Sesay, M. A., Dickert, L., Prasad, S. M., Ammon, H.L., Armstrong, R.N. and Gilliland, G.L. (1994) Structure and function of the xenobiotic substrate binding site of a glutathione S-transferase as revealed by X-ray crystallographic analysis of product complexes with the diastereomers of 9-(S-glutathione)-10-hydroxy-9,10-dihydrophenanthrene. *Biochemistry*. 33 (5), 1043-1052.

Ji, X., Tordova, M., O'Donnell, R., Parsons, J. F., Hayden, J. B., Gilliland, G. L. and Zimniak, P. (1997) Structure and function of the xenobiotic substrate binding site and the location of a

potential non-substrate-binding site in a class p glutathione S-transferase. *Biochemistry*. 36, 9690-9702.

Ji, X., von Rosenvinge, E. C., Johnson, W. W., Armstrong, R. N. and Gilliland, G. L. (1996) Location of a potential transport binding site in a sigma class glutathione transferase by X-ray crystallography. *Proceedings of the National Academy of Sciences of United States of America*. 93, 8208-8213.

Johri, A., Dhawan, A., Singh, L.R. and Parmar, D. (2006) Effect of prenatal exposure of deltamethrin on the ontogeny of xenobiotic-metabolizing cytochrome P450s in the brain and liver of offsprings. *Toxicology and Applied Pharmacology*. 214, 279-289.

Josephy, D. P. (2010) Genetic Variations in Human Glutathione Transferase Enzymes: Significance for Pharmacology and Toxicology. *Human Genomics and Proteomics*. 10, 1-14.

Joshi, R.M., Ghose, G., Som, T. K. and Bala, S. (2003) Study of the Impact of Deltamethrin Impregnated Mosquito Nets on Malaria Incidence at a Military Station. *Medical Journal Armed Forces India*. 59 (1), 12-14.

Jowsey, R., Thomson, E. R., Orton, C.T., Elcombe, R. C. and Hayes, D. J. (2003) Biochemical and genetic characterization of a murine class Kappa glutathione S-transferase. *Biochemical Journal*. 373, 559-569.

Karami-Mohajeri, S. and Abdollahi, M. (2011) Toxic influence of organophosphate, carbamate, and organochlorine pesticides on cellular metabolism of lipids, proteins, and carbohydrates: a systematic review. *Human and Experimental Toxicology*. 30 (9), 1119-1140.

Ketley, J. N., Habig, W. H. and Jakoby, W. B. (1975) Binding of nonsubstrate ligands to the glutathione S-transferases. *Journal of Biological Chemistry*. 250, 8670-8673.

Kolm, H. R., Sroga, E. G. and Mannervik B. (1992) Participation of the phenolic hydroxyl group of Tyr-8 in the catalytic mechanism of human glutathione transferase P1-1. *Biochemical Journal*. 285, 537-540.

Ladner, J.E., Parsons, J.F, Rife, C.L., Gilliland G.L. and Armstrong, R.N. (2004) Parallel evolutionary pathways for glutathione transferases: structure and mechanism of the mitochondrial class kappa enzyme rGSTK1-1. *Biochemistry*. 43 (2), 352.

Laemmli, U. K. (1970) Cleavage of structural proteins during the assembly of the head of bacteriophage T4. *Nature*. 227, 680-685.

Lobo, V., Patil, A., Phatak, A. and Chandra, N. (2010) Free radicals, antioxidants, and functional foods: Impact on human health. *Pharmacognosy Review*. 4, 118-126.

Mannervik, B., and Danielson, H. (1988) Glutathione Transferases- Structure and Catalytic Activity. *CRC Critical Reviews in Biochemistry*. 23 (3), 283-337.

Mannervik, B., Board, G. P., Hayes, D. J. Listowsky, I. and Pearson, R. W. (2005) Nomenclature for Mammalian Soluble Glutathione Transferases. *Methods In Enzymology*. 401,1-8.

Martí'nez, M. E., Romanos, L. A., Praena, C. M., Repetto, J. M, Martí'nez, R. D. (1993) Compuestos organoclorados: nivelessanguí'neosenmadres, recie'nnacidos, lactantes, enlechematernaydefo'rmula. Estudios en la provincia de Huelva. *Anales Espan'oles de Pediatría*. 39, 46-52: In Souza, M. S, Magnarelli, G. G., Rovedatti, M. G. Santa Cruz, S. and Pechen De D'angelo, A. M. (2005) Prenatal exposure to pesticides: analysis of human placental acetylcholinesterase, glutathione-S-transferase, and catalase as biomarkers of effect. *Biomarkers*. 10 (5), 376-389.

McTigue, M. A., Williams, D. R. and Tainer, J. A. (1995) Crystal structures of a schistosomal drug and vaccine target: glutathione S-transferase from *Schistosoma japonica* and its complex with the leading antischistosomal drug praziquantel. *Journal of Molecular Biology*. 246, 21-27.

Morel, F. and Aninat, C. (2011) The glutathione transferase kappa family. *Drug Metabolism Review*. 43, 281-291.

Morgenstern, R., Guthenberg, C. and Depierre W. J. (1982) Microsomal Glutathione S-Transferase: Purification, Initial Characterization, and Demonstration that It Is not Identical to the Cytosolic Glutathione S-Transferases A, B and C. *European Journal of Biochemistry*. 128, 243-248.

Oakley, J. A., Bello, L. M., Battistoni, A., Ricci, G., Rossjohn, J., Villar, O. H. and Parker, M. W. (1997) The Structures of Human Glutathione Transferase P1-1 in Complex with Glutathione and various inhibitors at High Resolution. *Journal of Molecular Biology*. 274, 84-100

Oakley, J. A., Bello, L.M., Nuccetelli, M., Mazzetti, P. A. and Parker, W. M. (1999) The ligandin (non-substrate) binding site of human pi class glutathione transferase is located in the electrophile binding site (H-site). *Journal of Molecular Biology*. 291 (4), 913-926.

Ofordile, O. N., Prentice, A. M., Moore, S. E. and Holladay, S. D. (2005) Early Pesticide Exposure and Later Mortality in Rural Africa: A New Hypothesis. *Journal of Immunotoxicology*. 2, 33-40.

Ozer, N., Erdemli, O., Sayek, I., and Ozer, I. (1990) Resolution and kinetic characterization of glutathione S-transferases from human jejunal mucosa. *Biochemical Medicine and Metabolic Biology*. 44 (2), 142-150.

Parrón, T., Requena, M., Hernández, A.F. and Alarcón, R. (2011) Association between environmental exposure to pesticides and neurodegenerative diseases. *Toxicology and Applied Pharmacology*. 256, 379-385.

Parsons, F.J., and Armstrong, N.R. (1996) Proton Configuration in the Ground State and Transition State of a Glutathione Transferase-Catalyzed Reaction Inferred from the Properties of Tetradeca(3-fluoro tyrosyl) Glutathione Transferase. *Journal of the American Chemical Society*. 118 (9), 2295-2296.

Pennetier, C., Costantini, C., Corbel, V., Licciardi, S., Dabiré, R. K., Lapied, B. and Hougard, J. (2008) Mixture for Controlling Insecticide-Resistant Malaria Vectors. *Emerging Infectious Diseases*. 14 (11), 1707-1714.

Perera, F.P, Rauh, V., Tsai, W., Kinney, P., Camann, D. and Barr, D. (2003) Effects of transplacental exposure to environmental pollutants on birth outcomes in a multiethnic population. *Environmental Health Perspectives*. 111, 201-206.

Petterson, E.F., Goddard, T.D., Huang, C.C., Couch, G.S., Greenblatt, D.M., Meng, E.C, Ferrin, T.E. (2004) UCSF Chimera—A Visualization System for Exploratory Research and Analysis. *Journal of Computational Chemistry*. 25(13), 1605-12.

Prade, L., Huber, R., Manoharan, H.T., Fahl, E. W. and Reuter, W. (1997) Structures of class pi glutathione S-transferase from human placenta in complex with substrate, transition-state analog inhibitor. *Structure*. 5 (10), 1287-1295.

Raijmakers, M.T., Steegers, E.A. and Peters, W.H. (2001) Glutathione S-transferases and thiol concentrations in embryonic and early fetal tissues. *Human Reproduction*. 16, 2445-2450.

Ralat, LA, and Colman, R.F. (2004) Glutathione S-transferase Pi has at least three distinguishable xenobiotic substrate sites close to its glutathione-binding site. *Journal of Biological Chemistry*. 279 (48), 50204-50213.

Rehman, H., Aziz, A-T., Saggu, S., Abbas, K. Z., Mohan, A. and Ansari, A. A. (2014) systematic review on pyrethroid toxicity with special reference to deltamethrin. *Journal of Entomology and Zoology studies*. 2 (6), 60-70.

Roth, C. (2017) Instruction for use of Roti®-Mark Standard Protein-molecular weight marker for SDS-PAGE. [https://www.carlroth.com/downloads/ba/en/T/BA\\_T851\\_EN.pdf](https://www.carlroth.com/downloads/ba/en/T/BA_T851_EN.pdf)

Rudnitskaya, A., Torok, B. and Torok, M. (2010) Molecular docking of enzyme inhibitors, a computational tool for structure-based drug design. *Biochemistry and Molecular Biology Education*. 38 (4), 261-265.

Saoudi, M., Messarah, M., Boumendjel, A., Jamoussi, K. and ElFeki, A. (2011) Protective effects of vitamin C against hematological and biochemical toxicity induced by deltamethrin in male Wistar rats. *Ecotoxicology and Environmental Safety*. 74, 1765-1769.

Schneidman-Duhovny, D., Inbar, Y., Nussinov, R., Wolfson, H.J. (2005) PatchDock and SymmDock: servers for rigid and symmetric docking. *Nucleic Acids Res*. 33 (Web Server issue): W363–W367.

Segel, I.H. (1975) Enzyme kinetics. New York: A Wiley-Interscience Publication.

Sheehan, D., Meade, G., Foley, M. V. and Dowd, A. C. (2001) Structure, function, and evolution of glutathione transferases: implications for classification of non-mammalian members of an ancient enzyme superfamily. *Biochemical Journal*. 360, 1-16

Singh, S.V., Leal, T., Ansari, G.S., Awasthi, Y. (1987) Purification and characterization of glutathione S-transferases of human kidney. *Biochemical Journal*. 246, 179-186.

Souza, M. S, Magnarelli, G. G., Rovedatti, M. G. Santa Cruz, S. and Pechen De D'angelo, A. M. (2005) Prenatal exposure to pesticides: analysis of human placental acetylcholinesterase, glutathione-S-transferase, and catalase as biomarkers of effect. *Biomarkers*. 10 (5), 376-389.

Souza, M. S, Magnarelli, G. G., Rovedatti, M. G. Santa Cruz, S. and Pechen De D'angelo, A. M. (2005) Prenatal exposure to pesticides: analysis of human placental acetylcholinesterase, glutathione-S-transferase, and catalase as biomarkers of effect. *Biomarkers*.10 (5), 376-389.

Steenland, K., Dick, R. B., Howell, R. J., Chrislip, D. W., Hines, C. J., Reid, T. M., et al (2001) Neurologic function among termiticide applicators exposed to chlorpyrifos. *Environmental Health Perspective*.108 (4), 293-300.

Tahir, M.K., Özer, N., Mannervik, B. (1988) Isoenzymes of glutathione transferase in rat small intestine. *Biochemical Journal*. 253, 759-764.

Taillebois, E., Alamiddine, Z., Brazier, C., Graton, J., Laurent, D. A. Thany, H.S. and Questel, J.Y. L. (2015) Molecular features and toxicological properties of four common pesticides, acetamiprid, deltamethrin, chlorpyrifos, and fipronil. *Bioorganic & Medicinal Chemistry*. 23, 1540-1550.

Tapia, B. Bortoni, G.P., Escobedo, E., Camann, D., Heilbrun, P. L., Whyatt, M. R. and Miller, S. C. (2012) A Comparative Study of Pesticide Use in Homes of Pregnant Women Living at the Texas-Mexico Border and in New York City. *Texas Public Health Journal*.64 (3), 18-23.

Tuna, G., Erkmen, K.G., Dalmizrak, O., Dogan, A., Hamdi O. I., Ozer, N., (2010) Inhibition characteristics of hypericin on rat small intestine glutathione-S-transferases. *Chemico-Biological Interactions*.188, 59-65.

Turk, S., Erkmen, K.G., Dalmizrak, O., Hamdi O. I. & Ozer, N. (2015) Purification of Glutathione S-Transferasepi from Erythrocytes and Evaluation of the Inhibitory Effect of Hypericin. *The Protein Journal*. 34 (6), 434–443.

Waliszewski, S.M., Aguirre, A., Infanzo'n, R. and Sí'liceo, J. (2000) Carry-over of persistent organochlorine pesticides through the placenta to the fetus. *Salud Publica de Mexico*. 42, 384-390.

Wang, X., Jia, H., Yang, H., Luo, M. and Sun T. (2017) Overexpression of Glutathione S-transferase P1 Inhibits the Viability and Motility of Prostate Cancer via Targeting MYC and Inactivating the MEK/ERK1/2 Pathways. To be published in *Oncology Research*. [In Print] Available from:<https://doi.org/10.3727/096504017X14978850961299>. [Accessed: 20th July 2017].

Whalen, R. and Boyer T.D. (1998) Human Glutathione S-Transferases. *Seminars in Liver Disease*. 18 (4), 345-358.

Wilce, M. C. J. and Parker, M. W. (1994) Structure and function of glutathione S-transferases. *Biochimica et Biophysica Acta*. 1205, 1-18.

Wu, B. and Dong, D. (2012) Human cytosolic glutathione transferases: structure, function, and drug discovery. *Trends in Pharmacological Sciences*. 33 (12), 656-668.

Yan, F., Yang, W., Li, X., Lin, T., Lun, Y., Lin, F., Lv, S., Yan, G., Liu, J., Shen, J., Mu, Y. & Luo, G. (2008) A trifunctional enzyme with glutathione S-transferase, glutathione peroxidase, and superoxide dismutase activity. *Biochimica et Biophysica Acta*. 1780 (6), 869-872.

Yekeen, T.A. and Adeboye, M.K. (2013) Cytogenotoxic Effects of Cypermethrin, Deltamethrin, Lambda-cyhalothrin, and Endosulfan Pesticides on *Allium Cepa* Root Cells. *African Journal of Biotechnology*. 12 (41), 6000-6006.

Zimniak, P. (2007) Substrate and Reaction Mechanism of Glutathione Transferase: In Awasthi, C.Y. (2007) Toxicology of Glutathione Transferase, *CRC Press, USA*, pp 71-95.







The Directorate of Graduate School of Health Sciences,

This study has been accepted by the thesis committee in Medical Biochemistry program as a Master of Science Thesis.

Thesis committee:

Chair: Professor Nazmi ÖZER, PhD  
Near East University

Member: Professor Naciye Leyla AÇAN, PhD  
Hacettepe University

Member: Assistant Professor Kerem TERALI, PhD  
Near East University

Supervisor: Professor Nazmi ÖZER, PhD  
Near East University

Approval:

According to the relevant article of the Near East University Postgraduate Study-Education and Examination Regulation, this thesis has been approved by the above-mentioned members of the thesis committee and the decision of the board of Directors of the Institute.

Professor K. Hüsnü Can BAŞER, PhD  
Director of Graduate School of Health Sciences

## DECLARATION

I hereby declare that the work in this thesis entitled “**HUMAN PLACENTAL GLUTATHIONE TRANSFERASE P1-1 (*hp*GSTP1-1): INHIBITORY ACTIVITY AND MOLECULAR DOCKING STUDIES OF DELTAMETHRIN**” is the product of my own research efforts undertaken under the supervision of Professor Nazmi Özer. No part of this thesis was previously presented for another degree or diploma in any University elsewhere, and all information in this document has been obtained and presented in accordance with academic ethical conduct and rules. All materials and results that are not original to this work have been duly acknowledged, fully cited and referenced.

Name, Last Name:

Signature:

Date:

## ACKNOWLEDGEMENT

My appreciation first goes to my supervisor, Professor Nazmi Özer. You are not just a teacher and supervisor, you are a father. It is a privilege sitting under your tutelage. Sir Isaac Newton once said, “If I have seen further than others, it is because I have stood on the shoulders of giants”. Thank you for lending me your shoulders to stand on and see ahead. Your love, patience, counsel, support, and contributions have been profound to my life. I sincerely appreciate all you have done for me.

I am also indebted to all staff of the Department of Medical Biochemistry, Faculty of Medicine Near East University. I cannot thank you enough. Your support and contribution to my studies, this work, and life as a whole, I cannot measure. To Professor Hamdi Ogus, Professor Nevbahar Turgan, Associate Professor Ozlem Dalmizrak, and Assistant Professor Kerem Teralı thank you so much.

To my sponsor, Kaduna State Government, I am grateful. I would not have come here without your sponsorship. Long live Kaduna State Government and the Federal Republic of Nigeria. I cannot forget you, all the Staff of Kaduna State Scholarship Board. Thank you for your support.

To my parents Mr. and Mrs. Markus A. Moolom, Grand Mother Mrs. Dagazau Madallah, Siblings Mrs. Samuel Dayer, Tiho C. Markus and Benedict U. Markus, Aunt Hannatu Dagazau (Miss), Hon. and Mrs. John Haruna, Uncle Moses A. Moolom, Cousins, friends and course mates, Near East Christian Fellowship (NECF) and WATCHMAN Family North Cyprus, you are most acknowledged and appreciated for the immeasurable support you have shown to my life. I love you.

Finally, let me express my gratitude to Dr. Timothy Bulus, Dr. Kinde David, Associate professor Mohammed Sani Abdulsalami and Associate Professor Iliya Haruna for your support, counsel, and encouragement. I cannot forget you Solomon Y. Tabat and Cornelius A. Oyamah for your help during my Laboratory work. I am grateful to you all.

## ABSTRACT

**Markus, V. Human Placental Glutathione Transferase P1-1 (*hpGSTP1-1*): Inhibitory Activity and Molecular Docking Studies of Deltamethrin. Near East University, Graduate School of Health Sciences, M.Sc. Thesis in Medical Biochemistry Program, Nicosia, 2017.**

Pyrethroids, which are widely used insecticides in agriculture and public health, have received considerable attention as an alternative to the highly toxic pesticides such as organophosphates. These pyrethroids, of which Deltamethrin (DEL) is a member, are the only class of insecticides recommended by both the Centre for Disease Control and Prevention (CDC) and the World Health Organization (WHO) to treat mosquito nets for the control of malaria. DEL has found enhanced usage due to high potency on a large number of pests and low toxicity to the non-target organism. However, recent studies revealed that DEL caused DNA damage and disruption in renal and hepatic function in pubescent female rats. Human studies on DEL toxicity are scarce; hence the need for this work. GSTP1-1 is a significant enzyme with important roles in the detoxification of endo- and xenobiotics by catalyzing their conjugation to reduced glutathione (GSH), and regulation of cell survival and apoptosis by inhibiting C-Jun-N terminal kinase-1 (JNK-1). First, the purity and subunit molecular mass of *hpGSTP1-1*, using native- and sodium dodecyl sulfate gel electrophoresis (SDS-PAGE) were determined. *hpGST P1-1* gave single band both on native- and SDS/PAGE. Subunit  $M_r$  was 21.4 kDa. The optimum pH, optimum temperature, activation energy ( $E_a$ ), temperature coefficient ( $Q_{10}$ ) of *hpGSTP1-1* were found to be 6.62, 35.4°C, 7.6 kcal mole<sup>-1</sup> and 1.52 respectively. In this study, the interaction of *hpGST P1-1* with DEL was investigated. The  $IC_{50}$  value (50% inhibition value) of *hpGSTP1-1* by DEL was 6.2 µM. The inhibition types and kinetic parameters were determined from graphs and using STATISTICA '99. The  $V_m$  and  $K_m$  at fixed [CDNB]-varied [GSH], and fixed [GSH]-varied [CDNB] were  $10.4 \pm 0.22$  and  $8.7 \pm 0.33$  U mg<sup>-1</sup> protein, and  $0.31 \pm 0.02$  and  $0.30 \pm 0.03$  mM, respectively. The inhibition types in both cases were non-competitive with the  $K_i$  values of  $5.61 \pm 0.32$  and  $7.96 \pm 0.97$  µM, respectively. The Molecular docking studies suggest that DEL binds to a site located at the intermonomer space of the *hpGSTp1-1* enzyme and caused conformational changes that inhibit the enzyme noncompetitively. Correspondingly, considerable maternal exposure to DEL may interfere with proper fetal development.

**Keywords:** Human placental GSTP1-1, Detoxification, Inhibitory Kinetics, Deltamethrin

## ÖZET

**Markus, V. İnsan Placentası Glutatiyon Transferazı P1-1 (*hpGSTP1-1*): Deltamethrin'in İnhibitör Aktivitesi ve Moleküler Doking Çalışmaları. Yakın Doğu Üniversitesi, Sağlık Bilimleri Enstitüsü, Tıbbi Biyokimya Programı, Yüksek Lisans Tezi, Lefkoşa, 2017.**

Pyrethroid'ler, çok toksik olan organofosfatlara alternatif insektisit olarak dikkat çekmiştir ve ziraat ve halk sağlığı alanlarında yaygın olarak kullanılmaktadır. Deltamethrin (DEL), hem Dünya Sağlık Örgütü (WHO) hem de Hastalık Kontrol ve Koruma Merkezi (CDC) tarafından sıtma aktarımına karşı cibinliklere eklenmesi önerilen tek insektisittir. DEL, etkisinin birçok zararlı böceğe karşı yüksek olması ve düşük toksisitesi nedeniyle geniş kullanım alanı bulmuştur. Ancak, son zamanlarda ergen farelerle yapılan çalışmalarda DEL'in DNA hasarı oluşturduğu ve böbrek ve karaciğer fonksiyonlarını bozduğu gösterilmiştir. İnsanlarda DEL'in etkileri konusunda çalışma yok denecek kadar azdır, o nedenle bu çalışma yapılmıştır. Glutatiyon transferaz P1-1 (GSTP1-1) endo- ve ksenobiyotikleri glutatiyon (GSH) ile konjuge ederek detoksifikasyonunda görev alan ve C-Jun-N terminal kinaz-1'i (JNK-1) inhibe ederek hücre yaşamını ve apoptozu düzenleyen önemli bir enzimdir. İlk önce, *hpGSTP1-1*'in saflığı ve alt birim moleküler kütlesi natif ve sodyum dodesil sülfat poliakrilamid jel elektroforezi (natif ve SDS/PAGE) kullanılarak belirlendi. GSTP1-1 natif ve SDS/PAGE'de tek band verdi. Altbirim Mr'ı 21.4 kDa olarak saptandı. GSTP1-1'in, optimum pH'sı, optimum sıcaklığı, aktivasyon enerjisi ( $E_a$ ) ve sıcaklık katsayısı, ( $Q_{10}$ ) sırası ile 6.62, 35.4°C, 7.6 kkal/mol, 1.52 olarak bulundu. Bu çalışmada, *hpGSTP1-1* ile DEL'in ilişkisi araştırıldı. DEL'in, GSTP1-1 için,  $IC_{50}$  değeri (enzimin%50'sini inhibe etmek için gerekli derişim) 6.2  $\mu$ M bulundu. DEL'in inhibisyon tipi ve kinetik sabitleri ise sabit [GSH]-değişken [CDNB] ve sabit [CDNB]-değişken [GSH] koşullarında grafiklerden ve ayrıca STATISTICA '99 kullanılarak belirlendi. Sabit [CDNB]-değişken [GSH], ve sabit [GSH]-değişken [CDNB] koşullarında  $V_m$  ve  $K_m$  değerleri, sırası ile  $10.4 \pm 0.22$  ve  $8.7 \pm 0.33$  U/mg protein, ve  $0.31 \pm 0.02$  ve  $0.30 \pm 0.03$  mM olarak saptandı. Her iki substrat ile inhibisyon tipi non-kompetitif ve  $K_i$  değerleri de sırası iledeğişken [GSH] ve değişken [CDNB] koşullarında;  $5.61 \pm 0.32$  ve  $7.96 \pm 0.97$   $\mu$ M olarak bulundu. Moleküler doking çalışması DEL'in enzim üzerinde alt birimler arasında bulunan L-bölgesine bağlandığı ve enzim dekonformasyon değişikliği yaparak non-kompetitif inhibisyona neden olduğu saptandı. Sonuç olarak, annenin DEL'e belli süre maruz kalması düzgün fetal gelişmeyi etkileyebilir.

**Anahtar Sözcükler** :İnsan plasentası GSTP1-1, Detoksifikasyon, İnhibitör Kinetiği, Deltamethrin

**TABLE OF CONTENTS**

	<b>Page No</b>
APPROVAL	iii
DECLARATION	iv
ACKNOWLEDGEMENTS	v
ABSTRACT	vi
OZET	vii
TABLE OF CONTENTS	viii
ABBREVIATIONS	xii
LIST OF FIGURES	xv
LIST OF TABLES	xvii
1. INTRODUCTION	1
2. GENERAL INFORMATION	5
2.1. Oxidative Stress and the Antioxidant System	5
2.2. Glutathione Transferases	8
2.3. Distribution of GSTs	8
2.4. Classification of GSTs	8
2.5. Nomenclature	10
2.6. Structure of GSTs	11
2.6.1. Active Sites of GSTs	13
2.7. Reaction Mechanism of Canonical GST	16
2.7.1 Binding and Activation of GSH	16
2.7.2 Electrophilic Substrate Binding (H-site)	17
2.8. Catalytic Activity of GSTs	18
2.8.1 Glutathione Transferase activity	18

2.8.1.1.	Major Types of Glutathione Transferase Reaction	18
2.8.1.1.1.	Aromatic NucleophilicSubstitutional Reaction	18
2.8.1.1.2.	Nucleophilic Additional Reaction to Double Bond	21
2.8.1.1.3.	Opening of Oxirane (Epoxide) Ring	21
2.9.	GSTs and Bioactivation of Toxins	21
2.10.	GST Peroxidase Activity	22
2.11.	GST Isomerase activity	22
2.12.	GSTs in the Metabolism of Eicosanoids	24
2.13.	Noncatalytic Activities of GSTs	25
2.13.1	Ligandin function	25
2.13.2.	Buffering	25
2.14.	Role of GST in Cellular Survival and Apoptosis	25
2.15.	GST Inhibitors	28
2.16.	Pesticides	28
2.17.	Deltamethrin	28
3.	MATERIALS AND METHODS	32
3.1.	Chemicals	32
3.2.	Methods	32
3.2.1.	Enzyme Preparation	32
3.2.2.	Native-Polyacrylamide Gel Electrophoresis (Native-PAGE) and Sodium Dodecyl Sulfate Polyacrylamide Gel Electrophoresis (SDS-PAGE)	32
3.2.3.	Casting of Gels for Native-PAGE and SDS-PAGE	35
3.2.4.	Sample Preparation for Native- and SDS-PAGE	35
3.2.4.1.	Sample Preparation for CBB Staining (Native-PAGE)	35
3.2.4.2.	Sample Preparation for Silver Staining (Native-PAGE)	36

3.2.4.3. Sample Preparation for CBB Staining (SDS-PAGE)	36
3.2.4.4. Sample Preparation for Silver Staining (SDS-PAGE)	36
3.2.5. Performing the Electrophoresis	36
3.2.6. Coomassie Brilliant Blue (CBB) Staining and Destaining	37
3.2.7. Silver Staining	37
3.2.8. Reaction Mixture for the <i>hp</i> GSTP1-1 Kinetics	37
3.2.9. Determination of the <i>hp</i> GSTP1-1 Enzyme Activity	38
3.2.10 Determination of Optimum pH	39
3.2.11. Determination of Optimum Temperature	39
3.2.12. Effect of DEL on <i>hp</i> GSTP1-1 and the Determination of $IC_{50}$	40
3.2.13 Confirmation of the reversible inhibition of <i>hp</i> GSTP1-1 by DEL	40
3.2.14. Inhibitory Kinetic Experiments with DEL.	40
3.2.15. Statistical Analysis	41
3.2.16. Molecular Docking of the GSTP1-1 Enzyme Inhibitor, DEL	41
4. RESULT	42
4.1. Characterization of Human Placental Glutathione Transferase P1-1	42
4.2. Determination of Optimum pH	44
4.3. Determination of Optimum Temperature	45
4.4. Inhibitory Kinetic Interaction of <i>hp</i> GSTP1-1 with DEL.	47
4.5. Molecular Docking of the GSTP1-1 Enzyme Inhibitor, DEL.	56
5. DISCUSSION	60
6. CONCLUSION	69
APPENDIX	70

REFERENCES

**ABBREVIATIONS**

APS	: Ammonium Persulfate
ASK1	: Apoptosis signal-regulating kinase 1
BPB	: Bromophenol blue
CB	: Cibacron blue
CBB	: Coomassie Brilliant Blue
CCCEH	: Center for Children's Environmental Health
CDC	: Center for Disease Control and Prevention
CDNB	: 1-chloro-2,4-dinitrobenzene
DEL	: Deltamethrin
DNA	: Deoxyribonucleic acid
$E_a$	: Energy of Activation
EA	: Ethacrynic acid
EC	: Enzyme Commission
EDTA	: Ethylenediaminetetraacetic acid
FDNB	: 1-fluoro-2,4-dinitrobenzene
GPX	: Glutathione peroxidase
GR	: Glutathione reductase
GS-DNB	: 1-(S-glutathionyl)-2,4-dinitrobenzene
GSH	: L-glutathione Reduced
G-site	: Glutathione binding site
GSSG	: Glutathione disulfide
GSTP1-1	: Glutathione transferase P1-1
GSTs	: Glutathione transferases
H <sub>2</sub> O <sub>2</sub>	: Hydrogen peroxide

HCl	: Hydrochloric acid
HO <sup>-</sup>	: Hydroxyl ion
HOCL	: Hypochlorous acid
<i>hp</i> GSTP1-1	: Human placenta glutathione transferase P1-1
H-site	: Electrophilic substrate binding site
<i>IC</i> <sub>50</sub>	: Half maximal inhibitory concentration
JNK	: C-Jun-N terminal kinase
kDa	: kilo Dalton
<i>K</i> <sub>i</sub>	: Inhibition constant
<i>K</i> <sub>m</sub>	: Michaelis-Mentenconstant
L-site	: Ligandin-binding site (or nonsubstrate-binding site)
MAPEG	: Membrane-associated Proteins in Eicosanoid and Glutathione metabolism
MES	: 2-(N-morpholino)-ethane sulfonic acid
Mr	: Relative molecular mass
MRP1	: Multidrug resistance protein 1
NMC	: N-methylcarbamates
Nrf2	: Nuclear transcription factor-erythroid 2 p45-related factor 2
O <sub>2</sub> <sup>-</sup>	: Superoxide ion
OC	: Organochlorines
ONOO <sup>-</sup>	: Peroxynitrite
OP	: Organophosphates
PDB	: Protein Data Bank
<i>pH</i> <sub>op</sub>	: Optimum pH
PPAR $\gamma$	: Peroxisome proliferator-activated receptor gamma
PYR	: Pyrethroids

$Q_{10}$	: Temperature Coefficient
RNS	: Reactive nitrogen species
ROOH	: Organic hydroperoxide
ROO <sup>•</sup>	: Peroxy radical
ROS	: Reactive oxygen species
RO <sup>•</sup>	: Alkoxy radical
SDS-PAGE	: Sodium dodecyl sulfate polyacrylamide gel electrophoresis
SOD	: Superoxide dismutase
SPB	: Sample preparation buffer
SSRIs	: Selective serotonin reuptake inhibitors
TCAs	: Tricyclic antidepressants
TEMED	: N,N,N',N'-Tetramethylethylenediamine
$T_{op}$	: Optimum Temperature
TRAF2	: Tumor Necrosis Factor Receptor-associated Factor 2
Tris	: Tris(hydroxymethyl)aminomethane
$V_m$	: Maximum velocity
WHO	: World Health Organization
$\beta$ -ME	: Beta Mercaptoethanol
<sup>•</sup> OH	: Hydroxyl Radical

## LIST OF FIGURES

	<b>Page No</b>
Figure 2.1. Schematic summary of detoxification and antioxidant systems	7
Figure 2.2. Classification of Human Glutathione transferases (GSTs)	9
Figure 2.3. The tertiary structure of a GST enzyme	12
Figure 2.4A. Important residues in the active-site of GSTs	14
Figure 2.4B. Structure-base sequence alignment of some human GST enzymes	15
Figure 2.5. Conjugation reaction of GSH with CDNB catalyze by GST	19
Figure 2.6. Molecular interactions between the artificial substrate CDNB molecules and the active sites of GSTM1-1	20
Figure 2.7. The isomerization steps and intermediates in the phenylalanine–tyrosine degradation pathway	23
Figure 2.8. The Proposed reaction mechanism for GSH-assisted conversion of $\Delta^5$ -androst-3, 17-dione ( $\Delta^5$ -AD) to $\Delta^4$ -androst-3, 17-dione ( $\Delta^4$ -AD)	24
Figure 2.9. Role of GSTP1-1 in cellular survival and apoptosis	27
Figure 2.10. The structure of DEL	29
Figure 4.1. <i>hp</i> GSTP1-1 on discontinuous Native-PAGE.	42
Figure 4.2. Determination of relative molecular mass of <i>hp</i> GSTP1-1	43
Figure 4.3. Specific activity, (U / mg Protein) vs. pH plot	44
Figure 4.4. Plots For Temperature Optimum, Energy of Activation and Temperature Coefficient	46
Figure 4.5. Confirmation of the reversibility of <i>hp</i> GSTP1-1inhibition by DEL	48

Figure 4.5.	Inhibition of <i>hp</i> GSTP1-1 by DEL	49
Figure 4.6.	Michaelis-Menten plot for <i>hp</i> GSTP1-1 enzyme with different concentration of DEL.	50
Figure 4.7.	Lineweaver-Burk plot for <i>hp</i> GSTP1-1 enzyme with different concentration of DEL	51
Figure 4.8.	Slope and intercept vs. [DEL] plot	52
Figure 4.9.	Michaelis-Menten plot for <i>hp</i> GSTP1-1 enzyme with different concentration of DEL	53
Figure 4.10.	Lineweaver-Burk plot for <i>hp</i> GSTP1-1 enzyme with different concentration of DEL	54
Figure 4.11.	Slope and intercept vs. [DEL] plot	55
Figure 4.12.	Three-dimensional structure of <i>hp</i> GSTP1-1 and DEL	56
Figure 4.13	Docking interaction of DEL with GSTP1-1	57
Figure 4.14.	Comparison of the binding sites of GSTP1-1	59

**LIST OF TABLES**

	<b>Page No</b>
Table 2.1. Free radicals	6
Table 3.1. Volumes Used in Gel Preparation for Native-PAGE	34
Table 3.2. Volumes used in gel preparation for SDS-PAGE	34
Table 4.1. Kinetic Parameters of <i>hp</i> GSTP1-1 Inhibition by DEL	55
Table 4.2. Interactions of GSTP1-1 with DEL	58